การประเมินการปนเปื้อนของแคดเมียมจากการเคลื่อนที่ของตะกอนท้องน้ำ ในห้วยแม่ตาว อำเภอแม่สอด จังหวัดตาก

นางสาวพิมพ์ประภา การุณมรรคผล

วิทยานิพนธ์นี้เป็นส่วนหนึ่งของการศึกษาตามหลักสูตรปริญญาวิทยาศาสตรมหาบัณฑิต
สาขาวิชาการจัดการสิ่งแวดล้อม (สหสาขาวิชา)
บัณฑิตวิทยาลัย จุฬาลงกรณ์มหาวิทยาลัย
ปีการศึกษา 2552

EVALUATION OF CADMIUM CONTAMINATION
DUE TO STREAM SEDIMENT TRANSPORT
IN MAE TAO CREEK, MAE SOT DISTRICT, TAK PROVINCE

Miss Pimprapa Karoonmakphol

A Thesis Submitted in Partial Fulfillment of the Requirements
for the Degree of Master of Science Program in Environmental Management
(Interdisciplinary Program)
Graduate School
Chulalongkorn University
Academic Year 2009

Thesis Title	EVALUATION OF CADMIUM CONTAMINATION DUE TO STREAM SEDIMENT TRANSPORT IN MAE TAO CREEK, MAE SOT DISTRICT, TAK PROVINCE
By	Miss Pimprapa Karoonmakphol
Field of Study	Environmental Management
Thesis Advisor	Pichet Chaiwiwatworakul, Ph.D.
Thesis Co-Advisor	Chantra Tongcumpou, Ph.D.

Accepted by the Graduate School, Chulalongkorn University in Partial Fulfillment of the Requirements for the Master's Degree

.... Dean of the Graduate School
(Associate Professor Pornpote Piumsomboon, Ph.D.)

THESIS COMMITTEE

.... Chairman
(Assistant Professor Manaskorn Rachakornkij, Ph.D.)

.... Thesis Advisor
(Pichet Chaiwiwatworakul, Ph.D.)

.... Thesis Co-Advisor
(Chantra Tongcumpou, Ph.D.)

.... Examiner
(Pisut Painmanakul, Ph.D.)

.... External Examiner
(Somchai Chonwattana, Ph.D.)

พิมพ์ประภา การุณมรรคผล : การประเมินการปนเปื้อนของแคดเมียมจากการเคลื่อนที่ของตะกอนท้องน้ำในห้วยแม่ตาว อำเภอแม่สอด จังหวัดตาก. (EVALUATION OF CADMIUM CONTAMINATION DUE TO SEDIMENT TRANSPORT IN MAE TAO CREEK, MAE SOT DISTRICT, TAK PROVINCE) อ. ที่ปรึกษาวิทยานิพนธ์หลัก: อ.ดร.พิเชฐ ชัยวิวัฒน์วรกุล, อ. ที่ปรึกษาวิทยานิพนธ์ร่วม: อ.ดร.จันทรา ทองคำเภา 109 หน้า.

พื้นที่ศึกษาของงานวิจัยนี้ ได้แก่ ลุ่มน้ำแม่ตาว ซึ่งเป็นพื้นที่ที่พบแคดเมียมปนเปื้อนอยู่มากที่สุดในประเทศไทย อีกทั้งมีการตรวจพบความเข้มข้นของแคดเมียมในตะกอนท้องน้ำในปริมาณมาก งานวิจัยนี้ จึงมุ่งเน้นในการศึกษาเกี่ยวกับตะกอนท้องน้ำและการเคลื่อนที่ของตะกอนท้องน้ำในห้วยแม่ตาว

อัตราการไหลในลำน้ำแม่ตาวของ 10 สถานีในช่วงหน้าฝนได้ถูกสำรวจ รวมถึงความเข้มข้นของแคดเมียมและขนาดของตะกอนท้องน้ำ ผลจากการจำลองการไหลในลำน้ำ ซึ่งประกอบด้วยระดับน้ำและอัตราการไหลถูกจำลองโดยใช้โปรแกรม MIKE SHE ควบคู่กับ MIKE 11 หลังจากนั้นการเคลื่อนที่ของตะกอนท้องน้ำถูกจำลองโดยส่วนจำเพาะการเคลื่อนที่ของตะกอนในโปรแกรม MIKE 11 ท้ายที่สุด ผลการเคลื่อนที่ของตะกอนท้องน้ำและค่าความเข้มข้นของแคดเมียมในตะกอนท้องน้ำ ถูกนำมาคำนวณและประเมินการแพร่กระจายของแคดเมียมในตะกอนท้องน้ำจากพื้นที่ทำการศึกษา อย่างไรก็ตาม เนื่องจากข้อมูลที่ต้องการมีไม่เพียงพอ ผลที่ได้จากการจำลองจึงอาจมีความไม่แน่นอนเกิดขึ้น ซึ่งสามารถปรับปรุงได้โดยการรวบรวมข้อมูลให้มากยิ่งขึ้น

การแพร่กระจายของการปนเปื้อนแคดเมียม เนื่องจากการเคลื่อนที่ของตะกอนท้องน้ำในลุ่มน้ำแม่ตาวเกิดขึ้นมากในช่วงหน้าฝน ซึ่งสามารถทำให้เกิดปัญหาการปนเปื้อนของแคดเมียมอย่างรุนแรง มิใช่เพียงในพื้นที่ศึกษาเท่านั้น แต่รวมไปถึงพื้นที่ข้างเคียงอีกด้วย

สาขาวิชา การจัดการสิ่งแวดล้อม ลายมือชื่อนิสิต....Pimpraapa K.....
ปีการศึกษา 2552 ลายมือชื่อ อ.ที่ปรึกษาวิทยานิพนธ์หลัก..........
ลายมือชื่อ อ.ที่ปรึกษาวิทยานิพนธ์ร่วม..........

5187553620: MAJOR ENVIRONMENTAL MANAGEMENT
KEYWORDS : CADMIUM / MAE TAO / MAE SOT / STREAM SEDIMENT / SEDIMENT TRANSPORT / MIKE SHE / MIKE 11

PIMPRAPA KAROONMAKPHOL : EVALUATION OF CADMIUM CONTAMINATION DUE TO STREAM SEDIMENT TRANSPORT IN MAE TAO CREEK, MAE SOT DISTRICT, TAK PROVINCE. THESIS ADVISOR: PICHET CHAIWIWATWORAKUL, Ph.D., THESIS CO-ADVISOR: CHANTRA TONGCUMPOU, Ph.D., 109 pp.

The Mae Tao subcatchment, the study area in this research, is known as the most worrisome site of cadmium contamination in Thailand. High cadmium levels in stream sediment are present, and this research concentrates on cadmium's presence in stream sediment and its transport throughout Mae Tao Creek.

The stream flow during storm events at 10 monitoring stations along Mae Tao Creek were surveyed, and the cadmium concentration and grain size distribution of stream sediment were quantified. The hydrodynamic results including water depth and water discharge were simulated using MIKE SHE coupled with MIKE 11, and stream sediment transport data were determined afterwards by the sediment transport module in MIKE 11. Finally, the sediment transport results and the measured cadmium concentration were calculated to evaluate the cadmium transport rate of stream sediment in the area. Nonetheless, due to the scarceness of supporting data, which can commonly occur in distributed model applications, the simulated results might still contain some degree of uncertainty and could be improved with more data collection.

In conclusion, the spread of cadmium contamination due to sediment transport in the Mae Tao subcatchment mainly occurs during storm events. These storms intensify cadmium contamination problems not only in the area but also in conterminous areas.

Field of Study: Environmental Management Student's Signature Pimprapa K.
Academic Year: 2009 Advisor's Signature
Co-Advisor's Signature

ACKNOWLEDGEMENTS

First of all, I would like to acknowledge the National Center of Excellence for Environmental and Hazardous Waste Management (NCE-EHWM), under the Graduate School of Chulalongkorn University for providing me a full scholarship and full financial support of this research.

This thesis could not have been completed without the assistance of my advisor, Dr. Pichet Chaiwiwatworakul, and my co-advisor, Dr. Chantra Tongcumpou. My gratitude is expressed to them for their patience, willingness to help, suggestions, guidance, and encouragement throughout my time in the program.

My appreciation is also extended to the chairman of the thesis committee, Assistant Professor Dr. Manaskorn Rachakornkij, and the thesis committee members, Dr. Pisut Painmanakul and Dr. Somchai Chonwattana, for their invaluable comments and time.

The MIKE student license was provided and supported by DHI Water • Environment • Health. My gratefulness is consigned to Dr. Douglas Graham for advising in the DHI software application as well as to Dr. Somchai Chonwattana and Miss Varaporn Buranautama for their very kind cooperation and assistance.

Much of the data was granted from the Department of Groundwater Resources, Department of Water Resources, Land Development Department, Royal Thai Survey Department, and Thai Meteorological Department. I would also like to gratefully recognize Mr. Panya Polsan, Mr. Sanong Pathanompee and surveying team from Royal Irrigation Department for their patience and field observation assistance.

Extraordinary thanks goes to Miss Akiko Uyeda for teaching and providing consultation on academic English writing as well as to the administrative officers for their great support. Also, I’d like to recognize Mr. Mongkolchai Assawaditlert and Miss Wilailuk Niyommanerat for their good advice and support as I performed my field study and laboratory work.

Finally, I would like to express my deepest gratitude to my beloved family and friends for their continuous love, encouragement, and support.

CONTENTS

PAGE

LIST OF TABLES

TABLE PAGE

LIST OF FIGURES

FIGURE PAGE

FIGURE PAGE

CHAPTER I

INTRODUCTION

1.1 Background and motivation

Despite having only the fifth-largest rice cultivation area in the world, Thailand is the world's largest rice exporter (Reuters, 2008). One of the areas knows for rice cultivation in Thailand is Mae Sot district in Tak province, located in the northern part of Thailand. This area has been well known not only as a high-quality jasmine rice producing area but also as the largest zinc deposit of Thailand (Department of Primary Industries and Mines (DPIM), 2006). Cadmium has been contaminating the area because it is extracted during the production of zinc.

High contaminations of cadmium in soil and rice grain were found in Phatat Pha Daeng and Mae Tao Mai sub-districts of Mae Sot district. This circumstance might not only have an effect on the quantity and quality of rice, but also cause health risks to the rice consumers. The local economy as a result has been impacted by the government's prohibition of rice cultivation in the area (Parada Maneewong, 2005).

A local farmer claimed that the villagers grow and eat local rice because it is their only option since they do not have enough money to buy rice from other locations. In 2004, there were 500 villagers suffering from kidney damage, another 700 villagers had been found to have high levels of cadmium in their blood, and 110,000 people were at risk for being affected by cadmium (The Nations, 2004).

The toxic leakages were believed to be essentially from forest destruction, forest encroachment, and mining activities from two zinc mines, belonging to Padaeng Industry Public Company Limited and the Tak Mining Company (DPIM, 2006).

Two subcatchments are of highest concern with regard to cadmium contamination: the Mae Tao and Mae Ku subcatchments, with the Mae Tao subcatchment having the larger zinc depository (Piyarat Kaowichakorn, 2006).

Consequently, the Mae Tao subcatchment was selected as the study area in this research because of the higher potential for cadmium contamination in the area.

Even though cadmium contamination in soil was higher than that of stream sediment, sediment can transport better than soil. As a result, this research focuses on the stream sediment or bed load in the Mae Tao Creek and its transport, which is one of the main mechanisms of cadmium spreading into the Mae Tao subcatchment.

1.2 Objectives

- To estimate water flow and water level of Mae Tao Creek in the year 2009.
- To demonstrate the stream sediment transport in the wet season.
- To identify the processes that play significant roles in the transport of sediment in the study area.
- To evaluate the transport of cadmium contamination in Mae Tao Creek.

1.3 Hypothesis

The transport of stream sediment within Mae Tao Creek during storm events is a significant process and causes the expansion of cadmium contamination.

1.4 Scope of the study

- Hydrological processes relating to the transport of cadmium contamination in the study area, Mae Tao subcatchment, were reviewed.
- Input data were collected from field surveys of the study area and applied into models (MIKE SHE and MIKE 11).
- An uncertainty analysis was conducted to identify the significant parameters for the transport of cadmium contamination.
- The model was validated to attain acceptable results.

1.5 Expected outcome

An evaluation of accumulated cadmium transfer due to stream sediment transport in Mae Tao Creek in the year 2009 is the expected outcome.

CHAPTER II

LITERATURE REVIEW

2.1 The study area

2.1.1 Location

The Mae Tao subcatchment, which belongs to the Salween River basin's upper Mae Moei catchment, is located in Mae Sot district, Tak province in the northern part of Thailand. The only creek in the Mae Tao subcatchment, as displayed in Figure 2-1, is called Mae Tao Creek; which could be separated into three parts: the main, left, and right parts of the creek. The location of zinc depository and two mines are approximately 16° 39' N and 98° 40' E. (Land Development Department (LDD) and Royal Thai Survey Department (RTSD)).

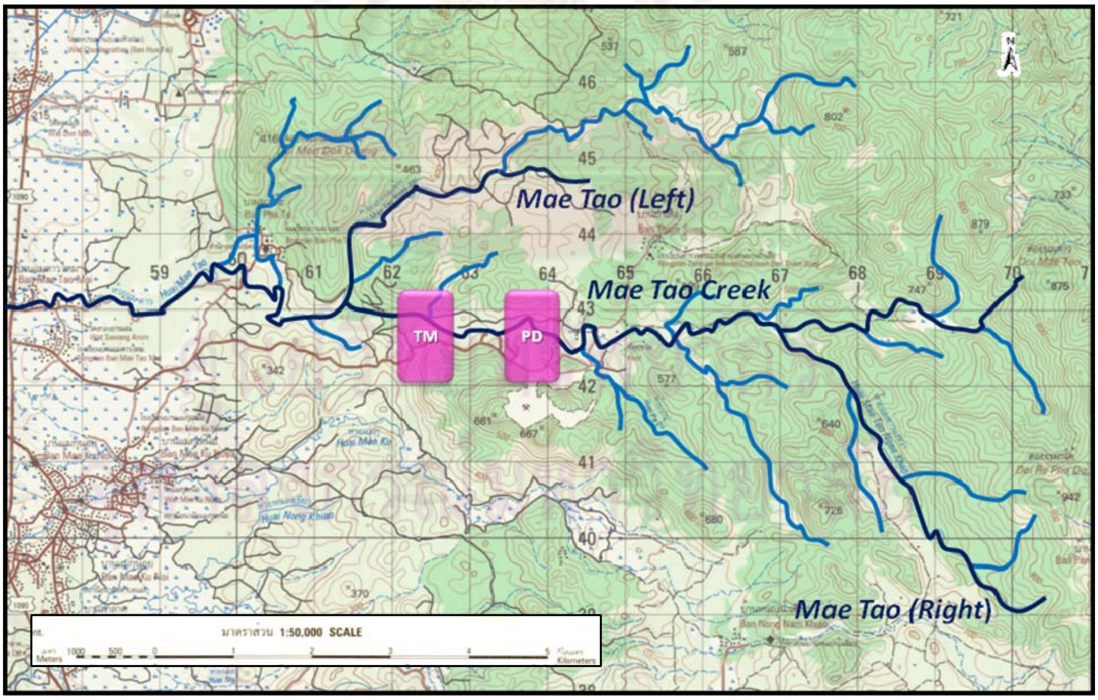

Figure 2-1 The study area, Mae Tao Creek and zinc mines, namely Tak Mining (TM) and Padaeng Industry Plc. (PD) (adapted from a topographic map with a scale of 1:50,000, Map sheet 4742III)

2.1.2 Climate and meteorology

The climate of the area is a tropical savanna. There are three seasons: summer, from March to May; the rainy season, from June to October; and winter, from November to February (Piyarat Kaowichakorn, 2006).

2.1.3 Hydrology

Mae Tao Creek, a 25 kilometers long stream, flows from the mountainous area in the east to the low land areas in the west; it passes through zinc deposits and finally discharges into the Mae Moei River. The irrigation water for the over 3,000 hectares of agricultural area is from Mae Tao Creek (Simmons *et al.*, 2009).

2.1.4 Landuse

Landuse of Mae Sot can be separated into five major groups (DPIM, 2006).

- Forest area: covers almost all of the eastern area as a mixed deciduous forest with lots of teak.
- Agricultural area: mainly paddy fields, which are cultivated during only one season a year. The other economic plants are soybeans, corn, and garlic, which are grown after the post rice harvest period.
- Residential area: mostly located along the floodplain area in the western part.
- Mining area: the zinc deposit is located at Doi Padaeng, Phra That Padaeng sub-district (16° 39’ N 98° 40’ E). There are two zinc mines in the area, namely, Padaeng Industry Public Company Limited and Tak Mining.
- Other: mostly for public purposes, such as reservoirs, roads, and creeks.

2.2 Contaminant

The ability of a trace element to cause environmental harm depends on its concentration in atmosphere or hydrosphere, its chemical speciation (form of occurrence), and the details of its biochemical cycling (Schnoor, 1996).

The fate of contaminants in soil can be divided into three processes. First, the retardation process consists of sorption, ion exchange and precipitation. Second, the attenuation process involves irreversible removal, transformation processes and the three mechanisms of redox, hydrolysis, and volatilization. Finally, mobility enhancement contains cosolvation, ionization, dissolution, and complexation. Meanwhile, the transport of contaminants in the subsurface can be divided into eight parts: (1) the hydrologic cycle, (2) the groundwater flow, (3) the hydraulic conductivity of geologic materials, (4) the flow in the unsaturated zone, (5) the contaminant transport mechanisms, (6) real-world contaminant transport, (7) the flow and transport equation, and (8) groundwater modeling (Yunus, slide).

2.3 Cadmium

Cadmium is one of the metallic components found in the earth's crust and ocean. It is naturally present everywhere in the environment (i.e. air, water, soils, plants, and foodstuffs) and is usually found as a mineral combined with other elements, namely oxygen, sulfur, or chlorine. It can be extracted during the production of other metals such as zinc, lead, or copper. It does not break down in the environment but can change into different forms. Cadmium, one of atmophile elements, can be either volatile or its compounds have low boiling points (Schnoor, 1996). Cadmium metal is harmless but its Cd^{2+} ion is harmful and can be dissolved in water.

Metal cadmium exhibits excellent resistance to corrosion, particularly in alkaline and seawater environments, possesses a low melting temperature and rapid electrical exchange activity, and has both high electrical and thermal conductivity. While cadmium compounds possess outstanding resistance to high stresses and high temperatures, and deter ultraviolet light degradation of certain plastics. Some cadmium electronic compounds exhibit semi-conducting properties and are utilized in solar cells and many electronic applications (International Cadmium Association (ICdA), 2009).

The Agency for Toxic Substances and Disease Registry (ATSDR), under the United States Public Health Service (1993), revealed that cadmium has no known good effects on human health. It results in high toxicity at low concentrations. It can cause lung cancer, kidney disease, fragile bones, and also death. Some researchers state that cadmium may cause birth defects and changes in the immune system.

2.3.1 Sources of cadmium

The Pollution Control Department (PCD), under the Ministry of Science and Technology (1998), lists two major source types of cadmium: natural sources and anthropogenic sources. Several activities that cause cadmium contamination in the environment (to the air, water, soil, plants, and animals) are listed in Table 2-1.

Piotrowski and Coleman (1980) stated that the major sources of cadmium in the environment are the mining and smelting of nonferrous metals, including zinc, lead, and copper, because cadmium is a by-product from the extraction, smelting, and refining of these metals. Cadmium and zinc are usually found together, the ratios of cadmium to zinc range between 1:100 and 1:1000, which are the same ratios in the study of Fulkerson and Goeller (1973) and Friberg *et al.* (1976), depending on the sources. More information on sources of cadmium emissions to soil is provided in Table 2-2.

Table 2-1 Activities that cause cadmium contamination in the environment

Compartment	Activities
Air	Coal or fossil fuel burning [1], [4]
	Oil and waste burning and scrap metal treatment [1], [2], [4]
	Metal mining, refining, and smelting [1], [4]
	Industries using cadmium in alkaline accumulators, alloys, paints, and plastics [2]
	Fertilizer utilization [1], [2]
	Use of pesticides containing cadmium [2]
	Forest fires [4]
	Volcanic activity [4]
Water	Disposal of wastewater [1], [3]
	Fertilizer utilization [1], [2], [4]
	Spills and leaks from hazardous waste and contaminated sites [1], [4]
	Metal or plastic pipes used in distribution [2]
	Use of pesticides containing cadmium [2]
	Atmospheric deposition [2], [3], [4]
	Non-ferrous metals production [4]
	Iron and steel industry activities [4]
	Weathering and erosion of soils and bedrock [4]
Soil	Fertilizer utilization [1], [2], [3], [4]
	Spills and leaks from hazardous waste sites [1]
	Atmospheric deposition [2], [4]
	Flooding or irrigation of cadmium contaminated water [2], [4]
	Airborne and waterborne cadmium [2], [3]
	Sludge from sewage treatments [3], [4]
	Underlying bedrock [4]
	Transported parent material such as glacial till and alluvium [4]
Plants and Animals	Uptaking cadmium from the environment [1], [2]

[1] ATSDR (1993: online)
[2] Friberg *et al.* (1976)
[3] Piotrowski and Coleman (1980)
[4] ICdA (2009)

Table 2-2 Sources of cadmium emissions to soil (ICdA, 2009)

Category	Activity
Inputs to agricultural soils	Atmospheric deposition
	Sewage sludge application
	Phosphate fertilizer application
Inputs to non-agricultural soils	Iron and steel industry activities
	Non-ferrous metals production
	Fossil fuel combustion
	Cement manufacture
Depositions in controlled landfills	Disposal of spent cadmium-containing products
	Non-cadmium containing products, which may contain cadmium impurities
	Naturally-occurring wastes

2.3.2 Cadmium applications

The ICdA (2009) stated that cadmium metal and its compounds are mainly used in rechargeable nickel-cadmium batteries because of its wide variety of unique properties. They can be also used as in pigments, stabilizers, coatings, specialty alloys, and electronic compounds. However, due to improvements to the production technology, usage, and disposal of products containing cadmium, cadmium in the environment reached a peak in the 1960s and has been constantly decreased.

2.3.3 Cadmium in the environment

Piotrowski and Coleman (1980), the ICdA (2009), and the PCD (1998) amassed the cadmium concentrations in several instances as shown in Table 2-3. In addition, the ICdA (2009) concluded that the mobility of cadmium to air is greater than it is to water and soil, while its mobility to soil is much less than it is to both air and water.

Table 2-3 Total cadmium concentration in various instances

Instances	Cadmium concentration	Unit
Atmosphere		
• Ambient air in rural areas [2]	0.1-5	ng/m^3
• Ambient air in rural areas [3]	0.1-43	ng/m^3
• Ambient air in urban areas [2]	2-15	ng/m^3
• Ambient air in urban areas [3]	2-700	ng/m^3
• Ambient air in industrialized areas [2]	15-150	ng/m^3
• Ambient air in rural area of industrialized countries [1]	0.1-20	ng/m^3
• Ambient air near stack [3]	10-5,000	ng/m^3
Foodstuffs		
• Cereals (e.g. wheat, rice) [1]	< 0.1	µg/g
• Rice crops from cadmium contaminated fields in Japan (1950s to 1960s) [2]	200-2,000	ppb
• Leafy vegetables (e.g. lettuce, spinach) [2]	30-150	ng/g
• Certain staples (e.g. potatoes, grain foods) [2]	30-150	ng/g
• Meat and Fish [2]	5-40	ng/g
• Animal offal (e.g. kidney, liver) [2]	> 1,000	ng/g
• Other food items [1]	< 0.05	µg/g
Materials		
• Raw materials for iron and steel production [2]	0.1-5.0	µg/g
• Raw materials for cement production [2]	2.0	µg/g
• Fossil fuels [2]	0.5-1.5	µg/g
• Phosphate fertilizers [2]	10-200	µg/g
• Marine phosphates and phosphorites [2]	~500	µg/g
• Cigarette [2]	0.5-2	µg/cigarette
• Inhaled tobacco smoke [2]	0.05-0.2	µg/cigarette

Instances	**Cadmium concentration**	**Unit**
Soil		
- Earth's crust [2]	0.1-0.5	µg/g
- Igneous rock [2]	0.02-0.2	µg/g
- Metamorphic rock [2]	0.02-0.2	µg/g
- Sedimentary rock [2]	0.1-25	µg/g
- Zinc ores [2]	200-14,000	µg/g
- Lead ores [2]	500	µg/g
- Copper ores [2]	500	µg/g
- Non-polluted agricultural soil [1]	0.01-0.7	µg/g
- Near smeltery [1]	300	µg/g
Water		
- Freshwater [1]	< 1	µg/L
- Freshwater [2]	< 0.1	µg/g
- Water in mining areas [1]	< 10	µg/L
- Sea-water [2]	~0.1	µg/L
- Mediterranean sea water [1]	0.02-1.9	µg/L
- Oceans (low concentration) [2]	< 20	ng/L
- Oceans (high concentration) [2]	20-110	ng/L
- Rainwater, fresh waters, and surface waters in urban and industrialized areas [2]	10-4,000	ng/L
Particles		
- Sediment in lakes and streams [2]	0.2-0.9	µg/g
- Marine sediment [2]	~1	µg/L
- Suspended particulates (High cadmium contamination) [1]	≤ 700	µg/L

[1] Piotrowski and Coleman (1980)
[2] ICdA (2009)
[3] PCD (1998)

1) Air

Cadmium from occupational environments and from cigarette smoke is directly transferred to humans. Cadmium in ambient air is generally deposited onto waters or soils (the deposition rates of cadmium are shown in Table 2-4), then transferred to plants and animals, and finally it enters the human body through the food chain (ICdA, 2009; Friberg *et al.*, 1976; Piotrowski and Coleman, 1980; and Liu *et al.*, 2007).

Table 2-4 Deposition rates of cadmium in different locations
(Piotrowski and Coleman, 1980)

Location	**The deposition rate ($\mu g/m^2$/month)**
Urban areas	40-400
Surrounding factories that emit cadmium	40,000
10 km from the factories	Up to 700

2) Water

Piotrowski and Coleman (1980) referred to the capability of cadmium dissolving in water as dependent on pH, while the ability of plants to uptake cadmium from soil is different. Additionally, rivers can transport cadmium for considerable distances, up to 50 km, from the source (ICdA, 2009).

3) Soil

Most cadmium emissions, around 80% to 90%, eventually return to soil because of deposition from both air and water. The major factors that identify cadmium speciation, adsorption, and distribution in soils are listed as the pH, soluble organic matter content, hydrous metal oxide content, clay content and type, presence of organic and inorganic, and competition from other metal ions. Most of the cadmium in soil is bounded to the non-exchangeable fraction, so its mobility and transfer into the food chain of animals and humans is rather limited (ICdA, 2009).

4) Plants and foodstuffs

The pathways that plants and foodstuff can uptake cadmium consist of natural soil cadmium, irrigation water, atmosphere, phosphorus containing fertilizers, as well as manures and organic wastes (Central Pollution Control Board, 2007). In addition, Piotrowski and Coleman (1980) determined that the average cadmium ratios of plant to soil are between 0.5 to 2. Some grasses, wheat, lettuce, and tobacco can notably uptake cadmium. Cadmium concentration in rice that is grown in highly contaminated soil exceeds the natural level in rice by 10-15 times. Furthermore, Friberg *et al.* (1976) also mentioned that rice and wheat are two important foodstuffs that are able to take up cadmium from soil, while wheat grains accumulate more cadmium than rice does. When the cadmium concentration in soil is above 10 mg/kg, the yields of both rice and wheat are less.

Cadmium accumulates in the kernel core of grains such as wheat and rice, while zinc is found mostly in the germ and bran coverings. The absorption rate of cadmium is approximately 20% and it is not easily eliminated (Haas, 2003).

5) Human

The ATSDR (2008: online) described the Minimal Risk Level (MRL) as the acceptable daily human exposure to a substance over a specified duration of exposure. MRLs are based on health effects of noncancerous but not consider carcinogenic effects. The MRLs of cadmium are shown in Table 2-5.

Table 2-5 ATSDR Minimal Risk Levels (MRLs) (ATSDR, 2008)

Route	Duration	MRL	Unit	Endpoint
Inhalation	Acute	0.00003	mg/m^3	Respiratory
Inhalation	Chronic	0.00001	mg/m^3	Renal
Oral	Intermediate	0.0005	mg/kg/day	Musculoskeletal
Oral	Chronic	0.0001	mg/kg/day	Renal

The ICdA (2009) declared that smoking tobacco is the primary source of air cadmium exposure for smokers and 10% of the cadmium content in cigarettes is inhaled when smoking, while Haas (2003) stated that about 30% of cadmium in cigarettes is absorbed into lungs while the remaining 70% goes into the atmosphere to be inhaled by others or to contaminate the environment. Moreover, the major route of cadmium intake for non-smokers is ingestion through food or water (approximately 95%), rather than from inhalation and dermal exposure of cadmium in air. This is largely due to the presence of trace amounts of cadmium in foodstuffs of natural origin or the use of phosphate fertilizers or sludge on agricultural soils.

Haas (2003) states that no cadmium was present in newborns because cadmium could not pass into the fetus during pregnancy or the breast milk with lactation. However, the tendency of cadmium levels in human increases with age and usually peaks around 50 years of age and it may cause chronic toxicity. Humans probably consume at least 40 µg/day, which is mainly by ingestion from terrestrial foods that uptake cadmium from soil, but average cadmium ingestion for non-smokers living in an uncontaminated area, estimated by the ICdA (2009), ranges from 10 to 25 µg/day, depending on the function of the type of food crop grown, agricultural practices pursued, and atmospheric deposition of cadmium onto the exposed plant parts.

Additionally, Haas (2003) also suggested two ways to limit cadmium toxicity. The first is to avoid cadmium exposure and intake from the mentioned sources in Table 2-1. The second way is to maintain good zinc levels by eating high-zinc foods, such as whole grains, legumes, and nuts. Taking additional zinc, such as 15-30 mg a day in a supplement, could offer more protection against cadmium toxicity.

2.4 Cadmium in Thailand

In the Hazardous Substances Acts of B.E. 2535 (1992), cadmium is classified in the third category of hazardous substances. The owners of the hazard substances that are produced, imported, exported, or acquired have to gain permission from the Department of Industrial Works. The standards of cadmium concentrations in the environment are shown in Table 2-6.

Table 2-6 Cadmium concentrations in Air, Water, and Soil Quality Standards under Thai environmental regulations

Circumstances	Cadmium Standard Value	Unit
Air emission [2]	1	mg/m^3
Dust in working area [2]	0.2	mg/m^3
Dust in working area (maximum allowance) [2]	0.6	mg/m^3
Fume in working area [2]	0.1	mg/m^3
Fume in working area (maximum allowance) [2]	3	mg/m^3
Emission Standard for Infected Waste Incinerator [1]	0.05	mg/m^3
Surface Water Quality Standards		
• Hardness $\leq$ 100 mg/L of $CaCO_3$ [1], [2]	5	mg/m^3
• Hardness > 100 mg/L of $CaCO_3$ [1], [2]	50	mg/m^3
Coastal Water Quality Standards [1]	5	mg/m^3
Groundwater Quality Standards [1]	3	mg/m^3
Ground Water Quality Standards for Drinking Purposes [1]	0-10	mg/m^3
Drinking Water Quality Standards [1], [2]	0-10	mg/m^3
Bottled Drinking Water Quality Standard [1]	5	mg/m^3
Appropriated Water Quality Criteria for Aquatic Living [1]	1	mg/m^3
Industrial Effluent Standards [1], [2]	30	mg/m^3
Zinc Smeltery Effluent Standards [2]	100	mg/m^3
Water Characteristics Discharged into Irrigation System [1]	30	mg/m^3
Water Characteristics Discharged into Deep Wells [1]	100	mg/m^3
Soil Quality Standards for Habitat and Agriculture [1]	37	mg/kg
Soil Quality Standards for Other Purposes [1]	810	mg/kg

[1] www.pcd.go.th
[2] PCD (1998)

2.5 Cadmium in Mae Sot district

A 2006 DPIM study found high cadmium contamination in soil and rice grain in Phatat Pha Daeng and Mae Tao Mai sub-districts, Mae Sot district, Tak province. Simmons *et al.* (2009) further explains that the dominant agricultural products in the area are paddy rice and soybean. Irrigation water for over 3000 hectares of the agricultural area is from Mae Tao Creek, which passes through a zinc deposit zone. The cadmium concentration of the soil in the study area was found to be from 0.5 to 280 mg/kg, while the normal Thai background concentrations are between 0.002 to 0.141 mg/kg. Therefore, the Thai Investigation Level for cadmium is 0.15 mg/kg (Zarcinas *et al.*, 2003). The results of the measured parameters in the contaminated areas in Mae Sot, Tak are shown in Table 2-7.

Table 2-7 Measured parameters of the contaminated area in Mae Sot (Simmons *et al.*, 2009)

Parameters	The measured values	Unit
Soil pH	5.4 to 7.68	-
Organic carbon remaining	1.86 ± 0.0168	%
Clay content	15.5 to 46.8	%
DTPA-extractable cadmium concentration	0.494 to 31.92	mg/kg

Anan Paengnoy (2004) refers to the study of the IWMI in the Mae Tao subcatchment, Mae Sot district. Cadmium was found in both soil and rice as shown in Table 2-8, which also compare the levels to those of the European safety standard. 106 tons (8.98%) of local rice contained less than 0.2 mg/kg of cadmium, 944 tons (80%) contained between 0.2 to 2.0 mg/kg of cadmium, and another 130 tons (11.02%) contained more than 2.0 mg/kg of cadmium. Moreover, cadmium has been found not only in local rice, but also in local garlic and soybean.

Table 2-8 Cadmium concentrations in the environment from a study by the IWMI (2003) compared with the European safety standard (Anan Paengnoy, 2004)

	Cadmium concentration from the study (mg/kg)	**European safety standard** (mg/kg)
Soil	3.4 – 284	3
Rice	0.1 – 4.4	0.2

Parada Maneewong (2005) studied the cadmium distribution in stream sediment and suspended sediment along Mae Tao Creek, Mae Ku Creek, and Nong Khieo Creek. Water, suspended sediment, and stream sediment were collected to measure the total concentration of cadmium and zinc for calculating their relationships in the media.

In the study, cadmium and zinc in the sampled water could not be detected by ICP, while DWR proved that the cadmium level of stream water in the area was also lower than the standard level. The results meant that the cadmium and zinc in this case were not in soluble forms. Cadmium and zinc were not mobile and could not get distributed away from the source by water movement. In addition, the mostly neutral to slightly high pH of the water, 7-8.5, was what caused them to exist in their insoluble forms.

Suspended solids and stream sediments were also collected and measured for their total cadmium and zinc concentrations by microwave and ICP-OES following the EPA standard method. The highest cadmium concentration of both suspended solids and sediment were discovered at Mae Tao Creek, whereas the maximum concentration of zinc was found at both Mae Tao Creek and Mae Ku creek, as shown in Table 2-9.

Table 2-9 Average total concentrations of cadmium and zinc and their ratios in both the suspended sediment and stream sediment of Mae Tao Creek, Mae Ku Creek, and Nong Khieo Creek (Parada Maneewong, 2005)

Creek	**Total Cd concentration (mg/kg)**	**Total Zn concentration (mg/kg)**	**Average ratio of Cd:Zn**
Suspended sediment			
Mae Tao	18.27	7,767.14	0.0023
Mae Ku	7.75	7,722.99	0.001
Nong Khieo	6.32	6,232.97	0.01
Stream sediment			
Mae Tao	37.11 ± 0.33	1,231.47 ± 10.76	0.03
Mae Ku	7.99 ± 0.01	316.55 ± 3.66	0.025
Nong Khieo	5.67 ± 0.10	63.08 ± 0.84	0.09

In addition, the relationships between the cadmium and zinc concentrations of the creeks were also concluded as the lower equations:

Mae Tao Creek: $Cd = 0.0314\,(Zn)$ $R^2 = 0.7597$
Mae Ku Creek: $Cd = 0.0227\,(Zn)$ $R^2 = 0.0772$
Nong Khieo Creek: $Cd = 0.0841\,(Zn)$ $R^2 = 0.7832$

2.6 Model Selection

Cunderlik (2003) summarized and compared many hydrological models to provide the information for selecting a suitable model for a variety of tasks and projects. The hydrological models can be classified into three main categories:

2.6.1 Lumped models

The parameters of these models do not vary spatially within the basin. The basin's response is evaluated only at the outlet, without obvious accounting for the response of individual sub-basins. These models are suitable for the primary prediction in the discharge. Examples of lumped models are IHACRES, SRM, and WATBAL.

2.6.2 Semi-distributed models

The parameters of these models are only partially allowed to vary in space, so the basin is divided into smaller sub-basins. Examples of these models include HBV-96, HEC-HMS, HFAM, HSPF, PRMS, SSARR, SWAT, SWMM, and TOPMODEL.

2.6.3 Distributed models

A distributed model's parameters are fully allowed to vary in space. Some preferable distributed models are CASC2D, CEQUEAU, GAWSER/GRIFFS, HYDROTEL, MIKE11/SHE, and WATFLOOD. These models can provide the highest degree of accuracy, but they require large amounts of data to perform simulations.

There are four main model selection criteria that modelers use to select a suitable model for their projects: the required model outputs, which are the importance of projects; hydrological processes, which are considered to estimate the desired outputs adequately; the availability of input data; and the price limitations of the project (Cunderlik, 2003).

Ali *et al.* (2008) summarized a comparison of different hydrological models as shown in Table 2-10.

Table 2-10 **Comparison of different hydrological models** (adapted from Ali *et al.*, slide)

Models	**Hydrological Processes**						
	Surface Water	**Unsaturated Flow**	**Groundwater Flow**	**Irrigation**	**Drainage**	**River/Lake**	**Flooding**
MODFLOW			✓				
Hydrus 2D		✓	✓				
E2		✓	✓				
CROPWAT (FOA)				✓			
SWIM	✓						
RAFTXP	✓						
USS	✓				✓		
ROB	✓						
CATCHSIM	✓		✓				
MIKE 11	✓			✓		✓	
MIKE 21	✓					✓	✓
MIKE FLOOD	✓			✓		✓	✓
MIKE SHE	✓	✓	✓	✓	✓	✓	✓

2.7 MIKE SHE and MIKE 11 models

The software selected for modeling the results in this research include MIKE SHE and MIKE 11, which have been developed by DHI Water • Environment • Health (DHI).

2.7.1 MIKE SHE

MIKE SHE, a physically based and distributed parameter model, simulates the hydrological cycle as displayed in Figure 2-2. It includes the overland flow (OL), evapotranspiration (ET) , unsaturated flow (UZ), saturated flow (SZ), and channel flow (OC). Related water quality modules consist of advection-dispersion, particle tracking, sorption and degradation, geochemistry, biodegradation, crop yield, and nitrogen consumption (DHI, 2009). MIKE SHE can be used to predict pollutant loading and transport, pesticide leaching, and outcomes of alternate best management practices (BMPs) on watersheds and their underlying aquifers. Therefore, MIKE SHE requires extensive model data and physical parameters (Yan and Zhang, 1999).

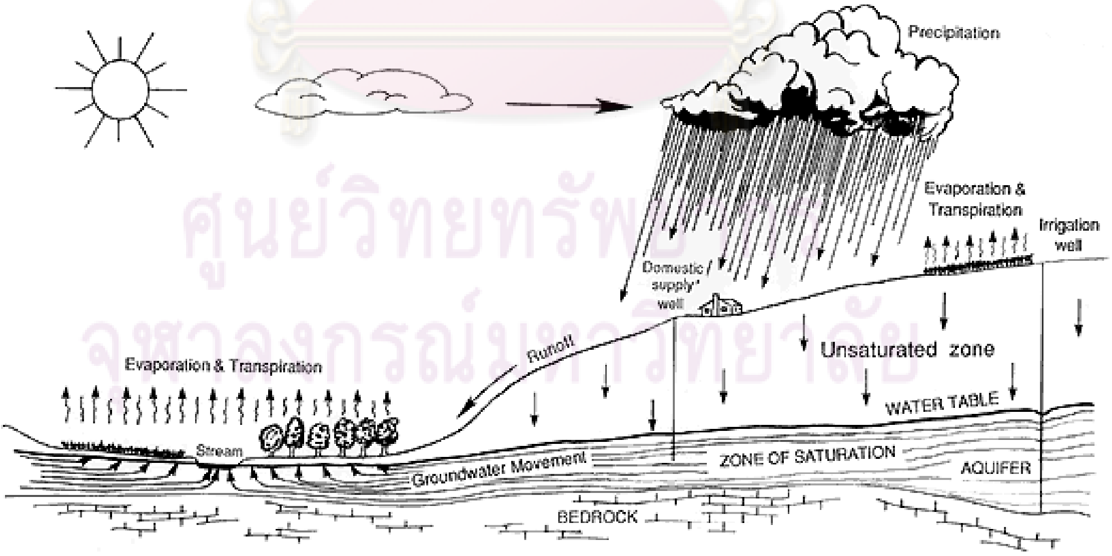

Figure 2-2 Hydrologic cycle (Kranz *et al.*, 1996)

Refsgaard and Kjelds (2001) selected MIKE SHE is the best tool to model groundwater-surface water related issues. MIKE SHE is able to provide the best and most comprehensive description of the surface water-groundwater interaction with a full dynamic coupled description of the relevant hydrological processes.

2.7.2 MIKE 11

MIKE 11 is a one-dimensional dynamic modeling tool for simulating phenomena in rivers, lakes, reservoirs, irrigation canals, and other inland water systems. The modules of MIKE 11 are shown in Figure 2-3; the hydrodynamic (HD) module is the core module of the model. Advection-dispersion (AD), sediment transport (ST), water quality (ECO Lab), and rainfall-runoff (RR) are examples of the included add-on modules. (DHI, 2009).

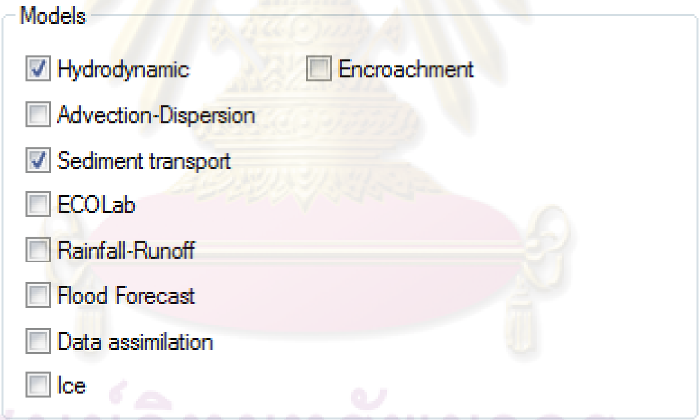

Models

☑ Hydrodynamic
☐ Advection-Dispersion
☑ Sediment transport
☐ ECOLab
☐ Rainfall-Runoff
☐ Flood Forecast
☐ Data assimilation
☐ Ice
☐ Encroachment

Figure 2-3 **The modules in MIKE 11.**

The hydrodynamic module (HD) contains an implicit, finite difference computation of unsteady flows in rivers. The module can describe both subcritical and supercritical flow conditions through a numerical scheme that adapts according to the local flow conditions (in time and space). The formulations could be applied to looped networks and quasi two-dimensional flow simulations on flood plains. The computational scheme is applicable for vertically homogeneous flow conditions ranging from steep river flows to tidal influenced estuaries.

The complete nonlinear equations of open channel flow (Saint Venant) can be solved numerically between all grid points at specified time intervals for given boundary conditions. Advanced computational modules could be used to describe flow over hydraulic structures such as broad-crested weirs, culverts, bridges, pumps, regulating structures, control structures, and dam-break structures.

There are two main modules for simulating sediment transport in channel system including advection-dispersion module (AD); which is suitable for cohesive sediment, such as, silts and clays; as well as sediment transport module (ST); which is appropriate for non-cohesive sediment namely gravels and sands.

The erosion, deposition, and transport of non-cohesive sediment module was applied in this research because of physical property of stream sediment was classified as mainly sand in the study area.

The Meyer-Peter and Muller model was selected to describe the stream sediment or bed load transport since this model could be used to focus on the stream sediment.

2.8 Unified Soil Classification System (USCS)

The Unified Soil Classification System (USCS), as displayed in Table 2-11, is a soil classification system widely applied in engineering fields to describe the texture and grain size of particles by analyzing the laboratory results of the grain size distribution and plasticity properties. The USCS is represented by a two letter symbol as stated below: (ASTM D2487)

Prefix:

- G = Gravel
- S = Sand
- M = Inorganic Silt
- C = Inorganic Clay
- O = Organic Silt or Clay

- Pt = Peat

Suffix:

- W = Well Graded
- P = Poorly Graded
- M = Silt
- C = Clay
- H = High plasticity; Liquid Limit > 50%
- L = Low plasticity; Liquid Limit ≤ 50%

Table 2-11 Unified Soil Classification System (USCS) (from ASTM D2487)

Major Divisions			**Group Symbol**	**Typical Names**
Coarse-Grained Soils More than 50% retained on the 0.075 mm (No. 200) sieve	**Gravels** 50% or more of coarse fraction retained on the 4.75 mm (No. 4) sieve	Clean Gravels	GW	Well-graded gravels and gravel-sand mixtures, little or no fines
			GP	Poorly graded gravels and gravel-sand mixtures, little or no fines
		Gravels with Fines	GM	Silty gravels, gravel-sand-silt mixtures
			GC	Clayey gravels, gravel-sand-clay mixtures
	Sands 50% or more of coarse fraction passes the 4.75 mm (No. 4) sieve	Clean Sands	SW	Well-graded sands and gravelly sands, little or no fines
			SP	Poorly graded sands and gravelly sands, little or no fines
		Sands with Fines	SM	Silty sands, sand-silt mixtures
			SC	Clayey sands, sand-clay mixtures
Fine-Grained Soils More than 50% passes the 0.075 mm (No. 200) sieve	**Silts and Clays** Liquid Limit 50% or less		ML	Inorganic silts, very fine sands, rock four, silty or clayey fine sands
			CL	Inorganic clays of low to medium plasticity, ravelly/sandy/silty/lean clays
			OL	Organic silts and organic silty clays of low plasticity
	Silts and Clays Liquid Limit greater than 50%		MH	Inorganic silts, micaceous or diatomaceous fine sands or silts, elastic silts
			CH	Inorganic clays or high plasticity, fat clays
			OH	Organic clays of medium to high plasticity
Highly Organic Soils			PT	Peat, muck, and other highly organic soils

CHAPTER III

METHODOLOGY

3.1 Data collection

The required data, input, were collected from many government departments, for example, the Department of Groundwater Resources (DGR), Department of Water Resources (DWR), Land Development Department (LDD), Royal Thai Survey Department (RTSD) and Thai Meteorological Department (TMD).

3.1.1 Topography

Mae Tao subcatchment is in the map sheet 4742III of series L7018, edition 1-RTSD with a scale of 1:50,000 as shown in Figure B-1, Appendix B. Elevation in the study area ranges from 220 to 950 m. The topography input is shown in Figure 3-1.

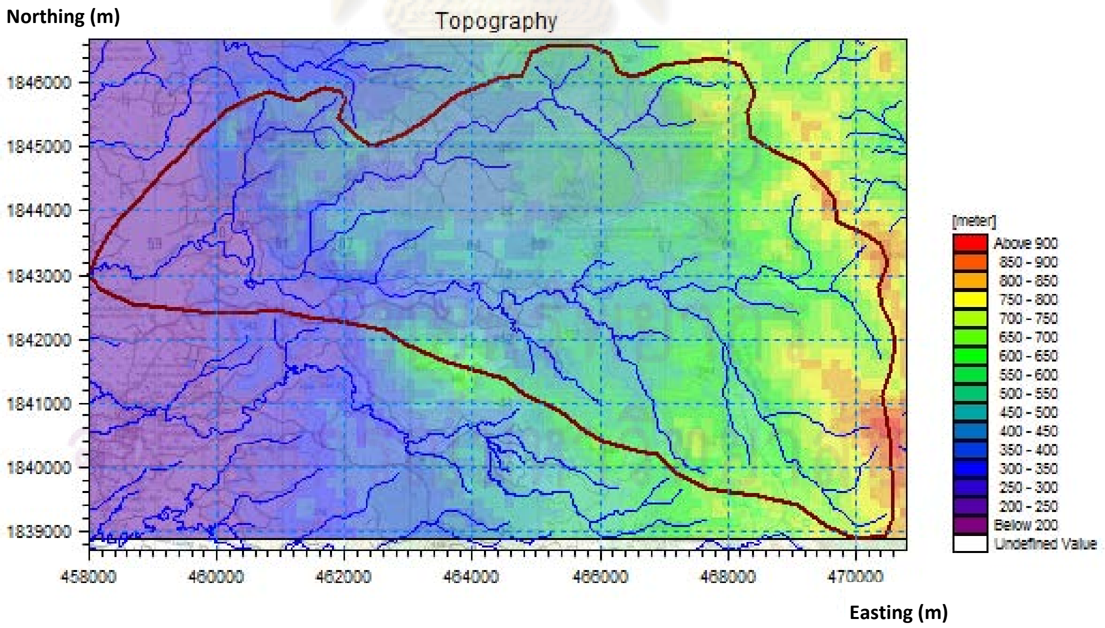

Figure 3-1 The topography of the study area

3.1.2 Meteorological data

The rainfall rate data in year 2009 (shown in Table B-1 and Figure B-2, Appendix B) and the evaporation rate data in year 2009 (displayed in Table B-2 and Figure B-3, Appendix B) were measured and collected at the Mae Sot station, TMD. Some of the significant annual rainfall and evaporation rate data for 2009 are provided in Table 3-1 and Table 3-2.

Table 3-1 Significant rainfall rate data in year 2009 at Mae Sot station, TMD

Data	**Rainfall rate** (mm/d)	**Remark**
The average rainfall rate	4.4	
The maximum rainfall rate	92.7	At 25th Sep 2009

Table 3-2 Significant evaporation rate data in year 2009 at Mae Sot station, TMD

Data	**Evaporation rate** (mm/d)	**Remark**
The average evaporation rate	4.3	
The maximum evaporation rate	9.8	On 16th Apr 2009
The minimum evaporation rate	1.2	On 9th Jun 2009

3.1.3 Saturated zone data

Average groundwater table in the study area was approximately 3.14 m lower than ground surface (DGR).

The properties of the saturated zone are displayed in Table 3-3.

Table 3-3 Properties of the saturated zone in the area

Properties of the saturated zone	**Value**	**Reference**
Horizontal hydraulic conductivity	10^{-11} - 10^{-8} m/s	Schnoor, 1996
Vertical hydraulic conductivity	10^{-13} - 10^{-7} m/s	Brassington, 1988
Specific yield	0% - 5%	Johnson, 1967
Specific storage	9.19×10^{-2} - 2×10^{-2} 1/m	Anderson and Woessner, 1972

3.1.3 Unsaturated zone data

The dominant ground surface soil in the area is peat. The properties of peat are displayed in Table 3-4.

Table 3-4 Properties of the unsaturated zone in the area

Properties of peat	**Value**	**Reference**
Hydraulic conductivity	10^{-4} - 10^{-5} m/s	Bear, 1972
Bulk density	≈ 1,600 kg/m^3	Scheffer and Blankenburg, 1993

3.2 Field observation

The 10 stations along Mae Tao Creek placed at upstream locations, junctions, and the outlet of the subcatchment were situated as presented in Figure 3-2. Each station was positioned by a handheld GPS with accuracy of ± 4 meters as shown in Table 3-5. The observation at every station included flow measurement including flow depth, channel width, cross-section area, velocity of water, and flow discharge; water characteristics namely pH of water, dissolved oxygen (DO), conductivity of water (*EC*), and water temperature (*T*); and also stream sediment properties consisted of cadmium concentration in the sediment and grain size distribution.

Table 3-5 **Position of the 10 observation stations along Mae Tao Creek.**

Station	**Northing** (m)	**Easting** (m)
1	1843017	457998
2	1843330	459400
3	1843034	461274
4	1843110	461376
5	1843286	461438
6	1842870	462046
7	1842718	465638
8	1842750	466937
9	1842559	467228
10	1842736	467088

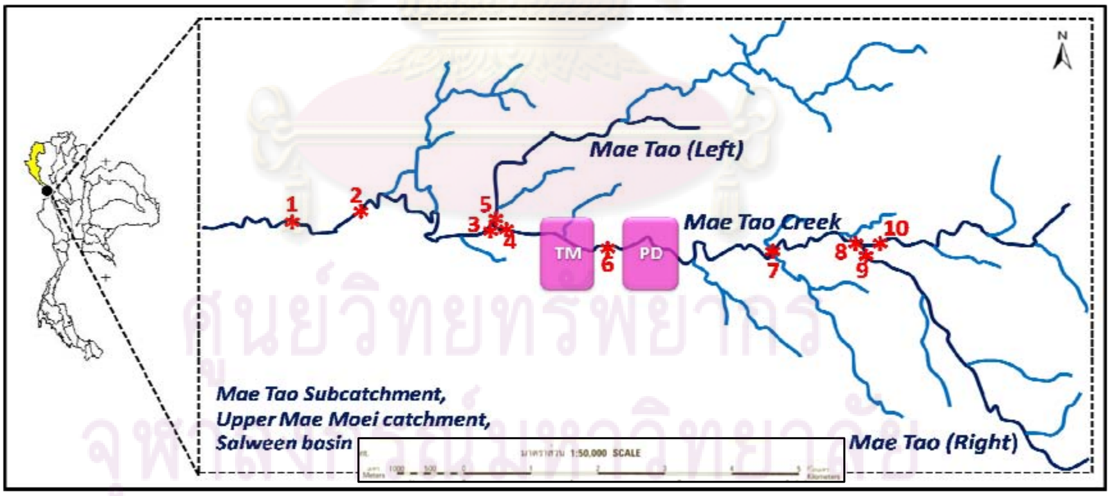

Figure 3-2 **Map of Mae Tao Creek and the locations of the 10 marked stations**

3.2.1 Flow measurement

The discharge of stream can be defined by measuring the volume of the water that flows through a cross-section within a period of time. The area-velocity method is the recommended method for calculating stream flow.

The area-velocity method measures the velocity of water (*V*) and cross-section area (*A*) by dividing the area into many sections with constant intervals, as shown in Figure 3-3. The wide interval (*W*) depends on the width of the cross-section and surveying time. (Keerati Leewatchanakul, 1994) ???

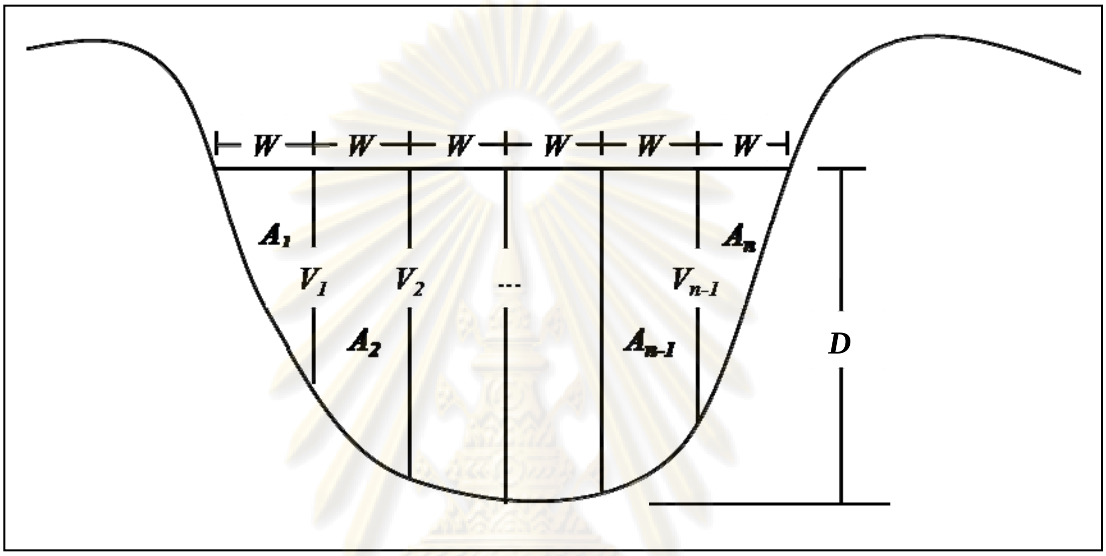

Figure 3-3 The area-velocity method

A) Instruments

The following instruments were used:

- A propeller type current meter
- An automatic leveler
- 3-4 m staff gauges
- Measuring tape
- Pegs

B) Methods

Velocity measurement

After dividing a cross-section into many sections, the water depth of a section was evaluated. Table 3-6 was used to select a measuring level and mean velocity equation based on the water depth at each measuring point. A propeller current meter was set at the particular measuring level of each section. The velocities of the measuring points were recorded for calculating the mean velocity of the section by following the equation in Table 3-6. The average velocity of each section was applied to determine the transport rate of the section by applying Eq. (3.6).

Table 3-6 **Relationship between the depth of water, the velocity measuring level, and the mean velocity of the section.** (Keerati Leewatchanakul, 1994)

Depth of water at each measuring point (m)	**Measuring level from water surface** (m)	**Mean velocity in the section** (m/s)
< 0.60	0.6*D*	$V_{0.6D}$ (3.1)
0.60 – 3.05	0.2*D* and 0.8*D*	$\frac{V_{0.2D} + V_{0.8D}}{2}$ (3.2)
3.05 – 6.10	0.2*D*, 0.6*D* and 0.8*D*	$\frac{V_{0.2D} + 2V_{0.6D} + V_{0.8D}}{4}$ (3.3)
> 6.10	surface, 0.2*D*, 0.6*D*, 0.8*D*, and bottom	$\frac{V_S + 3V_{0.2D} + 2V_{0.6D} + 3V_{0.8D} + V_B}{10}$ (3.4)

D = flow depth (m)
V_B = water velocity at 0.3 m higher than bottom (m/s)
V_S = water velocity at 0.3 m lower than surface (m/s)
$V_{0.2D}$ = water velocity at 0.2 times depth from water surface (m/s)
$V_{0.6D}$ = water velocity at 0.6 times depth from water surface (m/s)
$V_{0.8D}$ = water velocity at 0.8 times depth from water surface (m/s)

Cross-section surveying method

Cross-section surveying is a type of hydrological surveying that is used for acquiring the physical data of a stream. The cross-section area is widely used for many applications such as stream changing analysis and hydraulic design.

The surveying of cross-section areas started at a known leveling point, like a benchmark (BM) or staff gauge. The depth of each section was measured at the measuring point for computing each section area before combining the areas of all sections for determining and plotting the cross-section area. Thus, the water discharge rate of the cross-section was calculated by using the following equations:

$$A = A_1 + A_2 + A_3 + \dots + A_n \tag{3.5}$$

$$Q = A_1 V_1 + A_2 V_2 + A_3 V_3 + \dots + A_n V_n \tag{3.6}$$

$$V_{av} = \frac{Q}{A} \tag{3.7}$$

where

A = total cross-section area (m^2)
A_i = area of section i (m^2)
V_i = water velocity of section i (m/s)
V_{av} = average velocity of the cross-section (m/s)
Q = water discharge (m^3/s)

3.2.2 Field measurement and sediment sampling

Both water and sediment at each station were sampled by a random sampling method. pH, DO, conductivity, and temperature of the sampled water were measured at the site by a pH meter, DO meter, and conductivity meter. Approximately 1 kg of stream sediment at each station was sampled and taken back for further experiments.

3.3 Laboratory

3.3.1 Sample preparation

The sediment must be dehydrated before measuring the total cadmium concentration by flame atomic absorption spectroscopy and determining the particle size distribution by sieve analysis.

A) Instruments

- Trays
- Oven
- Mortar
- Pestle

B) Methods

Each sample was set in a tray. The samples were dehydrated at 85 °C for 48 hours. After that, they were aired cooled to room temperature. The dehydrated sediment was grinded before being used in both analyses.

3.3.2 Total cadmium concentration

US Environmental Protection Agency (2009) mentioned US EPA 3051A method “Microwave Assisted Acid Digestion of Sediments, Sludge, Soils, and Oils” to perform an analytical procedure that was applied for determining total cadmium concentration in this study.

A) Materials and Instruments

- 65% Nitric acid
- Hydrochloric acid
- Standard cadmium concentration
- Deionized water
- Whatman disc filter paper No. 5
- PTFE vessels and covers
- Volumetric flasks

- FLAAS sample vessels
- Polyethylene bottles
- Sieve No. 65
- Weighing apparatus
- Microwave
- Flame atomic absorption spectroscopy (FLAAS)

B) Methods

Digestion

The dehydrated sediment of each station was put through a selected sieve (65-mesh sieve). Approximately 0.5 g (± 0.01 g) of the sifted sediment was weighted and placed in each PTFE vessel. Then 9 ml of 65% nitric acid and 3 ml of hydrochloric acid was mixed with the sediment. After covering the containers, the vessels were placed into a microwave system. The samples were heated up to 175 °C (± 5 °C) for 5.5 min (± 0.25 min), remained at 175 °C (± 5 °C) for 4.5 min, and then cooled down to room temperature. Each cooled sample was filtered into a volumetric flask by using Whatman disc filter paper No. 5. The filtered samples were diluted to adjust the volume to 50 ml before being placed into polyethylene bottles.

Flame Atomic Absorption Spectroscopy

The flame atomic absorption spectroscope (FLAAS) was set and calibrated by following the manual instructions to measure the total cadmium concentration. All prepared samples were decanted into sample vessels, each of which was put into a compartment of the instrument. The standard cadmium concentration and deionized water were inserted between each of the 10 samples to check and clean it in order to get trustworthy data. The FLAAS was turned on to measure the cadmium concentration of each station. After the FLASS finished measuring, the obtained data were placed in an excel file to calculate the cadmium concentration in the sediment.

3.3.3 Grain size distribution

The grain size distribution method was adapted from ASTM C136-06, the "Standard Test Method for Sieve Analysis of Fine and Coarse Aggregates" and ASTM D422-63, the "Standard Test Method for Particle-Size Analysis of Soils".

1) Instruments

- Sieves (No. 3/4", 3/8", 4, 10, 20, 35, 65, 100, 150 and 200)
- Automatic shaker
- Weighing apparatus
- Cleaning implements

2) Method

After being dehydrated and grinded up, the sample sediment from each station was weighed. Each selected sieve (No. 3/4", 3/8", 4, 10, 20, 35, 65, 100, 150 and 200) was also weighed. The sieves were ranked by the mesh number. A sieve receiver was placed onto the automatic shaker. The smallest mesh (mesh no. 200) was at the bottom. The sieves were stacked from smallest to largest mesh. The sample was filled to the top of the sieve set before being covered with a sieve lid. The automatic shaker was turned on and shaken for around 30 minutes. Each sieve and retained sediment sample was then weighed. The total weight of sediment after sieving was checked by comparing with the total weight of the sample before sieving. If they differed by more than 2%, the experiment was repeated because loss of sediment was too high. Moreover, if the sample passing sieve No. 200 was more than 10%, hydrometer analysis was performed to acquire more accurate results.

3) Data Analysis

The retained weight of the sediment, percent passing, percent retained, cumulative percent retained were calculated using the following equations:

- Percent Retained

$$\text{Percent Retained} = \frac{\text{Weight of retained sample on each sieve}}{\text{Weight of total sample}} \times 100\% \qquad (3.8)$$

- Cumulative Percent Retained

$$\text{Cumulative percent retained} = \sum(\text{Percent retained of all larger mesh sieves}) \quad (3.9)$$

- Percent Passing

$$\text{Percent Passing} = \frac{\text{Weight of passed sample of each sieve}}{\text{Weight of total sample}} \times 100\% \qquad (3.10)$$

or

$$\text{Percent Passing} = 100\% - \text{Cumulative percent retained of that sieve mesh} \quad (3.11)$$

3.3.4 Soil Classification

The type of collected sediment at each station was classified by the Unified Soil Classification System (USCS) (ASTM D2487). Each sample was classified as coarse-grained soil or fine-grained soil using sieve No. 200. If the percent of the sample passing sieve No. 200 was less than 50%, the sample was classified as having coarse-grained particles, including gravel (G) or sand (S). If the percent of the sample passing sieve No. 200 was greater than 50%, the sample was classified as having fine-grained particles, namely inorganic silt (M), inorganic clay (C), organic silt or clay (O), or peat (Pt). The coarse-grained particles were classified by the coarse fraction (CF), which is the ratio determined by the following equation.

$$\text{CF} = \frac{\text{C}}{\text{F}} = \frac{\%\text{ Coarser than 4-mesh sieve}}{\%\text{ Coarser than 200-mesh sieve}} \qquad (3.12)$$

If the CF was less than 50%, the sample was classified as sand (S). If the CF was greater than 50%, the sample was classified as gravel (G).

The fine-grained particles were categorized by the plasticity chart shown in Figure 3-4, which is a plot of the plasticity index (PI) with regard to the liquid limit (LL), while the A-line was determined by the equation below.

$$\text{PI} = 0.73\,(\text{LL}-20) \qquad (3.13)$$

If the ratio between the LL and PI was under the A-line, the sample was classified as inorganic silt (M), organic silt or clay (O). If the ratio between the LL and PI was above the A-line, the sample was classified as inorganic clay (C).

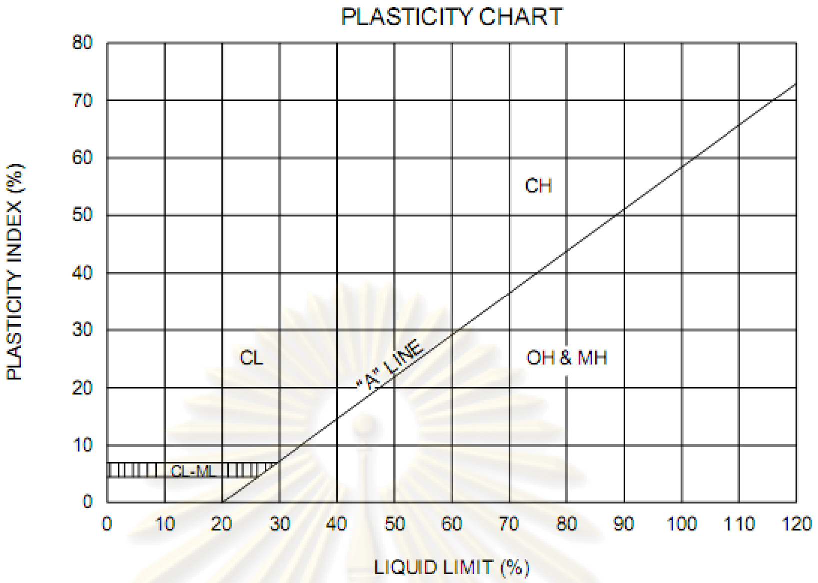

Figure 3-4 Plasticity chart and the A-line (ASTM D2487)

3.4 Simulation

Simulations in this study consisted of two steps. The hydrodynamic simulation was firstly done using MIKE SHE (with all processes) coupled with MIKE 11 (without the sediment transport module) as displayed in Figure 3-5. The coupling model was calibrated with the observed water level and discharge. Secondly, the hydrodynamic results were inputted into the MIKE 11 program (with the sediment transport module) to obtain the stream sediment transport in the creek as shown in Figure 3-6.

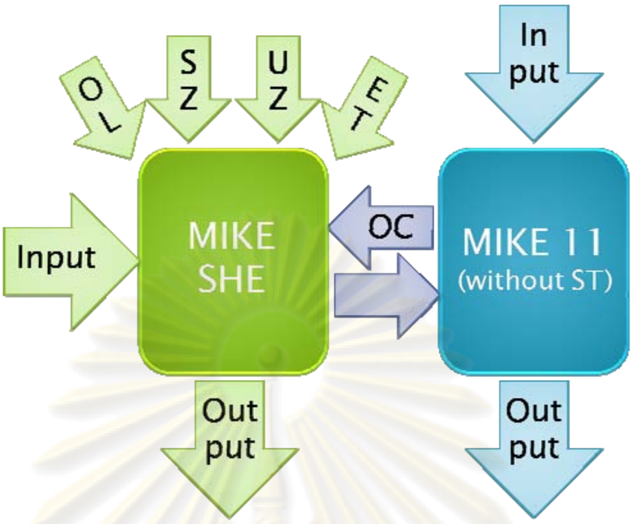

Figure 3-5 **Model setup (1st step)**

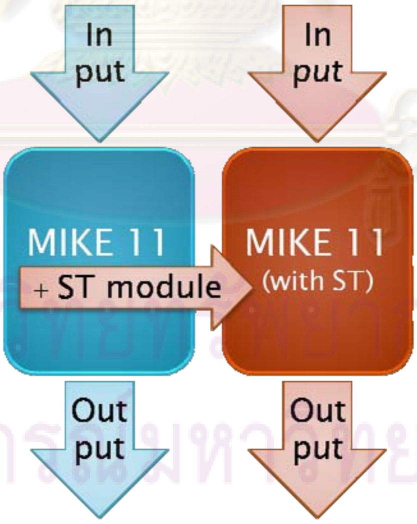

Figure 3-6 **Model setup (2nd step)**

3.4.1 MIKE SHE (DHI, 2009d, 2009e, 2009f)

1) Overland Flow (OL)

When the net precipitation rate is greater than the infiltration capacity of an unsaturated zone, water that ponds on the ground surface still contains some losses due to evaporation and infiltration. The remaining water is available as surface runoff before running downhill towards the river system. The direction and quantity of the flow in finite difference are controlled by the topography and flow resistance of the area.

The diffusive wave approximation equation applied in this research was simplified from the Saint Venant equations to reduce the complexity by ignoring lateral inflows perpendicular to the flow direction and momentum losses due to local and convective acceleration.

Equations (3.14) and (3.15) show the two-dimensional diffusive wave approximation equations that were used to simulate surface runoff. The relation between the velocities and the depths are written as follows:

$$uh = K_x \left(-\frac{\partial z}{\partial x} \right)^{\frac{1}{2}} h^{\frac{5}{3}} \qquad (3.14)$$

$$vh = K_y \left(-\frac{\partial z}{\partial y} \right)^{\frac{1}{2}} h^{\frac{5}{3}} \qquad (3.15)$$

$$z = z_g + h \qquad (3.16)$$

where

u = flow velocity in x-direction (m/s)
v = flow velocity in y-direction (m/s)
K_x = Strickler coefficient in x-direction ($m^{1/3}$)
K_y = Strickler coefficient in y-direction ($m^{1/3}$)
h = flow depth (above ground surface) (m)
z = flow depth (referred to datum) (m)
z_g = ground surface level (referred to datum) (m)

The rate of overland flow is controlled by surface roughness, so the Strickler roughness coefficient is defined as being equivalent to the Manning M. Since the values of n are typically in the range of 0.01 (smooth channels) to 0.10 (thickly vegetated channels), the Manning M value, varying from 10 (thickly vegetated channels) to 100 (smooth channels), is determined by the following equation.

$$K = M = \frac{1}{n} \tag{3.17}$$

where

M = Manning M ($m^{1/3}$)

n = Manning n ($m^{-1/3}$)

A finite-difference form of the velocity term is derived from the approximations.

$$\frac{\partial}{\partial x}(uh) \cong \frac{1}{\Delta x}[(uh)_{east} - (uh)_{west}] \tag{3.18}$$

$$\frac{\partial}{\partial y}(vh) \cong \frac{1}{\Delta y}[(vh)_{north} - (vh)_{south}] \tag{3.19}$$

where

$(uh)_{east}$ = discharge per unit length across the eastern boundary (m^2/s)

$(uh)_{west}$ = discharge per unit length across the western boundary (m^2/s)

$(vh)_{north}$ = discharge per unit length across the northern boundary (m^2/s)

$(vh)_{south}$ = discharge per unit length across the northern boundary (m^2/s)

Δx = side of length in x-direction (m)

Δy = side of length in y-direction (m)

Equation (3.20), adapted from Eq. (3.14) and (3.15), was applied to estimate the flow between grid squares as well as the flow across open boundaries at the edge of the model is calculated with the following equation, using the specified boundary water level.

$$Q = \frac{K\,\Delta x}{\Delta x^{\frac{1}{2}}} (Z_U - Z_D)^{\frac{1}{2}} \, h_u^{\frac{5}{3}} \tag{3.20}$$

where

Q = water discharge (m^3/s)

K = appropriate Strickler coefficient and water depth (m$^{1/3}$)

Z_U = higher depth of the two water levels (referred to datum) (m)

Z_D = lower depth of the two water levels (referred to datum) (m)

h_u = depth of water that can freely flow into the next cell (m)

= actual water depth minus detention storage

Successive over-relaxation (SOR) was the numerical method selected for solving the overland flow equation. Since water balance correction plays a role in reducing the calculated flows in some situations, this equation is used to avoid an internal water balance error and divergence of the solution scheme.

$$\sum|Q_{out}| \le \sum Q_{in} + i\Delta x^2 + \frac{\Delta x^2 h(t)}{\Delta t} \tag{3.21}$$

where

$\sum Q_{out}$ = sum of outflows (m^3/s)

$\sum Q_{in}$ = sum of inflows (m^3/s)

i = net input to overland flow (net rainfall less infiltration) (m/s)

$h(t)$ = water depth (m)

Δt = time difference (s)

2) Evapotranspiration (ET)

Evapotranspiration is the largest part of the water balance. Total evapotranspiration, which could be predicted from the meteorological and vegetative data, is calculated from the interception of rainfall by a canopy, drainage from the canopy to the soil surface, evaporation from the canopy surface, evaporation from the soil surface, and uptake of water by plant roots and its transpiration based on soil moisture in the unsaturated root zone. Moreover, evapotranspiration is directly linked to runoff, infiltration, and groundwater flow.

The primary ET model used is based on empirically derived equations that follow the work of Kristensen and Jensen (1975).

(A) Canopy Interception

Interception is defined as the process whereby precipitation is retained on vegetation. This intercepted water directly evaporates. The interception storage capacity (I_{max}) relies on type of vegetation and its stage of development, which are characterized by the leaf area index (LAI).

$$I_{max} = C_{int} \cdot LAI \qquad (3.22)$$

where

I_{max} = size of the interception storage capacity (mm)

C_{int} = interception coefficient (mm)

LAI = leaf area index (-)

The interception coefficient (C_{int}) is time-step dependent. A usual value of C_{int} is about 0.05 mm. Furthermore, the leaf area index (LAI) characterizes the ratio of the leaves' surface area divided by the ground surface area upon which vegetation grows. LAI values typically varies between 0 (bare ground) and 7 (dense forest). (DHI, 2009)

(B) Evaporation from the Canopy

The amount of evaporation from the canopy in temperate climates is generally small compared to the precipitation; on the other hand, semi-dry climates may impact the water balance of the model.

$$E_{can} = \min(I_{max}, E_p \Delta t) \qquad (3.23)$$

where

E_{can} = canopy evaporation (m)

E_p = potential evapotranspiration rate (m/s)

(C) Plant Transpiration

The transpiration from the vegetation (E_{at}) depends on the density of the crop material, the soil moisture content in root zone, and the root density.

$$E_{at} = f_1(LAI) \cdot f_2(\theta) \cdot RDF \cdot E_p \tag{3.24}$$

where

E_{at} = actual plant transpiration (m/s)
$f_1(LAI)$ = function based on leaf area index (-)
$f_2(\theta)$ = function based on soil moisture content in root zone (-)
RDF = root distribution function (-)

The function $f_1(LAI)$ expresses the dependency of the transpiration on leaf area of the vegetation, while $f_2(\theta)$ is related to the soil moisture content in the root zone.

$$f_1(LAI) = C_2 + C_1 \cdot LAI \tag{3.25}$$

$$f_2(\theta) = 1 - \left(\frac{\theta_{FC} - \theta}{\theta_{FC} - \theta_W}\right)^{C_3/E_p} \tag{3.26}$$

where

θ_{FC} = volumetric moisture content at field capacity (-)
θ_W = volumetric moisture content at the wilting point (-)
θ = actual volumetric moisture content (-)
C_1 = empirical evapotranspiration parameter (-)
C_2 = empirical evapotranspiration parameter (-)
C_3 = empirical evapotranspiration parameter (mm/d)

Water extraction by roots varies over the cultivation season. The exact root development in nature is dependent on the climatic conditions and moisture conditions in the soil.

$$\log R(z) = \log R_0 - AROOT \cdot z \tag{3.27}$$

where

$R(z)$ = root extraction vary logarithmically with depth
R_0 = root extraction at the soil surface
$AROOT$ = root mass distribution (-)
z = depth below ground surface (m)

The value of the Root Distribution Function (RDF) of each layer is then calculated by dividing the amount of water extracted in the layer by the total amount of water extracted by the roots.

$$RDF_i \;=\; \frac{\int_{z_1}^{z_2} R(z)\,dz}{\int_{0}^{L_R} R(z)\,dz} \qquad (3.28)$$

where

RDF_i = root distribution function of layer *i* (-)

z_1 = depth below the ground surface bounded above layer *i* (m)

z_2 = depth below the ground surface bounded below layer *i* (m)

L_R = maximum root depth (m)

(D) Soil Evaporation

Evaporation from the soil (E_s) occurs at the top unsaturated layer. This is described by the following equations:

$$E_s \;=\; E_p \cdot f_3(\theta) + (\,E_p - E_{at} - E_p \cdot f_3(\theta)\,) \cdot f_4(\theta) \cdot (1 - f_1(LAI)) \qquad (3.29)$$

$$f_3(\theta) \;=\; \begin{cases} C_2 & ;\theta > \theta_W \\ C_2 \dfrac{\theta}{\theta_W} & ;\theta_r \le \theta \le \theta_W \\ 0 & ;\theta < \theta_r \end{cases} \qquad (3.30)$$

$$f_4(\theta) \;=\; \begin{cases} \dfrac{\theta - \dfrac{\theta_W + \theta_{FC}}{2}}{\theta_{FC} - \dfrac{\theta_W + \theta_{FC}}{2}} & ;\theta \ge \dfrac{\theta_W + \theta_{FC}}{2} \\ 0 & ;\theta < \dfrac{\theta_W + \theta_{FC}}{2} \end{cases} \qquad (3.31)$$

where

E_s = soil evaporation (m/s)

The empirical evapotranspiration coefficients, C_1, C_2, and C_3, are parts of actual soil evaporation and plant transpiration equations.

C_1 is plant dependent. This parameter influences the ratio of soil evaporation to transpiration. A smaller C_1 value results in more soil evaporation relative to transpiration. C_1 is estimated to be about 0.3 for agricultural crops and grass.

C_2 also involves the allocation of soil evaporation over transpiration. High values of C_2 lead to smaller values of total actual evapotranspiration because more water is extracted from the top node, which subsequently dries out faster. C_2 is estimated to be around 0.2 for agricultural crops and grass grown on clayey loamy soils.

C_3 has not been evaluated by experiment yet. A value of C_3 is generally 20 mm/d.

3) Unsaturated Flow (UZ)

Unsaturated flow is one of the central processes not only in most model applications but also in MIKE SHE. The unsaturated zone is usually heterogeneous. Unsaturated flow is primarily vertical since gravity plays the major role during infiltration. Therefore, unsaturated flow in MIKE SHE is calculated only vertically in one-dimension, which is sufficient for most applications. However, this may limit the validity of the description in some situations, such as on very steep hill slopes with contrasting soil properties in the soil profile.

A simplified gravity flow, which assumes a uniform vertical gradient but ignores capillary force, was selected for calculating vertical flow in the unsaturated zone. The driving force for the transport of water in the unsaturated zone is the gradient of hydraulic head (h) including a gravitational component (z) and a pressure component (ψ).

$$h = z + \psi \tag{3.32}$$

where

h	=	hydraulic head	(m)
z	=	gravitational head	(m)
ψ	=	pressure head	(m)

The gravitational head (z) is elevation of a point above the datum (z is positive upward), while the pressure component (ψ), for which its reference level is the atmospheric pressure, is negative under unsaturated conditions due to capillary force and short range adsorptive forces between the water molecules and the soil matrix. However, in the gravity flow module, the pressure head term is ignored and the driving force is due entirely to gravity, making the vertical gradient of the hydraulic head 1.

The volumetric flux of the gravity flow module is obtained from Darcy's law:

$$q = -K(\theta)\frac{\partial h}{\partial z} = -K(\theta) \tag{3.33}$$

where

q	=	volumetric flux	(m/s)
$K(\theta)$	=	unsaturated hydraulic conductivity	(m/s)

Assuming that the soil matrix is incompressible and the soil water has a constant density, the continuity equation for this case is as follows:

$$\frac{\partial \theta}{\partial t} = -\frac{\partial q}{\partial z} - S(z) \tag{3.34}$$

where

θ	=	actual volumetric moisture content	(-)
S	=	root extraction sink term	(1/s)
t	=	time	(s)

4) Saturated Flow (SZ)

The saturated zone (SZ) component of MIKE SHE calculates the saturated subsurface flow in the area. MIKE SHE allows for a fully three-dimensional flow in a heterogeneous aquifer with shifting conditions between unconfined and confined conditions.

The three-dimensional Darcy equation mathematically describes the spatial and temporal variations of the dependent variable (the hydraulic head).

The finite difference method is utilized to simulate 3D groundwater flow that discharges groundwater drainage directly to the surface water. The principal flow equation for a three-dimensional saturated flow in saturated porous media is defined as follows:

$$\frac{\partial}{\partial x}\left(K_{xx}\frac{\partial h}{\partial x}\right) + \frac{\partial}{\partial y}\left(K_{yy}\frac{\partial h}{\partial y}\right) + \frac{\partial}{\partial z}\left(K_{zz}\frac{\partial h}{\partial z}\right) - Q = S\frac{\partial h}{\partial t} \tag{3.35}$$

where

K_{xx} = hydraulic conductivity along x axis (m/s)

K_{yy} = hydraulic conductivity along y axis (m/s)

K_{zz} = hydraulic conductivity along z axis (m/s)

h = hydraulic head (m/s)

Q = source/sink terms (1/s)

S = specific storage coefficient (1/m)

Pre-conditioned conjugate gradient (PCG) solver was applied in the study. The potential flow was calculated using Darcy's law.

$$Q = (\Delta h)\, C \tag{3.36}$$

where

Δh = piezometric head difference (m)

C = conductance (m^2/s)

Horizontal conductance between node *i* and *i*-1 is shown as follows:

$$C_{i-\frac{1}{2}} = \frac{KH_{i\text{-}1,\,j,\,k}\;KH_{i,\,j,\,k}\,(\Delta z_{i\text{-}1,\,j,\,k} + z_{i,\,j,\,k})}{(KH_{i\text{-}1,\,j,\,k} + KH_{i,\,j,\,k})} \tag{3.37}$$

where

$C_{i-\frac{1}{2}}$ = horizontal conductance (m^2/s)

KH = horizontal hydraulic conductivity (m/s)

Δz = saturated layer thickness of the cell (m)

Vertical conductance between two cells was calculated from the middle of layer *k* to the middle of the layer *k*+1. Thus,

$$C_v = \frac{\Delta x^2}{\dfrac{\Delta z_k}{2K_{z,\,k}} + \dfrac{\Delta z_{k+1}}{2K_{z,\,k+1}}} \tag{3.38}$$

where

C_v = vertical conductance between two cells (m^2/s)

Dewatering conditions were divided into two conditions: the dewatering conditions in a lower cell and in the cell above.

If the cell below becomes dewatered, the actual flow between cell *k* and *k*+1 is calculated as follows:

$$q_{k+\frac{1}{2}} = C_{v,\,k+\frac{1}{2}}\,(z_{top,\,k+1} - h_k) \tag{3.39}$$

If the cell above becomes dewatered, the actual flow from cell *k*-1 to *k* is calculated as follows:

$$q_{k-\frac{1}{2}} = C_{v,\,k-\frac{1}{2}}\,(h_{k-1} - z_{top,\,k}) \tag{3.40}$$

where

$q_{k+\frac{1}{2}}$ = the actual flow from cell *k* to *k*+1 (m^3/s)

$q_{k-\frac{1}{2}}$ = the actual flow from cell *k*-1 to *k* (m^3/s)

The storage capacity was computed by

$$\frac{\Delta w}{\Delta t} = \frac{S2(h^n - z_{top}) + S1(z_{top} - h^{n-1})}{\Delta t} \tag{3.41}$$

where

$\frac{\Delta w}{\Delta t}$ = storage capacity (-)

n = time step (-)

$S1$ = storage capacity at the start of the iteration at time step n (1/m)

$S2$ = storage capacity at the last iteration (1/m)

The storage capacities for confined and unconfined cells are determined as follows:

For confined cells $S = \Delta x^2 \, \Delta z \, S_{art}$ (3.42)

For unconfined cells $S = \Delta x^2 \, S_{free}$ (3.43)

where

S = storage capacity for the cells (1/m)

5) Channel Flow (OC)

The channel modeling component of MIKE SHE is the MIKE 11 model. MIKE 11 is a dynamic one-dimensional model for simulating the flow in a channel system. MIKE SHE can be directly coupled with MIKE 11.

The following section provides more information on the MIKE 11 model.

3.4.2 MIKE 11 (DHI, 2009a, 2009b, 2009c)

The hydrodynamic module and sediment transport module were applied in this research. The hydrodynamic module is the core module of the MIKE 11 model. This is applied together with MIKE SHE to obtain hydrodynamic results, while the sediment transport module is utilized for simulating sediment transport results by inputting the hydrodynamic results.

1) Hydrodynamics module

There are two significant equation series in the hydrodynamics module, namely the continuity equation and momentum equation.

(A) Continuity equation

$$\frac{\partial A}{\partial t} + \frac{\partial Q}{\partial x} = q \qquad (3.44)$$

where

A = Cross-section area (m^2)

Q = Discharge (m^3/s)

q = Lateral inflow per unit width (m^2/s)

x = distance (ms)

t = time (s)

The continuity equation at grid point j time step $n+\frac{1}{2}$

$$\frac{\partial A}{\partial t} \approx \frac{A_j^{n+1} - A_j^n}{\Delta t} \tag{3.45}$$

$$\frac{\partial Q}{\partial x} \approx \frac{\left(\frac{Q_{j+1}^{n+1}+Q_{j+1}^{n}}{2}\right)-\left(\frac{Q_{j-1}^{n+1}+Q_{j-1}^{n}}{2}\right)}{\Delta x_j + \Delta x_{j+1}} \tag{3.46}$$

where

Δt = time difference between time step n and n+1 (s)

Δx = distance between point j and j-1 (m)

(B) Momentum equation

$$\frac{\Delta M}{\Delta t} = \frac{\Delta(M \bullet U)}{\Delta x} + \frac{\Delta P}{\Delta x} - \frac{F_f}{\Delta x} + \frac{F_s}{\Delta x} \tag{3.47}$$

$\frac{\Delta M}{\Delta t}$ represents Momentum = Mass per unit length • velocity

$\frac{\Delta(M \bullet U)}{\Delta x}$ represents Momentum flux = Momentum • velocity

$\frac{\Delta P}{\Delta x}$ represents Pressure force = Hydrostatic Pressure

$\frac{F_f}{\Delta x}$ represents Friction force = Force due to bed resistance

$\frac{F_s}{\Delta x}$ represents Gravity force = Contribution in x-direction

There are four main momentum equation selections: kinematic wave, diffusive wave, fully dynamic wave, and higher order fully dynamic wave.

- Kinematic wave

  This option is suitable for steep rivers, while both backwater effects and tidal flows are not applicable. Thus, the momentum flux and pressure force terms are ignored.

$$\frac{\Delta M}{\Delta t} = -\frac{F_f}{\Delta x} + \frac{F_s}{\Delta x} \tag{3.48}$$

- Diffusive wave

  This option is applied for relatively steady backwater effects and slowly propagating flood waves. However, tidal flows are not considered. Thus, the momentum flux term is ignored.

$$\frac{\Delta M}{\Delta t} = \frac{\Delta P}{\Delta x} - \frac{F_f}{\Delta x} + \frac{F_s}{\Delta x} \tag{3.49}$$

- Fully dynamic wave

  This option is suitable for fast transients, tidal flows, rapidly changing backwater effects, and flood waves.

$$\frac{\Delta M}{\Delta t} = \frac{\Delta(M \bullet U)}{\Delta x} + \frac{\Delta P}{\Delta x} - \frac{F_f}{\Delta x} + \frac{F_s}{\Delta x} \tag{3.50}$$

- Higher order fully dynamic wave

  Finally, this option is very similar to the fully dynamic wave option but this is more specific for steep channels. Thus, the pressure force term can be optionally further identified.

$$\frac{\Delta M}{\Delta t} = \frac{\Delta(M \bullet U)}{\Delta x} + \frac{\Delta P}{\Delta x} - \frac{F_f}{\Delta x} + \frac{F_s}{\Delta x} \tag{3.51}$$

2) Sediment transport

(A) Sediment continuity equation

The major equation for erosion, deposition, and transport of the non-cohesive sediment module is the sediment continuity equation (Eq. (3.52)), which is used for predicting bed level changes.

$$\frac{\partial S}{\partial x} + \left(1 - \varepsilon\right) w \cdot \frac{\partial z}{\partial t} = 0 \qquad (3.52)$$

where

S = sediment transport rate (m^3/s)

t = time (s)

w = channel width (m)

x = longitudinal co-ordinate (m)

z = bed level (m)

ε = sediment porosity (-)

(B) Meyer-Peter and Muller Model

As stated before, the primary focus of this research is on stream sediment, so the Meyer-Peter and Muller model was selected to simulate the stream sediment or bed load transport. Thus, the sediment transport rate in the study was implied by bed load transport rate ($S \approx Q_b$).

Bed load sediment transport equation is

$$Q_b = q_b w \qquad (3.53)$$

where

Q_b = bed load transport rate (m^3/s)

q_b = absolute bed load transport per unit river width (m^2/s)

The absolute bed load transport per unit width of the river was found through the following equation:

$$q_b = \Phi_b \sqrt{(s-1)gd^3} \tag{3.54}$$

where

d = diameter of the grain (m)

g = acceleration due to gravity (m/s^2)

s = relative density of sediment (-)

Φ_b = dimensionless bed load transport (-)

The dimensionless bed load transport equation is

$$\Phi_b = 8(\theta_{eff} - 0.047)^{1.5} \quad \text{when } \theta_{eff} > 0.047 \tag{3.55a}$$

$$\Phi_b = 0 \quad \text{when } \theta_{eff} \leq 0.047 \tag{3.55b}$$

where

θ_{eff} = dimensionless effective shear stress (-)

The dimensionless effective shear stress equation is

$$\theta_{eff} = \frac{u_{eff}^2}{(s-1)gd} \tag{3.56}$$

where

u_{eff} = effective velocity (m/s)

Effective velocity was determined by the following equations:

$$u_{eff} = u'_f \cdot \left(\frac{n_b}{n}\right)^{0.75} \tag{3.57}$$

$$n_b = 0.0192(d_{90})^{\frac{1}{6}} \tag{3.58}$$

where

d_{90} = diameter of which 90% are finer (m)

n = resistance number (m$^{1/6}$)

u_{eff} = effective velocity (m/s)

u'_f = bed friction velocity (m/s)

(C) Additional equations

Related additional equations are as follows:

- Relative density or specific gravity of sediment

$$s = \frac{\rho_{sediment}}{\rho_{water}} \tag{3.59}$$

where

$\rho_{sediment}$ = density of sediment (kg/m^3)

ρ_{water} = density of water (kg/m^3)

- The relation between current velocity and bed friction velocity

$$\frac{u}{u'_f} = 2.5\left[\ln\left(\frac{30D'}{2.5d}\right)-1\right] \tag{3.60}$$

$$D' = D\frac{\theta'}{\theta} \tag{3.61}$$

$$\theta' = \frac{u'^2_f}{(s-1)gd} \tag{3.62}$$

$$\theta = \sqrt{\frac{(\theta'\text{-}0.06)}{0.4}} \tag{3.63}$$

where

D = flow depth (m)

D' = boundary layer thickness (m)

θ = dimensionless shear stress (-)

θ' = dimensionless skin friction (-)

- Resistance number

$$n = \begin{cases} 1 & ; D_{gr} < 1 \\ 1-0.56\log D_{gr} & ; 1 < D_{gr} < 60 \\ 0 & ; D_{gr} > 60 \end{cases} \tag{3.64}$$

where

D_{gr} = dimensionless grain diameter (m)

- Dimensionless grain diameter

$$D_{gr} = d\left[\frac{g(s-1)}{\upsilon^2}\right]^{\frac{1}{3}} \qquad (3.65)$$

where

υ = kinematic viscosity (m^2/s)

3.5 Evaluation

The sediment transport data simulated from the models and cadmium concentration in the stream sediment measured by FLASS were calculated to evaluate cadmium transport rate in the stream sediment (g/d) using the equation below.

$$\text{Cadmium transport rate} = \left(S \times \rho_{sediment}\right) \times [Cd]_{sed} \qquad (3.66)$$

where

S = sediment transport rate (m^3/d)

$\rho_{sediment}$ = density of sediment (kg/m^3)

$[Cd]_{sed}$ = cadmium concentration in stream sediment (mg/kg)

CHAPTER IV

RESULTS AND DISCUSSIONS

4.1 Field observation results

4.1.1 Flow measurement results

The flow measurement results along Mae Tao Creek were computed using the area-velocity method as presented in Table 4-1, while the cross-section profile of each station is displayed in Figure C-1 to Figure C-10, Appendix C.

Table 4-1 Flow measurement results from the 10 stations

Station	**Northing** (m)	**Easting** (m)	***D*** (m)	***w*** (m)	***A*** (m^2)	***V*** (m/s)	***Q*** (m^3/s)
1	1843017	457998	0.90	8.50	5.98	0.41	2.43
2	1843330	459400	1.00	12.10	8.52	0.28	2.38
3	1843034	461274	0.60	10.00	4.70	0.49	2.28
4	1843110	461376	1.09	9.50	5.96	0.40	2.39
5	1843286	461438	0.60	7.30	2.77	0.23	0.62
6	1842870	462046	1.10	9.60	6.95	0.33	2.26
7	1842718	465638	0.45	6.50	1.91	0.74	1.42
8	1842750	466937	0.45	5.70	1.39	1.00	1.40
9	1842559	467228	0.20	5.00	0.71	0.92	0.65
10	1842736	467088	0.55	4.50	1.84	0.30	0.56

D = flow depth (m)
w = channel width (m)
A = cross-sectional area (m^2)
V = velocity of water (m/s)
Q = water discharge (m^3/s)

The flow depth and water velocity of the small sections, which were divided at constant width intervals, were measured and recorded in the calculation sheets; thus the flow depth (*D*), water velocity (*V*), and channel width (*w*) of the cross-section at each station were determined, as represented in Table 4-1. The cross-section areas (*A*) were subsequently computed and their profiles were plotted as displayed in Figure C-1 to Figure C-10. The water discharge (*Q*) of each cross-section was finally calculated from Eq. (3.6). The water discharge increased along the flow direction in Mae Tao (starting from station 10 to station 1), as demonstrated in Figure 4-1.

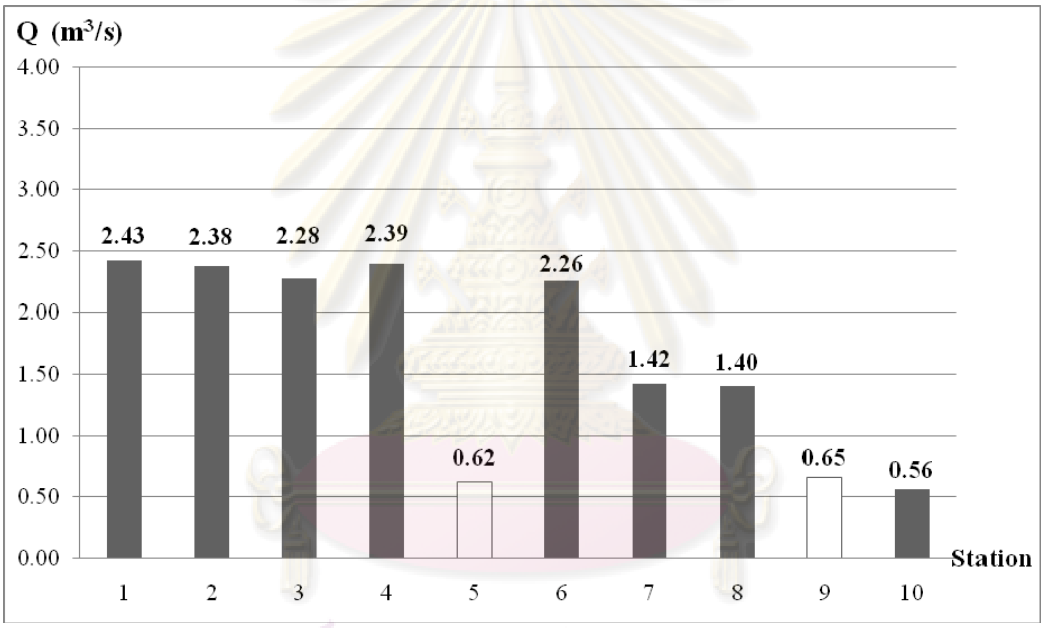

Figure 4-1 Water discharge of the stations along Mae Tao Creek (Remark: Stations 5 and 9 were not along the main stream)

The noteworthy two connection points found in the field observation as shown in Figure 3-2 were station 3, the connection between station 4 (main creek of Mae Tao) and station 5 (Mae Tao Creek (Left)), as well as station 8, the connection between station 10 (main creek of Mae Tao) and station 9 (Mae Tao Creek (Right)). Referring to volume balance, a summation of the water discharge of stations 4 and 5 should be equal to that of station 3. Similarly, the water discharge of station 8 should total of the discharges of station 9 and station 10. However, the field observation of each station was not done on the same date and there was rainfall precipitation during that time, so a computation of the flow balance could not be done.

4.1.2 Field measurement results

The field measurement data comprising of the pH, DO, conductivity, and temperature of the water at each station are provided in Table 4-2.

Table 4-2 Field measurement data at each station including pH, DO, conductivity, and temperature of water

Station	**Northing** (m)	**Easting** (m)	**pH**	**DO** (mg/L)	**EC** (µS)	**T** (°C)
1	1843017	457998	8.26 ± 0.05	6.95 ± 0.57	357 ± 2	25.1 ± 0.0
2	1843330	459400	8.29 ± 0.04	7.33 ± 0.01	351 ± 0	25.9 ± 0.0
3	1843034	461274	8.35 ± 0.03	7.48 ± 0.28	348 ± 2	25.4 ± 0.0
4	1843110	461376	8.44 ± 0.09	7.30 ± 0.29	327 ± 1	25.6 ± 0.0
5	1843286	461438	8.30 ± 0.08	7.07 ± 0.19	332 ± 1	26.2 ± 0.0
6	1842870	462046	8.33 ± 0.02	6.77 ± 0.42	342 ± 1	25.6 ± 0.6
7	1842718	465638	8.16 ± 0.04	6.60 ± 0.08	311 ± 2	25.9 ± 0.0
8	1842750	466937	8.42 ± 0.03	6.62 ± 0.10	306 ± 1	25.7 ± 0.7
9	1842559	467228	8.19 ± 0.15	6.60 ± 0.43	271 ± 1	25.7 ± 0.3
10	1842736	467088	8.46 ± 0.02	6.37 ± 0.41	328 ± 2	25.2 ± 0.2

pH = potential of the hydrogen ion
DO = dissolved oxygen (mg/L)
EC = conductivity of water (µS)
T = temperature (°C)

The pH values of the water at every station were for the most part slightly high, ranging from 8.16 to 8.46, demonstrated as Figure 4-2. Slightly alkali water causes more insoluble forms of heavy metals in water, so cadmium could not be well distributed or widespread through water media. The measured values of DO, which were between 6.37 and 7.48 mg/L, as shown in Figure 4-3, represented the clean natural water of Mae Tao Creek. Conductivity values at the stations varied between 271.00 and 356.67 µS, as displayed in Figure 4-4, whereas water temperatures were measured to be around 25.1 to 26.2 °C (see Figure 4-5).

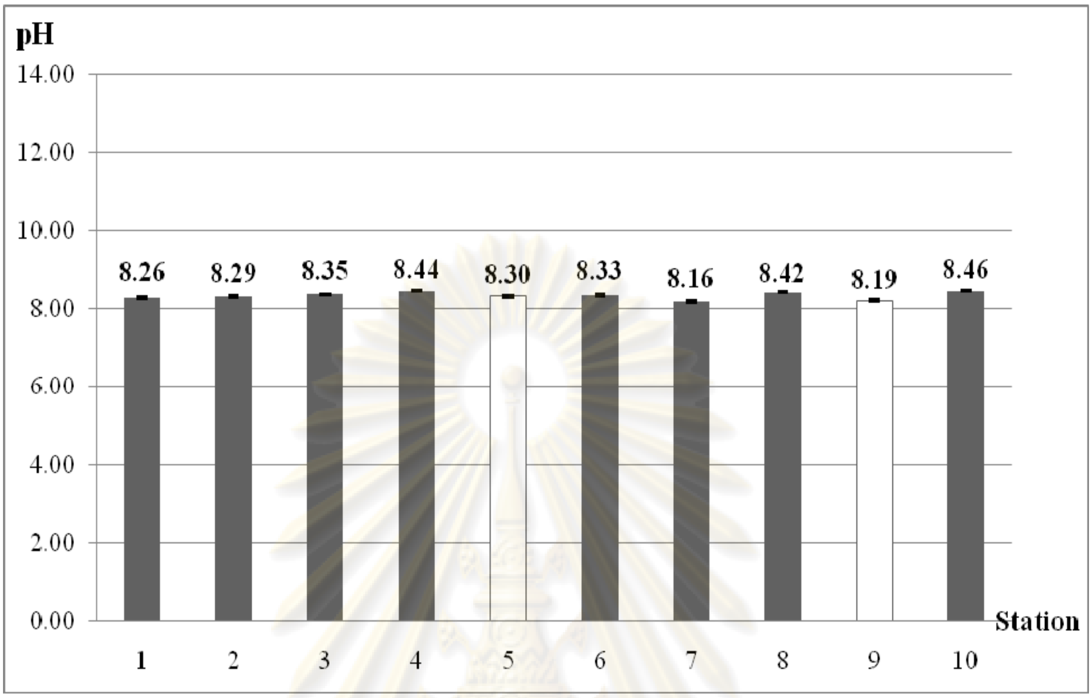

Figure 4-2 **Water pH at each station along Mae Tao Creek**
(Remark: Station 5 and 9 were not along the main stream)

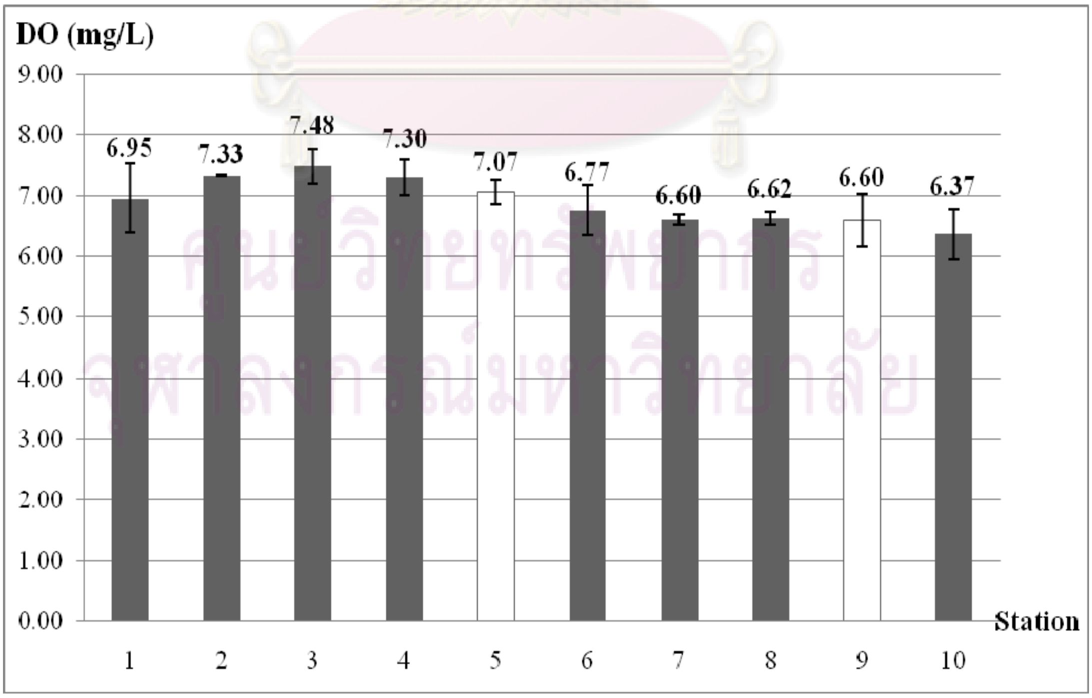

Figure 4-3 **Dissolved oxygen in water at each station along Mae Tao Creek**
(Remark: Station 5 and 9 were not along the main stream)

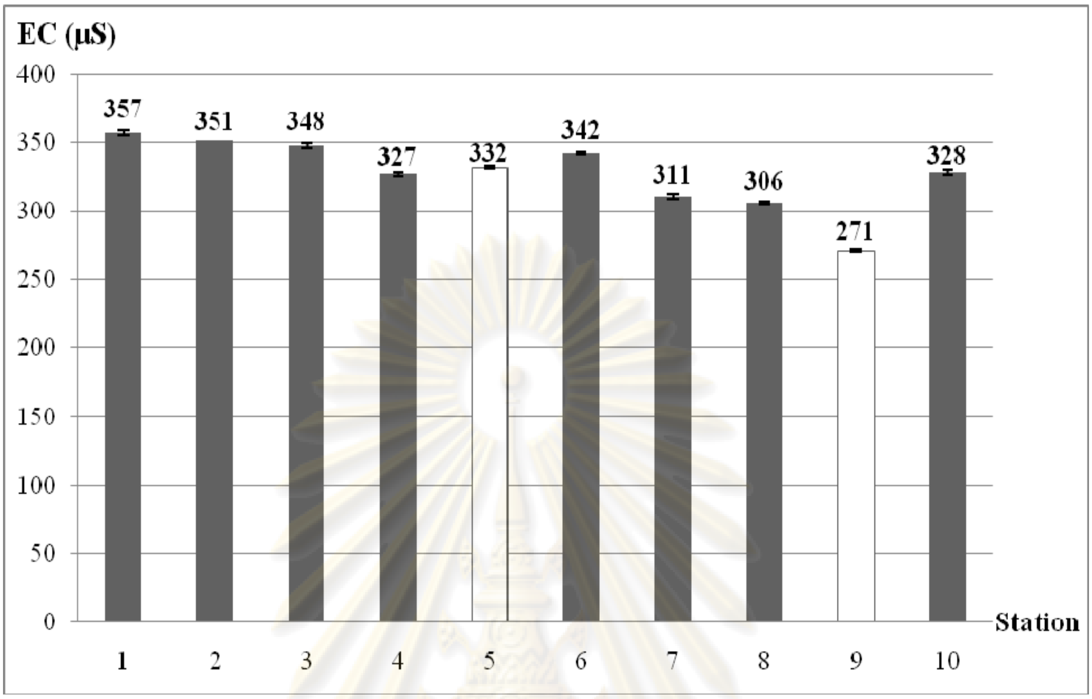

Figure 4-4 Water conductivity at each station along Mae Tao Creek (Remark: Station 5 and 9 were not along the main stream)

Figure 4-5 Water temperature at each station along Mae Tao Creek (Remark: Station 5 and 9 were not along the main stream)

4.2 Laboratory results

4.2.1 Cadmium concentration results

The cadmium concentration of the stream sediment, which was collected and measured by a FLASS (Flame Atomic Absorption Spectroscopy), is provided in Table 4-3. Moreover, the concentrations at the stations are also reported in Figure 4-6.

Table 4-3 Cadmium concentration of the stream sediment at each station

Station	**Northing** (m)	**Easting** (m)	**Cadmium concentration in stream sediment, $[Cd]_{sed}$**	
			(mg of Cd per kg of sediment)	(mg of Cd per L of sediment)
1	1843017	457998	33.93 ± 1.35	65.22 ± 2.60
2	1843330	459400	13.34 ± 0.74	25.64 ± 1.43
3	1843034	461274	6.07 ± 0.12	11.66 ± 0.23
4	1843110	461376	28.79 ± 9.46	55.34 ± 18.19
5	1843286	461438	LD	LD
6	1842870	462046	15.05 ± 1.21	28.92 ± 2.32
7	1842718	465638	1.12 ± 0.04	2.15 ± 0.07
8	1842750	466937	1.45 ± 0.28	2.78 ± 0.53
9	1842559	467228	1.35 ± 0.39	2.59 ± 0.75
10	1842736	467088	LD	LD

* Assumption: density of wet sediment = 1922 kg/m^3
* LD = Lower than the detected limit of the FLASS

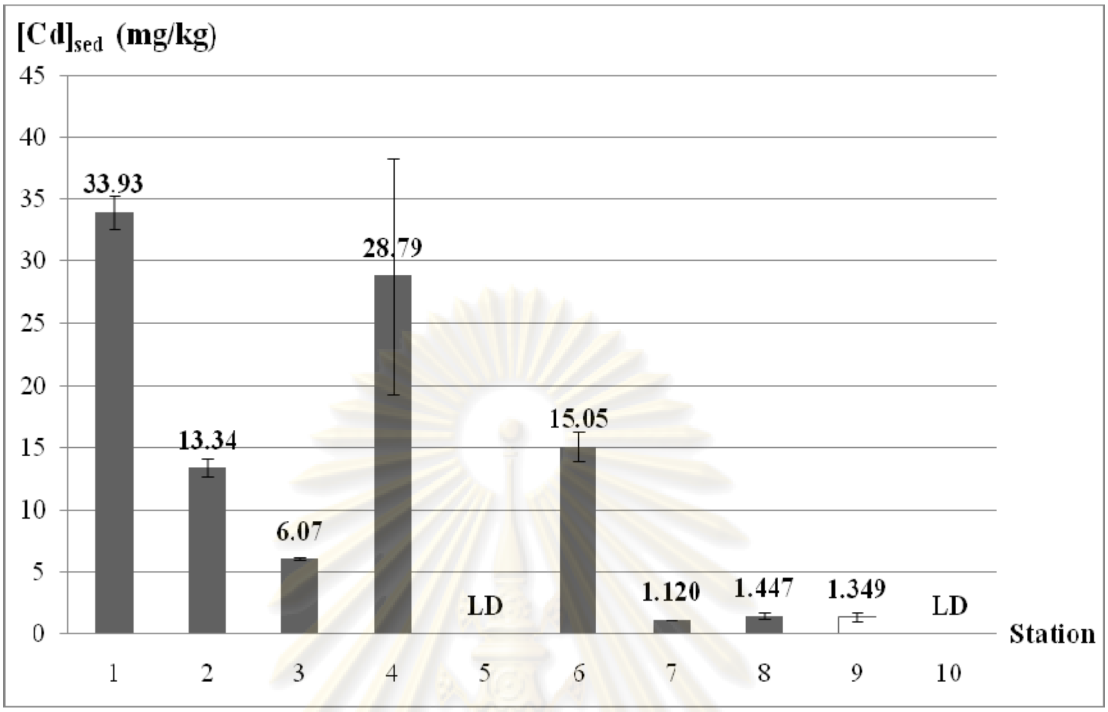

Figure 4-6 **Cadmium concentration at each station along Mae Tao Creek (Remark: Station 5 and 9 were not along the main stream)**

Detected cadmium concentrations in the stream sediment along Mae Tao Creek ranged from 1.120 to 33.93 mg of cadmium per kg of stream sediment; however, cadmium concentrations could not be detected at two of the stations (station 5 and station 10) by the FLASS.

The cadmium concentration level was higher along Mae Tao Creek. There was some cadmium contamination upstream, represented by stations 9 and 10. This signified that cadmium could also exist naturally, though the concentration was very low.

However, the concentration was particularly much higher when passing the first mine (Padaeng Industry Plc.), as indicated by the concentration at station 7 to station 6. The cadmium concentration continued to increased through to the second mine, belonging to Tak Mining, which can be deduced by the concentrations from station 6 to station 4. Station 3 symbolized the connection of Mae Tao Creek (main) and Mae Tao Creek (left). The concentration at this station was lower than it was at station 4, which was primarily due to the turbulent mixing that occurs at the junction, causing little sediment to be deposited at this location. Moreover, dilution from the station 5 concentration, which was lower than detected limit by the FLASS, also supported this circumstance.

Finally, the cadmium concentration at station 1, located downstream of the Mae Tao subcatchment, was measured to be equal to 33.93 mg of cadmium per kg of stream sediment or 65.22 mg of cadmium per L of stream sediment, which was calculated by assuming that the density of wet sediment was 1922 kg/m^3.

4.2.2 Grain size distribution

The mean diameter and standard deviation of the stream sediment at each station were determined by the grain size distribution, as shown in Table 4-4. For this, the percentage of lost sample should be lower than 2% for acceptable results.

Because of the high potential of cadmium contamination and movement, small sediment capable of passing through a 65-mesh sieve was considered in this study. The mean diameter and standard deviation of the small sediment at all stations are listed in Table 4-5.

Classification of the stream sediment was completed by following the Unified Soil Classification System (USCS) as demonstrated in Table 4-6. Since the percentage of stream sediment passing through sieve No. 200 was lower than 50% at every station, the sediment was categorized as gravel (G) or sand (S). Moreover, the coarse fraction (CF) of every station was lower than 0.5, so the stream sediment in the study area was identified as being mainly sand.

In addition, grain-size distribution curves of all 10 stations along Mae Tao Creek (see Figure 4-7 to 4-16) determined the equations for identifying sizes of stream sediment at the stations, i.e., d_{10}, d_{50}, and d_{90} as displayed in Table 4-7.

Table 4-4 Grain-size distribution of stream sediment at each station

Sieve	**Mesh No.**	**Sieve opening**	**Mean size**	**Weight of the sediment at each station** (g)									
		(mm)	(mm)	**Sta 1**	**Sta 2**	**Sta 3**	**Sta 4**	**Sta 5**	**Sta 6**	**Sta 7**	**Sta 8**	**Sta 9**	**Sta 10**
Weight of sample before sieving				1741.9	1838.1	1743.7	1977.5	1572.1	1338.7	1570.0	1366.7	1896.8	1269.9
1	3/4"	19.000	19.000	40.0	0.0	7.4	45.7	0.0	0.0	35.3	13.5	73.3	12.2
2	3/8"	9.500	14.250	275.1	40.1	12.8	171.8	4.9	0.0	41.7	4.8	424.7	9.9
3	4	4.750	7.125	214.0	23.2	37.2	147.8	12.5	0.0	15.5	9.9	283.6	31.1
4	10	2.000	3.375	201.1	149.1	114.5	145.2	45.3	0.0	19.5	6.5	250.3	58.0
5	20	0.850	1.425	223.7	258.8	206.5	257.2	205.3	0.8	36.1	9.0	128.7	119.9
6	35	0.500	0.675	269.4	337.7	239.3	362.7	246.0	9.8	170.2	43.3	103.3	167.7
7	65	0.231	0.366	338.2	408.4	606.6	618.5	607.7	511.9	945.8	520.5	354.6	418.1
8	100	0.150	0.191	0.4	2.7	50.4	10.1	88.6	78.9	64.7	118.9	0.7	61.5
9	150	0.100	0.125	154.6	541.6	381.8	192.6	265.2	659.2	202.2	493.3	215.0	306.6
10	200	0.075	0.088	0.0	1.1	2.2	0.0	0.9	0.8	0.3	4.8	0.1	2.1
Receiver		-	0.075	24.9	73.9	83.2	25.9	95.5	75.9	38.1	136.0	59.1	81.5
Total (g)				1741.4	1836.7	1741.9	1977.5	1571.7	1337.3	1569.4	1360.5	1893.4	1268.6
Loss (g)				0.5	1.4	1.8	0.0	0.4	1.4	0.7	6.3	3.4	1.4
Loss (%)				0.03	0.076	0.10	0.0	0.02	0.10	0.04	0.46	0.18	0.11
% Passing Sieve No. 200				1.43	4.02	4.77	1.31	6.07	5.67	2.43	9.95	3.12	6.42
Mean Diameter (mm)				4.323	1.121	0.985	2.895	0.668	0.223	1.270	0.547	5.664	1.011
S.D. (mm)				4.176	1.075	0.942	2.785	0.640	0.217	1.221	0.525	5.485	0.967

Table 4-5 **Grain size of small sediment that could pass through 65-mesh sieve (diameter < 0.231 mm)**

Sieve	**Mesh No.**	**Sieve opening**	**Mean size**	**Weight of the sediment at each station** (g)									
		(mm)	(mm)	**Sta 1**	**Sta 2**	**Sta 3**	**Sta 4**	**Sta 5**	**Sta 6**	**Sta 7**	**Sta 8**	**Sta 9**	**Sta 10**
Weight of sample before sieving				1741.9	1838.1	1743.7	1977.5	1572.1	1338.7	1570.0	1366.7	1896.8	1269.9
8	100	0.150	0.191	0.4	2.7	50.4	10.1	88.6	78.9	64.7	118.9	0.7	61.5
9	150	0.100	0.125	154.6	541.6	381.8	192.6	265.2	659.2	202.2	493.3	215.0	306.6
10	200	0.075	0.088	0.0	1.1	2.2	0.0	0.9	0.8	0.3	4.8	0.1	2.1
Receiver		-	-	0.075	73.9	83.2	25.9	95.5	75.9	38.1	136.0	59.1	81.5
Mean Diameter (mm)				0.118	0.119	0.123	0.122	0.127	0.127	0.133	0.126	0.114	0.125
S.D. (mm)				0.115	0.116	0.115	0.117	0.119	0.119	0.121	0.115	0.110	0.114

Table 4-6 Stream sediment classification of each station by USCS

Sieve	Mesh No.	Sieve opening	Mean size	Weight of the sediment at each station (g)									
		(mm)	(mm)	Sta 1	Sta 2	Sta 3	Sta 4	Sta 5	Sta 6	Sta 7	Sta 8	Sta 9	Sta 10
Weight of sample before sieving				1741.9	1838.1	1743.7	1977.5	1572.1	1338.7	1570.0	1366.7	1896.8	1269.9
1	3/4"	19.000	19.000	40.0	0.0	7.4	45.7	0.0	0.0	35.3	13.5	73.3	12.2
2	3/8"	9.500	14.250	275.1	40.1	12.8	171.8	4.9	0.0	41.7	4.8	424.7	9.9
3	4	4.750	7.125	214.0	23.2	37.2	147.8	12.5	0.0	15.5	9.9	283.6	31.1
4	10	2.000	3.375	201.1	149.1	114.5	145.2	45.3	0.0	19.5	6.5	250.3	58.0
5	20	0.850	1.425	223.7	258.8	206.5	257.2	205.3	0.8	36.1	9.0	128.7	119.9
6	35	0.500	0.675	269.4	337.7	239.3	362.7	246.0	9.8	170.2	43.3	103.3	167.7
7	65	0.231	0.366	338.2	408.4	606.6	618.5	607.7	511.9	945.8	520.5	354.6	418.1
8	100	0.150	0.191	0.4	2.7	50.4	10.1	88.6	78.9	64.7	118.9	0.7	61.5
9	150	0.100	0.125	154.6	541.6	381.8	192.6	265.2	659.2	202.2	493.3	215.0	306.6
10	200	0.075	0.088	0.0	1.1	2.2	0.0	0.9	0.8	0.3	4.8	0.1	2.1
Receiver		-	0.075	0.075	73.9	83.2	25.9	95.5	75.9	38.1	136.0	59.1	81.5
Total (g)				1741.4	1836.7	1741.9	1977.5	1571.7	1337.3	1569.4	1360.5	1893.4	1268.6
% Passing Sieve No. 200				1.43	4.02	4.77	1.31	6.07	5.67	2.43	9.95	3.12	6.42
F = % Coarser than sieve No. 200				98.6	95.9	95.1	98.7	93.9	94.2	97.5	89.6	96.7	93.5
C = % Coarser than sieve No. 4				30.4	3.44	3.29	18.5	1.10	0	5.89	2.06	41.2	4.18
CF = Coarse Fraction				0.308	0.0359	0.0346	0.187	0.0118	0	0.0604	0.0230	0.426	0.0448
Stream sediment categorization				Sand	Sand	Sand	Sand	Sand	Sand	Sand	Sand	Sand	Sand

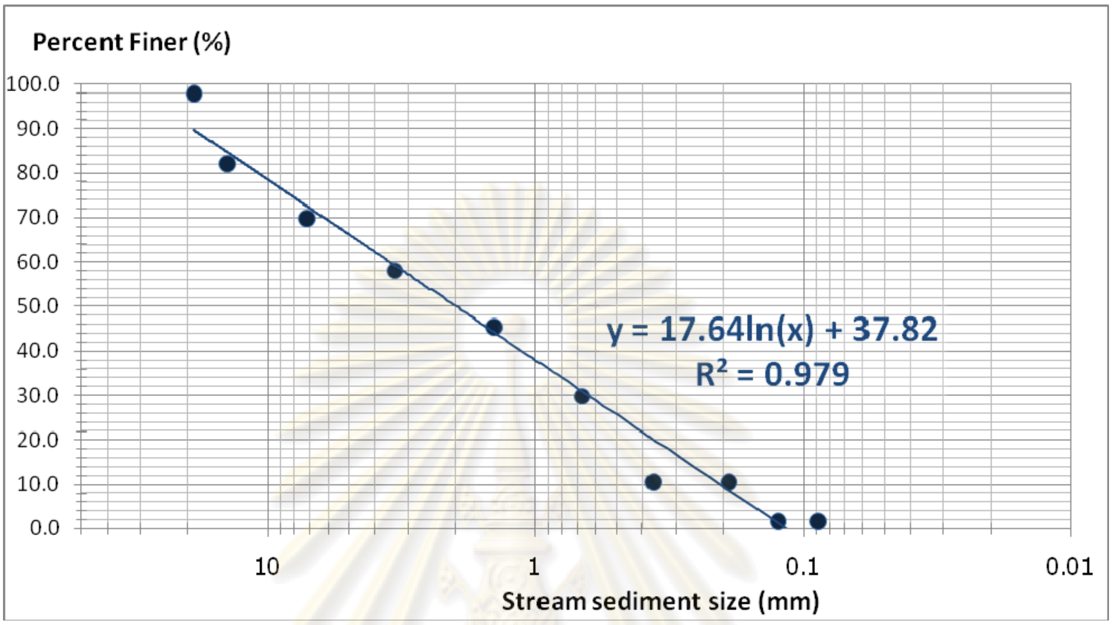

Figure 4-7 Grain-size distribution curve (Station 1)

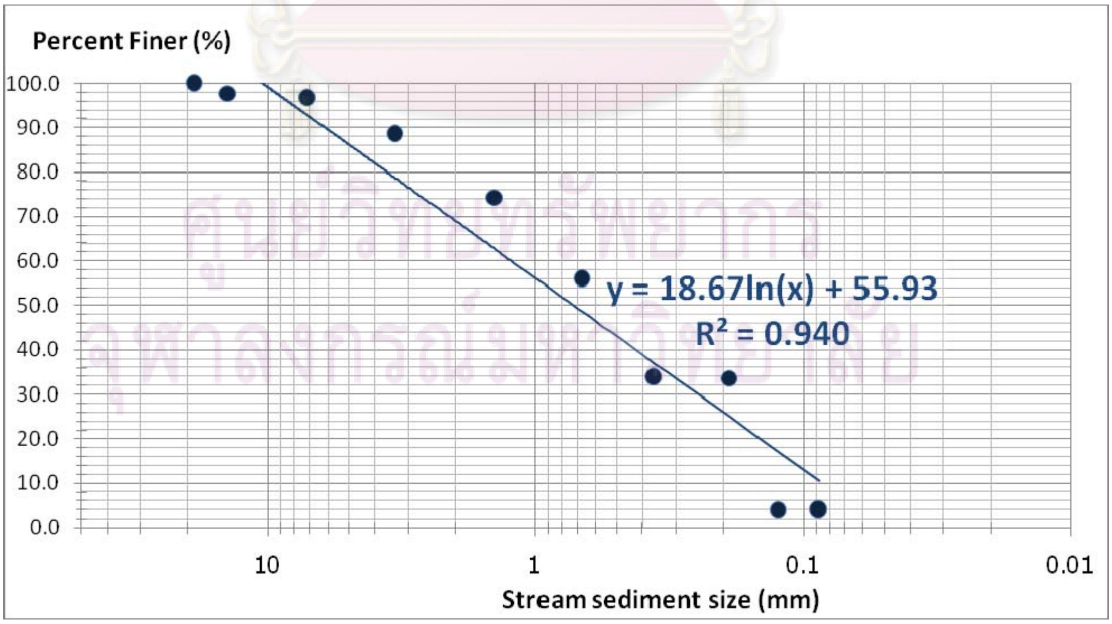

Figure 4-8 Grain-size distribution curve (Station 2)

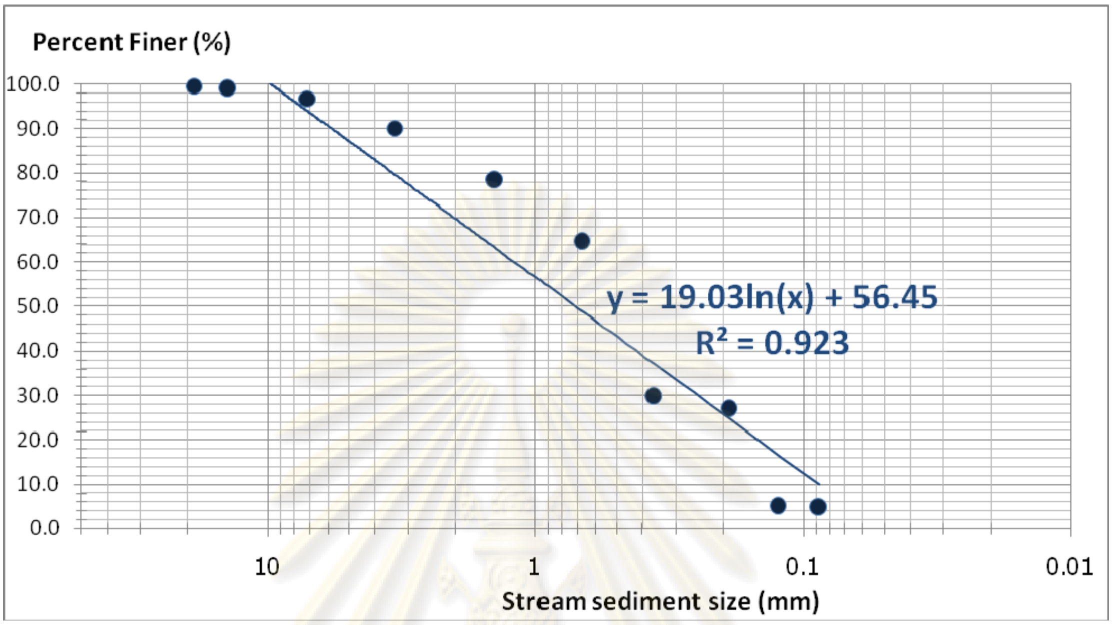

Figure 4-9 Grain-size distribution curve (Station 3)

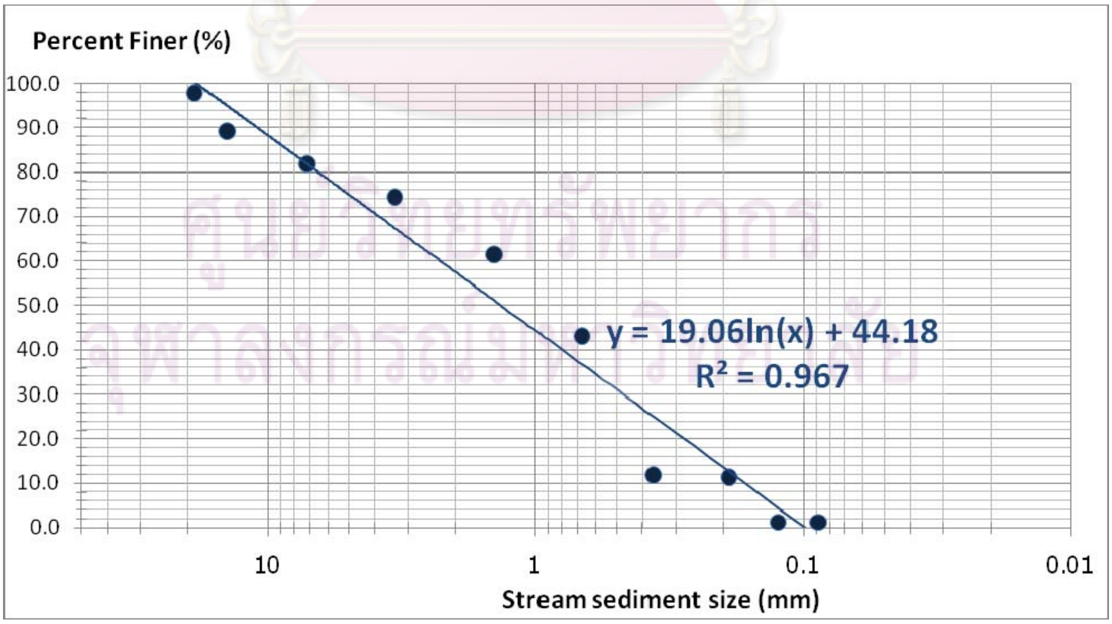

Figure 4-10 Grain-size distribution curve (Station 4)

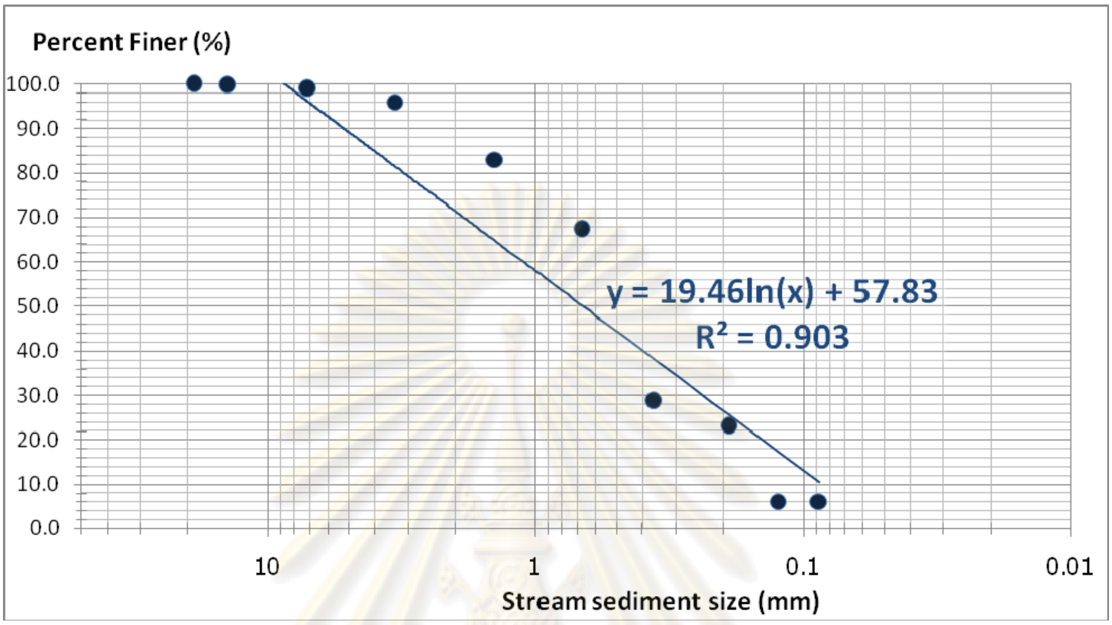

Figure 4-11 Grain-size distribution curve (Station 5)

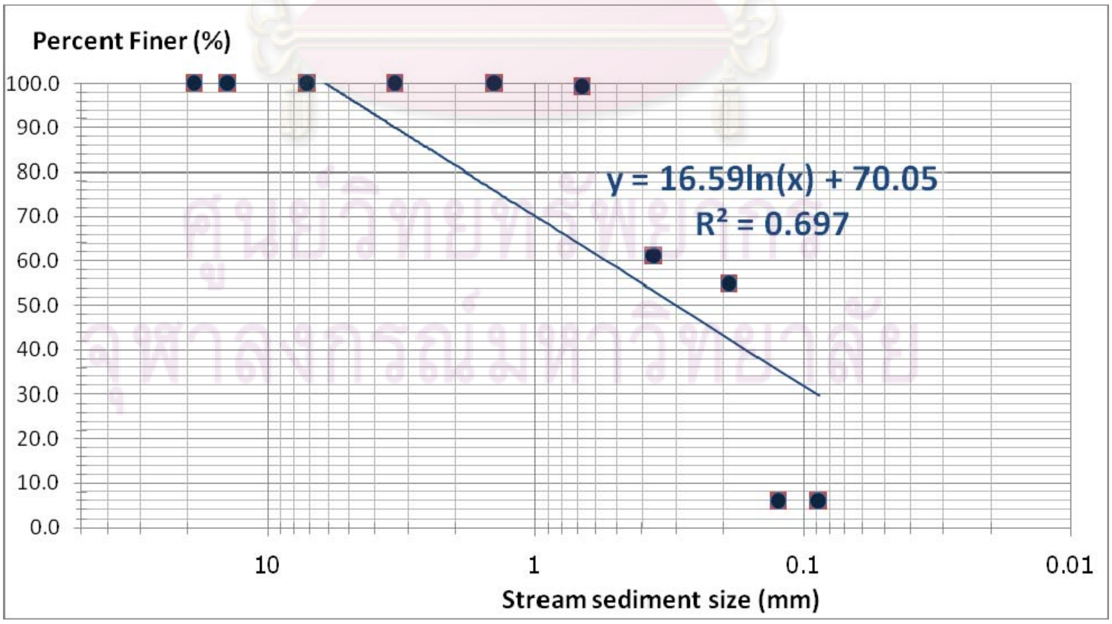

Figure 4-12 Grain-size distribution curve (Station 6)

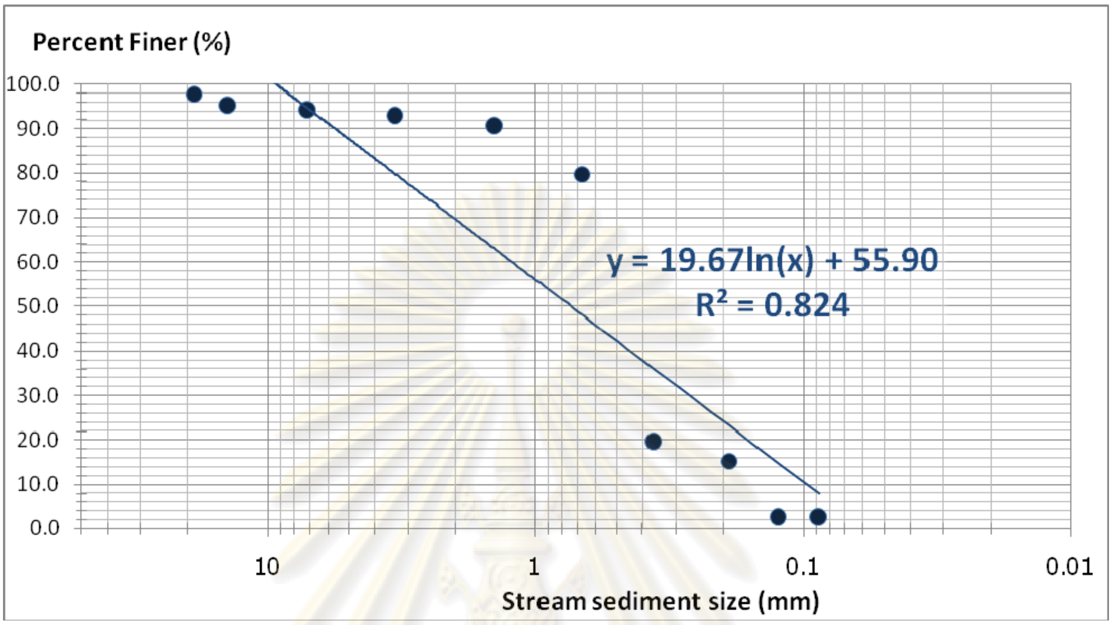

Figure 4-13 Grain-size distribution curve (Station 7)

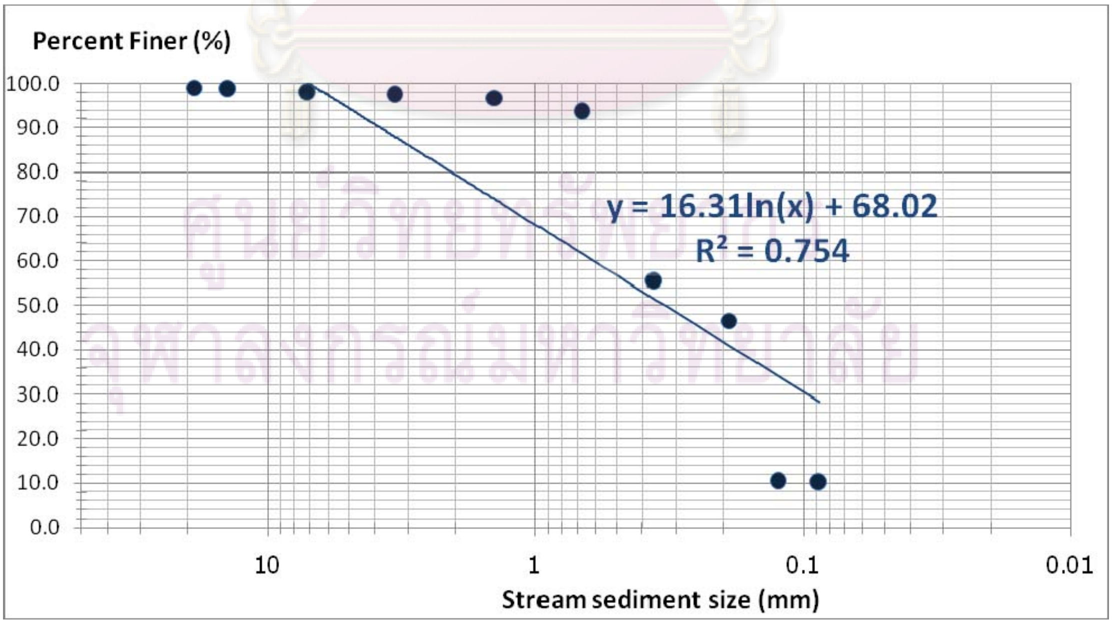

Figure 4-14 Grain-size distribution curve (Station 8)

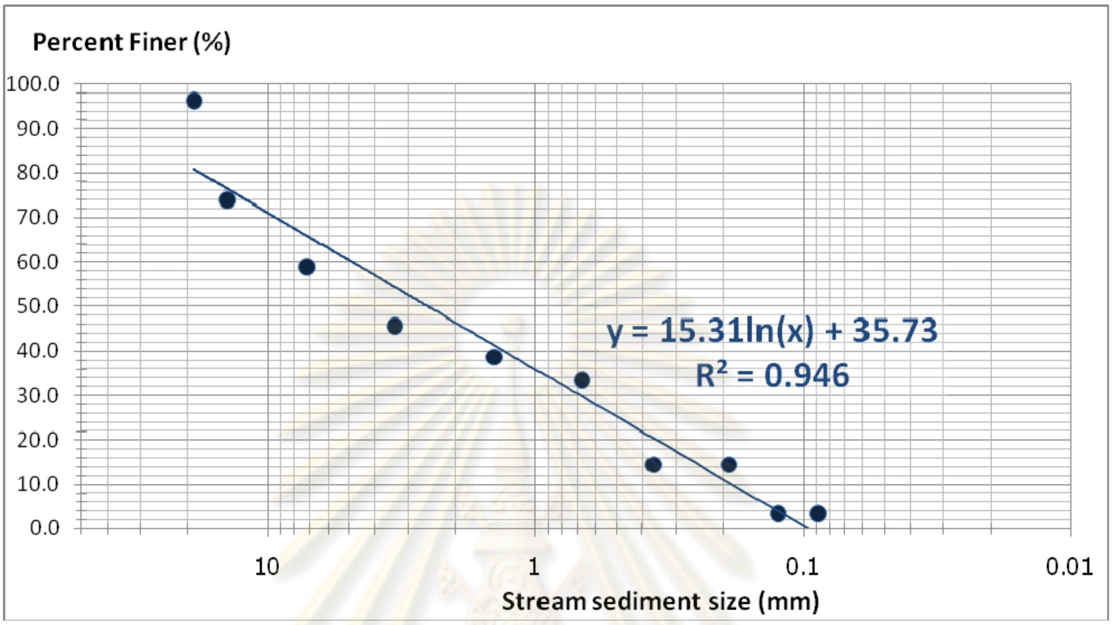

Figure 4-15 Grain-size distribution curve (Station 9)

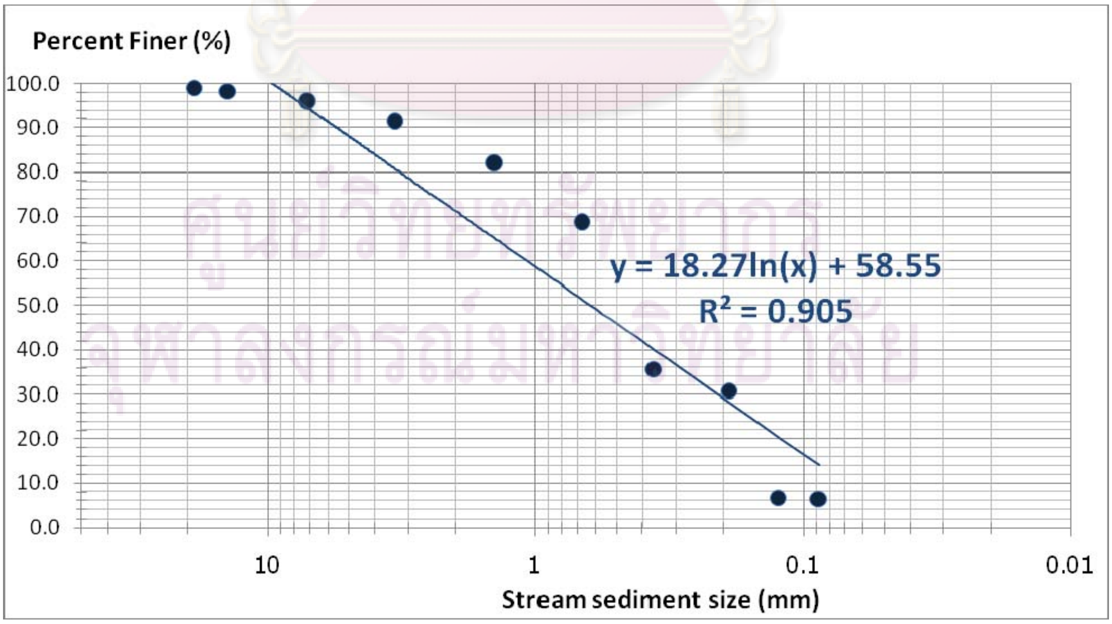

Figure 4-16 Grain-size distribution curve (Station 10)

Table 4-7 Grain size of stream sediment along Mae Tao Creek

Station	d_{10} (mm)	d_{50} (mm)	d_{90} (mm)
1	0.206	1.995	19.260
2	0.085	0.728	6.202
3	0.087	0.712	5.830
4	0.166	1.357	11.067
5	0.086	0.669	5.223
6	0.027	0.299	3.328
7	0.097	0.741	5.661
8	0.028	0.331	3.848
9	0.186	2.540	34.631
10	0.070	0.626	5.592

d_{10} = size at which 10% of sediment are smaller than the specified diameter (mm)

d_{50} = size at which 50% of sediment are smaller than the specified diameter (mm)

d_{90} = size at which 90% of sediment are smaller than the specified diameter (mm)

4.3 Simulation results

4.3.1 Hydrodynamic results

Since water discharge data, which was not provided by any of the departments, is one of important inputs for calculating sediment transport, MIKE SHE was applied to estimate the flow from the hydrological data of the area.

The hydrodynamic results obtained by running MIKE SHE coupled with MIKE 11 were the water depth and water discharge. Figure 4-17 represented time series-water discharge of all 10 observation stations. Water discharge at upstream is very few and the discharge is more and more several consequently along Mae Tao Creek until the downstream of Mae Tao subcatchment (Station 1), whereas water discharges from Mae Tao Creek (Right) and Mae Tao Creek (Left) were minority comparing with the discharge from Mae Tao Creek (Main).

Water depth and water discharge downstream data of the Mae Tao subcatchment from 1st January 2009 to 31st December 2009 are given in Figure 4-18 and Figure 4-19.

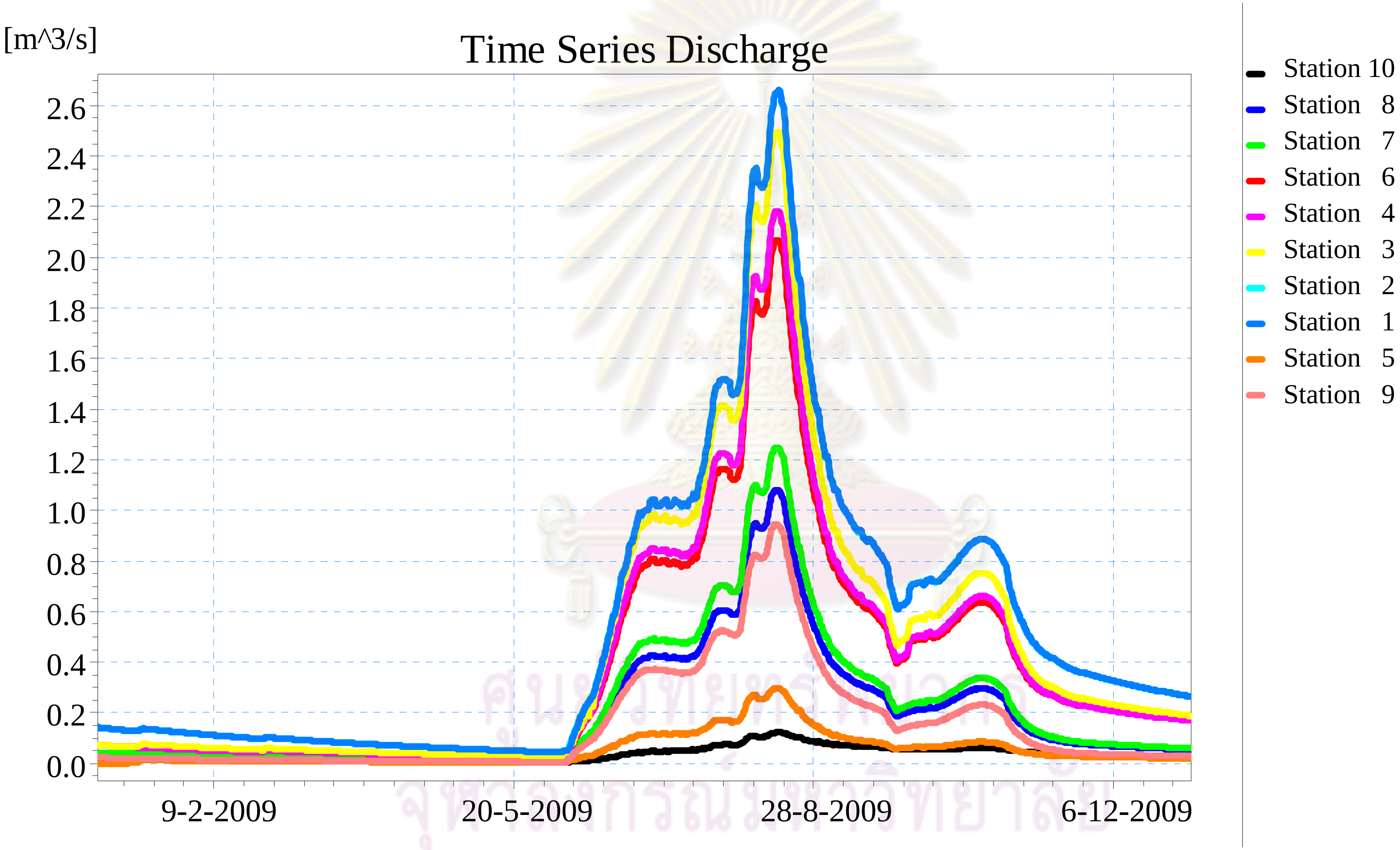

Figure 4-17 Water discharge of all stations

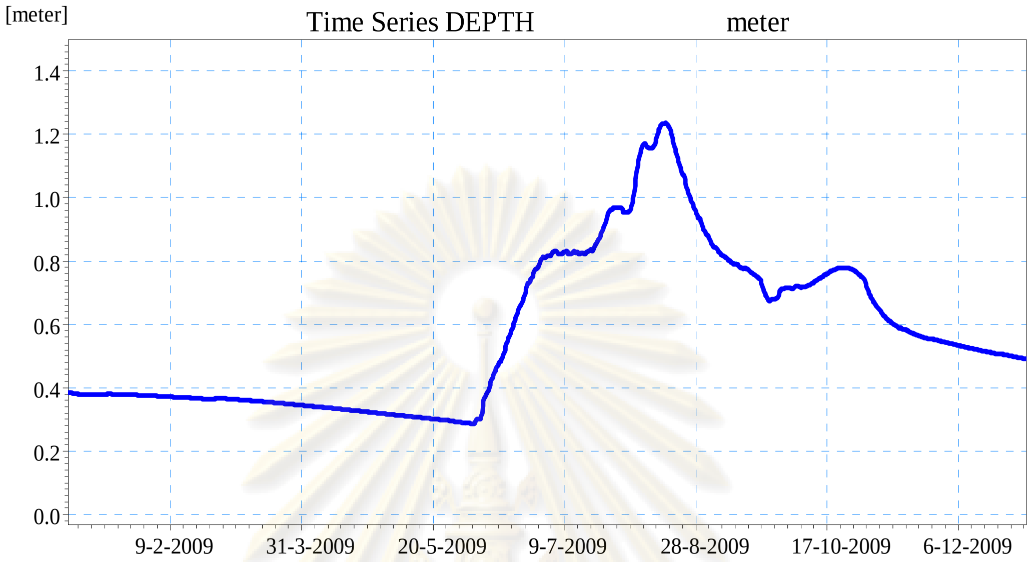

Figure 4-18 Water depth downstream (Station 1)

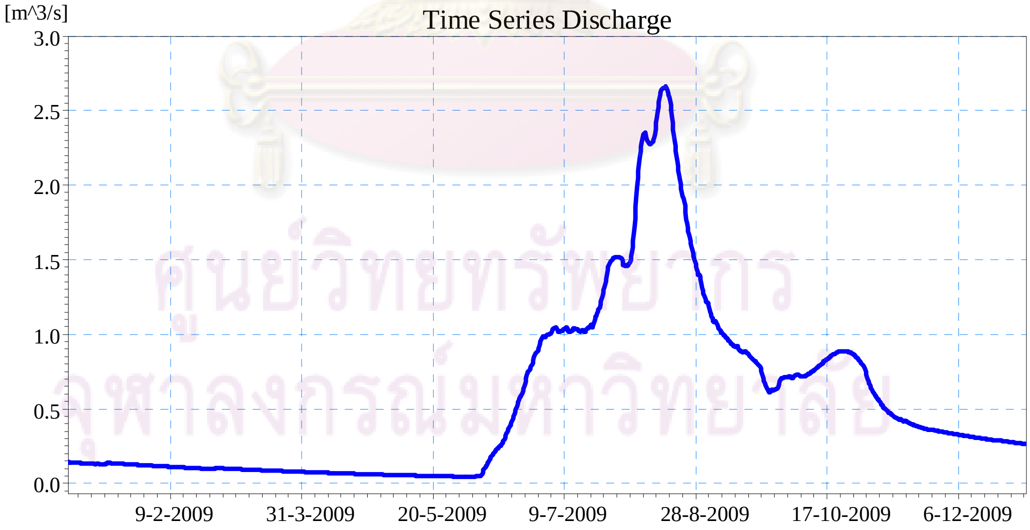

Figure 4-19 Water discharge downstream (Station 1)

A chart summarizing the total water balance in the study area is given in Figure 4-20. 1734 mm of rainfall precipitated in the area in 2009. Approximately 878 mm (50.63%) of it was evapotranspiration, making evapotranspiration the largest compartment in the water cycle. 838 mm of water infiltrated from the unsaturated zone to the saturated zone; however, 523 mm evaporated and infiltrated up to the unsaturated zone. In addition, 41 mm of unsaturated water flowed out of the area as boundary flow, whereas 23 mm of the saturated flow drained out of the saturated zone. According to the river system, 93 mm of water went as overland flow into the river, while 189 mm of groundwater drained into the river.

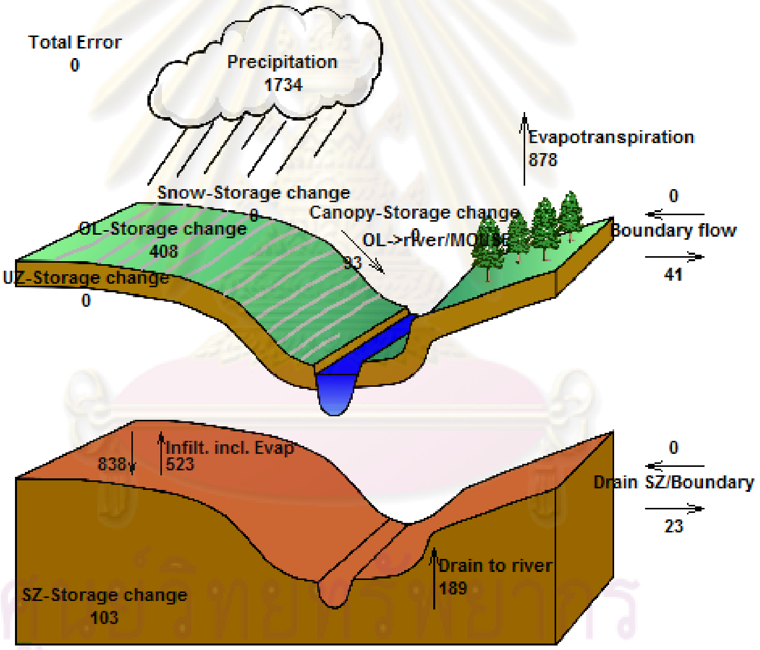

Figure 4-20 Total water balance chart of the Mae Tao subcatchment in year 2009 (unit: mm)

In addition, the maximum values of water depth and water discharge of each station along Mae Tao Creek are presented in Table 4-8.

Table 4-8 Maximum values of water depth and water discharge at each station

Station	Date	Water depth (m)	Water discharge (m^3/s)
1	16/08/09	1.236	2.661
2	16/08/09	1.298	2.660
3	16/08/09	0.768	2.496
4	16/08/09	0.960	2.183
5	16/08/09	0.527	0.298
6	16/08/09	0.636	2.069
7	15/08/09	0.632	1.247
8	15/08/09	0.743	1.080
9	15/08/09	0.291	0.944
10	17/08/09	0.165	0.124

4.3.2 Uncertainty Analysis

Since the input data of the study were inadequate, an uncertainty analysis was needed for assessing the confidence level of the results. The uncertainty analysis graphs of the compartments in the total water balance chart are presented in Figure 4-21 to Figure 4-29.

The parameters that applied in the uncertainty analysis include the following:

- Drain level: It is determined from a saturated zone layer from which drain water is extracted. It is stage routing surface drainage calculated from the drainage levels in each cell. Thus, the drain flow continues until it crosses a river or the model boundary.

- Saturated hydraulic conductivity of unsaturated zone: It is a function of the soil texture. It represents the ease at which the water can flow through the soil. It decreases as the moisture content decreases from the saturated condition. The experimental procedure for measure hydraulic conductivity is rather difficult and not very reliable.
- Lower level: It is applied to define the bottom of the geologic layers and lenses. This level is used to interpolate geologic and source properties to the model cells.

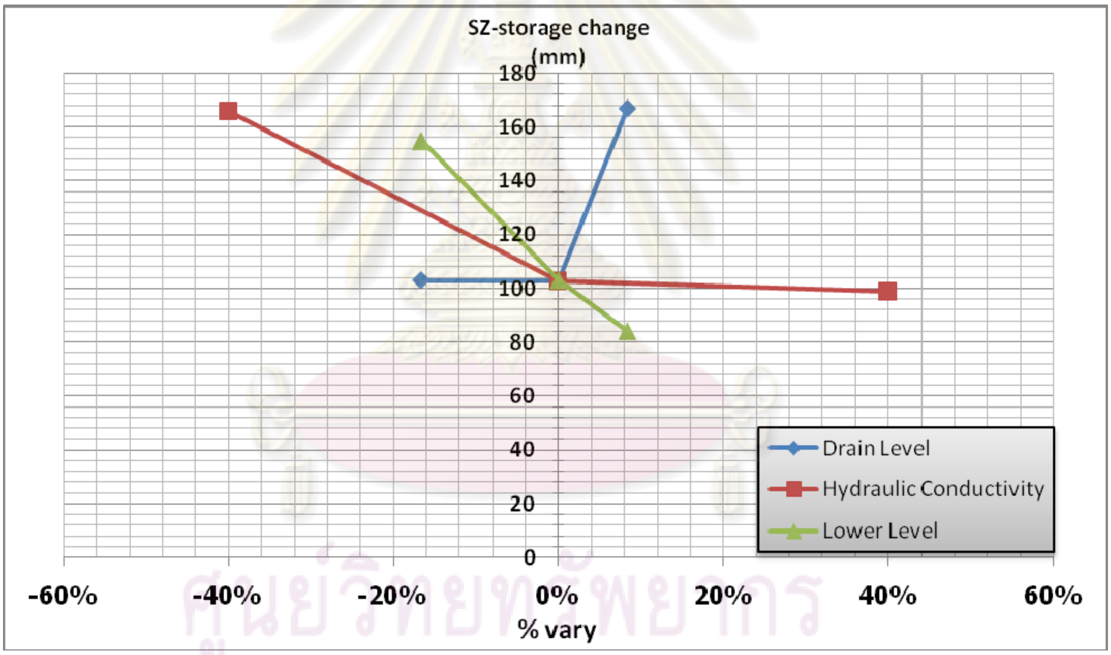

Figure 4-21 Uncertainty analysis of saturated zone-storage changes

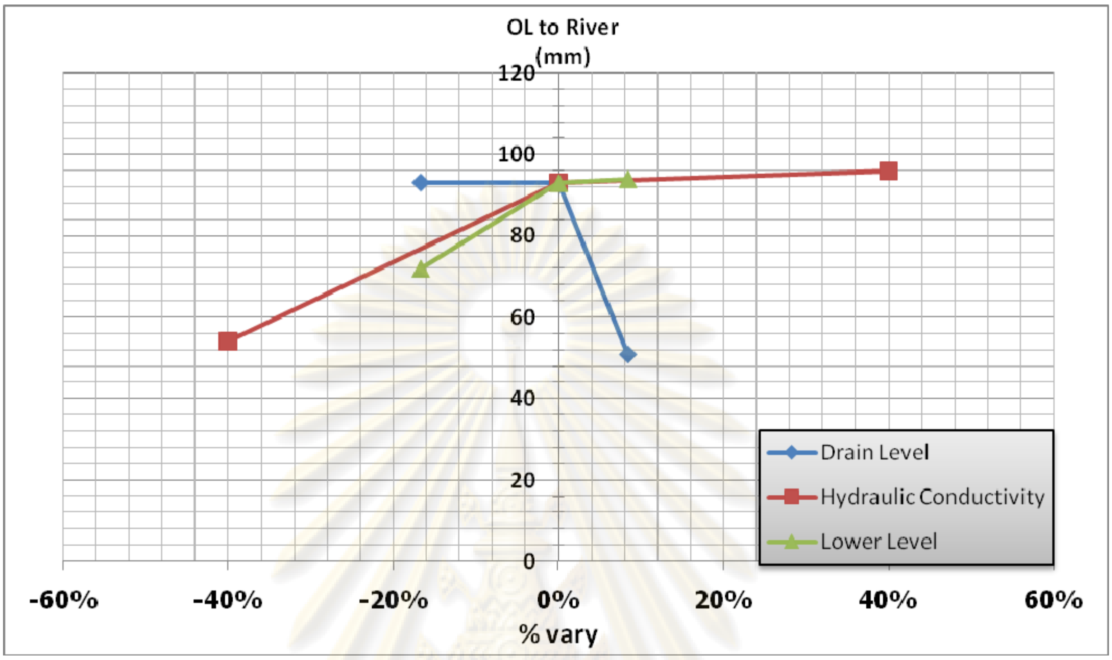

Figure 4-22 Uncertainty analysis of the overland flow to the river

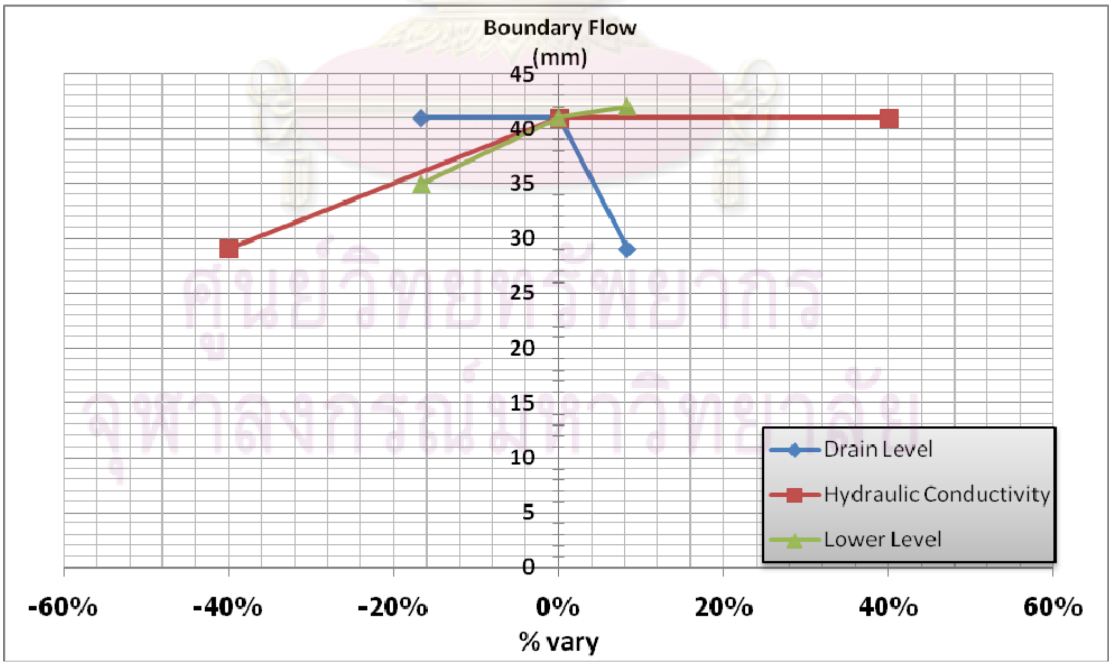

Figure 4-23 Uncertainty analysis of boundary flow in the unsaturated zone

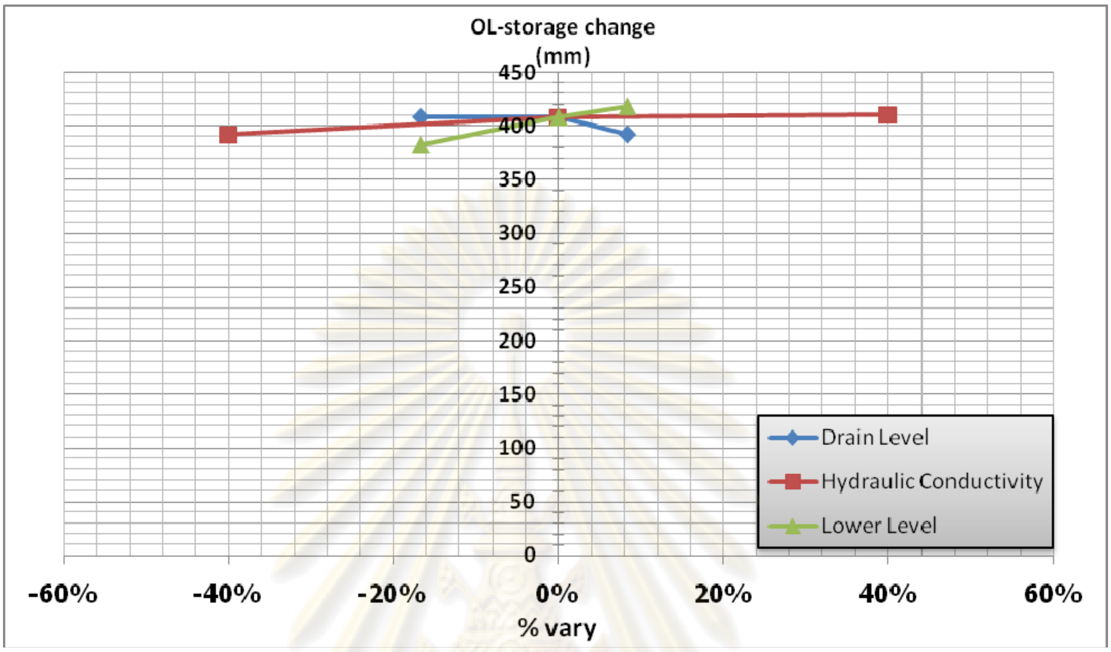

Figure 4-24 Uncertainty analysis of overland flow-storage changes

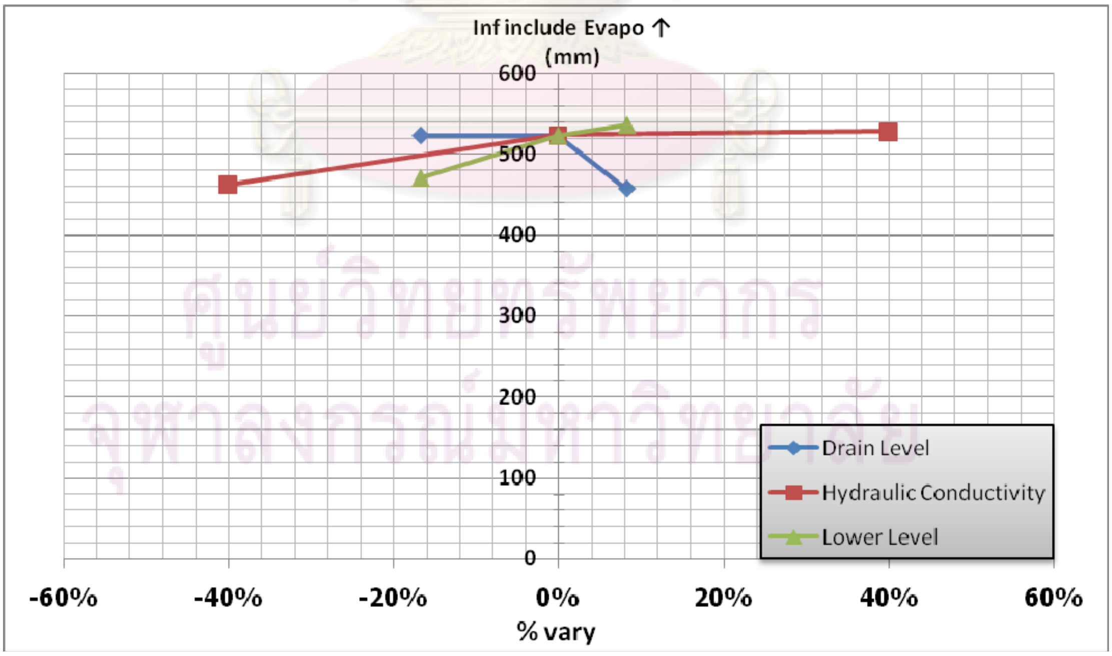

Figure 4-25 Uncertainty analysis of infiltration including evapotranspiration (upward)

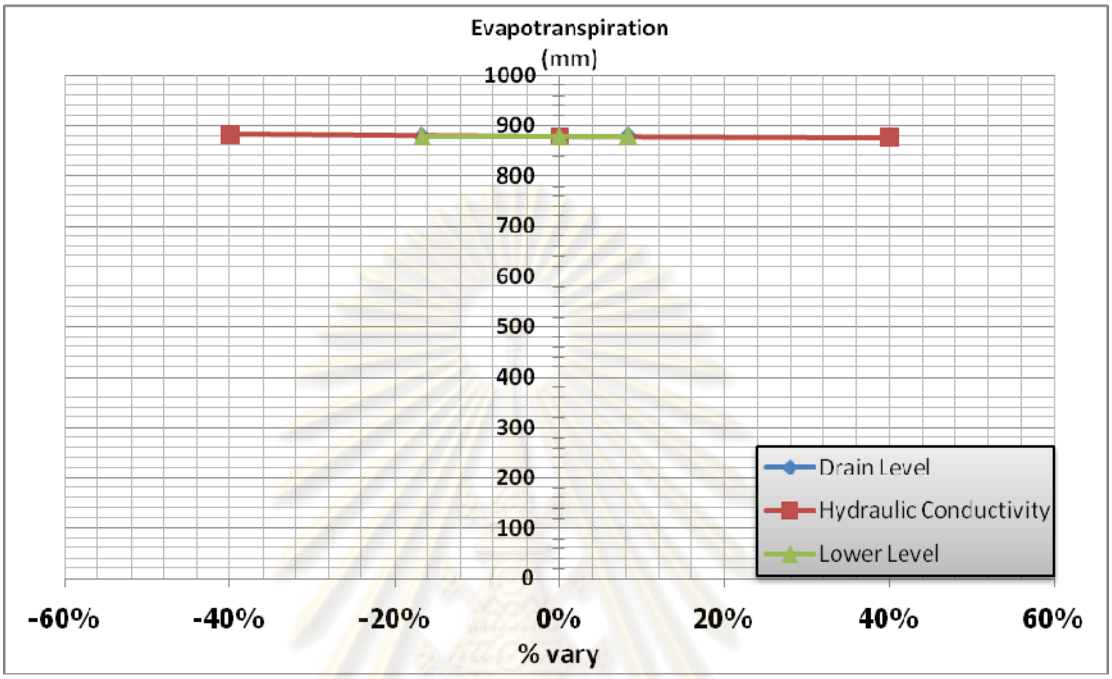

Figure 4-26 Uncertainty analysis of evapotranspiration

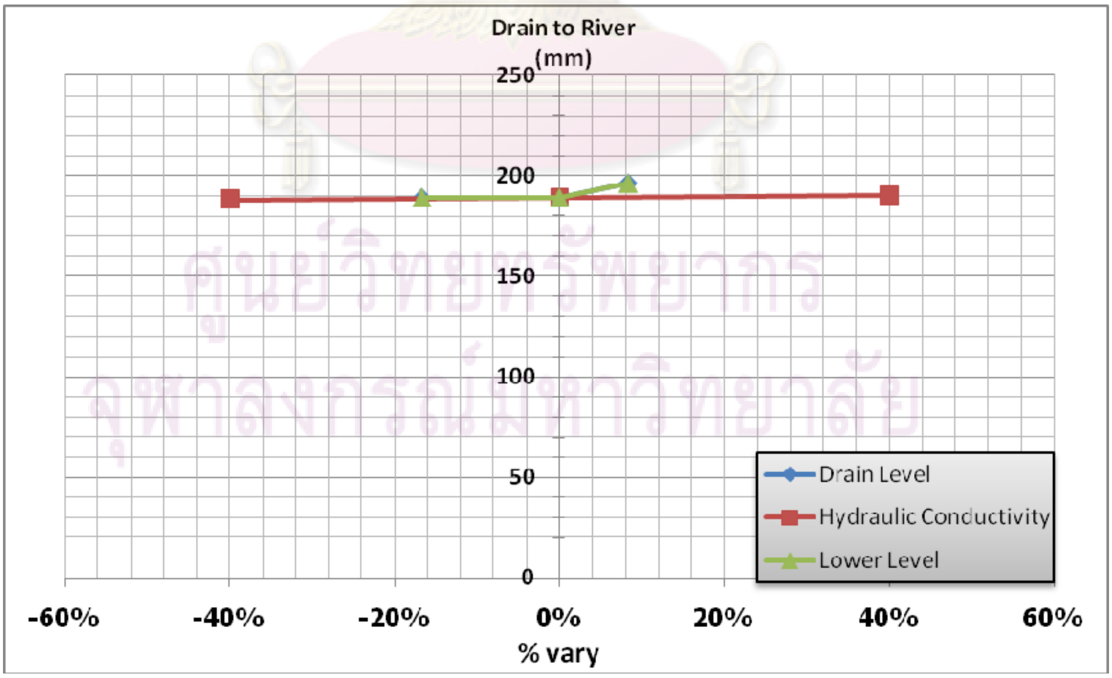

Figure 4-27 Uncertainty analysis of groundwater drainage to the river

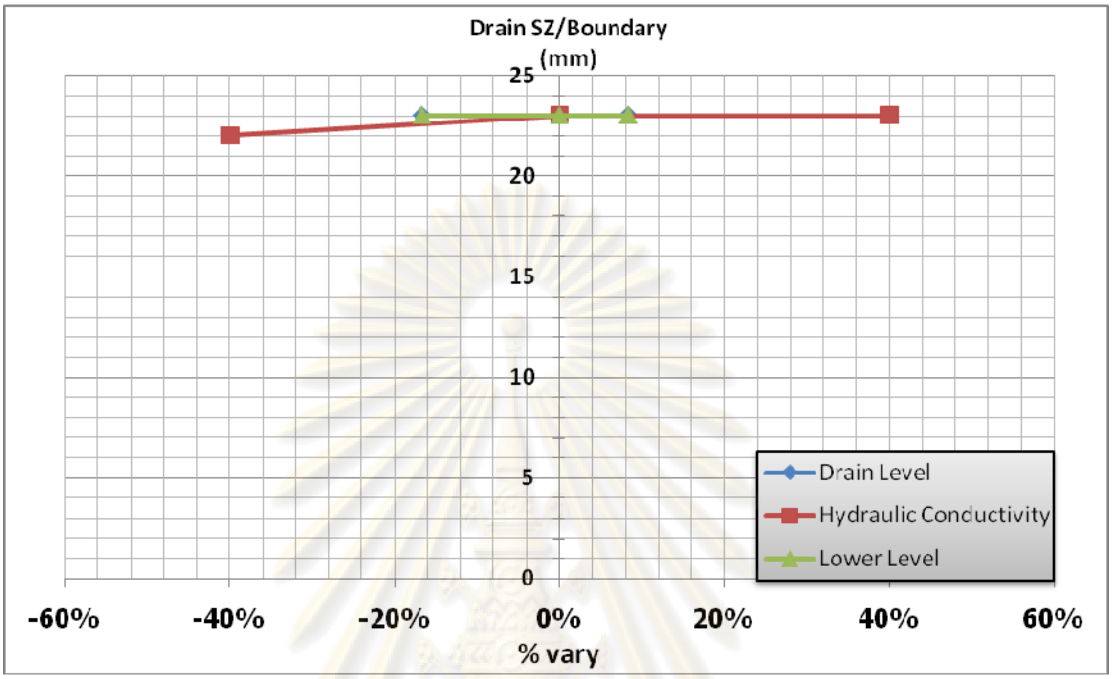

Figure 4-28 Uncertainty analysis of boundary flow out from the saturated zone

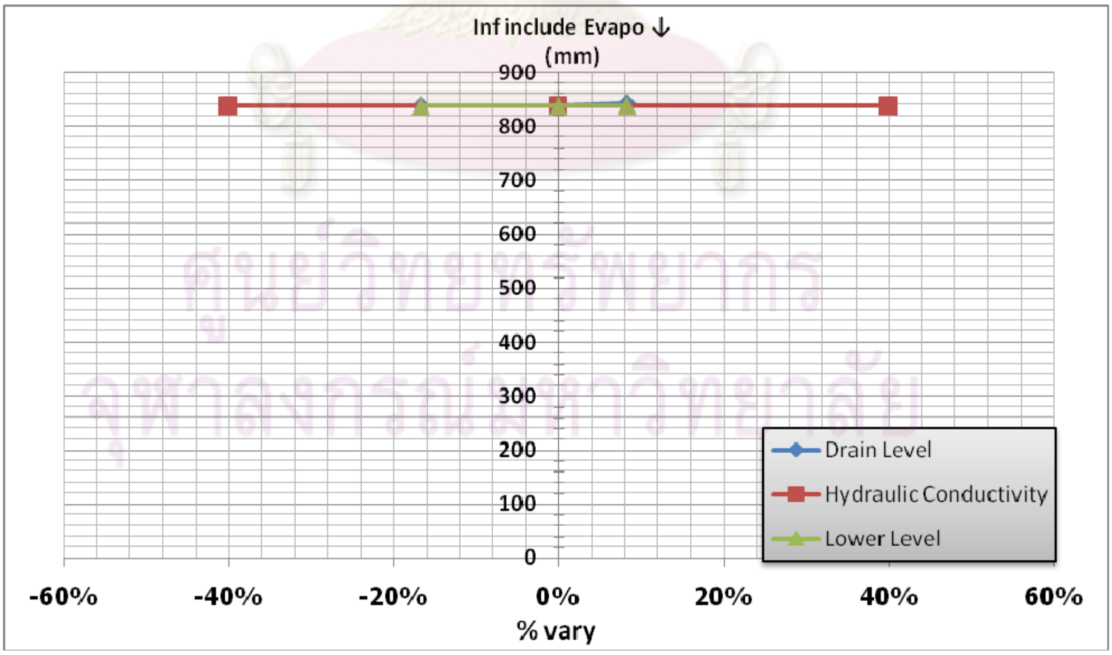

Figure 4-29 Uncertainty analysis of infiltration including evapotranspiration (downward)

At a low drainage level stage, groundwater was able to change to the overland flow; thus overland flow-storage change and overland flow to river were greater. In addition, since water in the unsaturated zone was consumed and stored in the saturated zone prior to flowing out as boundary flow, much of the water infiltrated and evaporated in the upward direction.

The higher value of hydraulic conductivity allowed more water to flow in the unsaturated zone and also as boundary flow, while the saturated zone-storage change became less. More infiltration including evapotranspiration in the upward direction could bring about the entrance of surface water into the river system.

The lower level near to the ground also caused the saturated zone near the ground. Less saturated zone-storage change led to more boundary flow in the unsaturated zone. This initiated more changes to overland flow storage and infiltration, including evapotranspiration in the upward direction; thus more surface water was able to flow to river.

Moreover, boundary flow out from the saturated zone and water in the saturated zone draining to river were slightly sensitive compared to the other components, whereas evapotranspiration and downward infiltration including evapotranspiration were mostly insensitive parameters.

Finally, both overland flow to the river and groundwater draining to river were the significant compartments that majorly affected the channel flow. However, since groundwater draining to river was quite insensitive, the overland flow to the river played a key role causing uncertainty in the hydrodynamic results. According to the data in Figure 4-11, low hydraulic conductivity, subjacent lower level, or high stage of drain level was the cause of the low overland flow to the river.

4.3.3 Sediment transport results

After simulating water discharge along Mae Tao Creek, the hydrodynamic results from the MIKE SHE simulation were applied in MIKE 11 with the sediment transport module for computing the time series results for 2009, including sediment transport as displayed in Figure 4-30 and accumulated sediment transport, as shown in

Figure 4-31. Sediment transport could be distinguished by the wet and dry seasons. The sediment transport values in the wet season were much higher than the values in the dry season (see Figure 4-30).

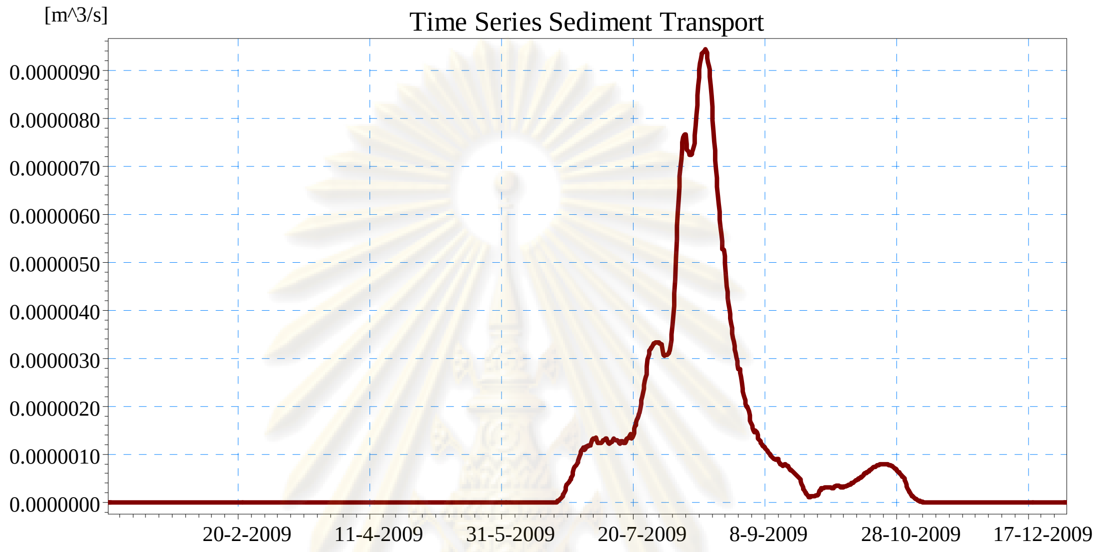

Figure 4-30 Sediment transport rate downstream

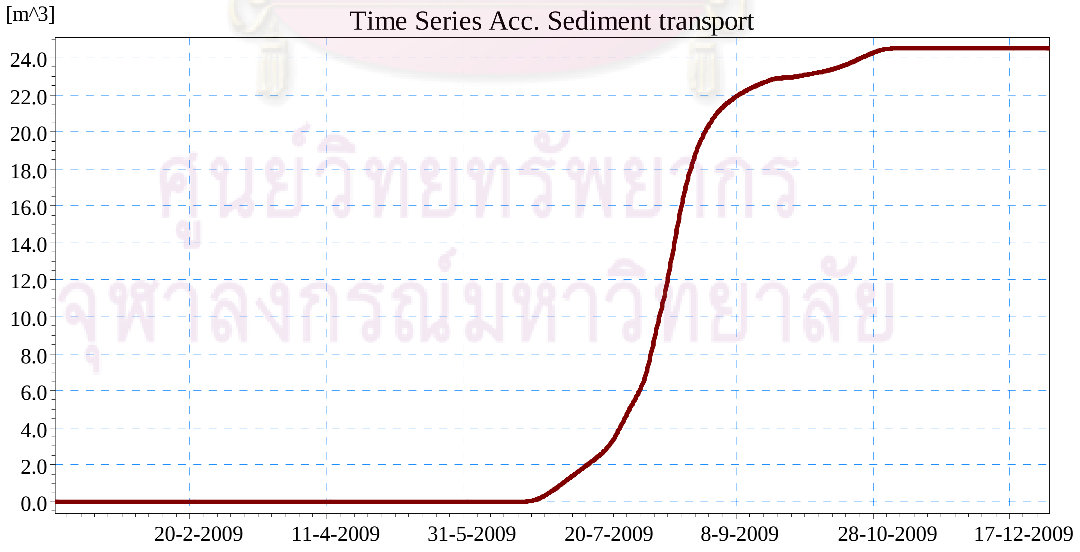

Figure 4-31 Accumulated sediment transport downstream

The 2009 annual accumulated sediment transport downstream was simulated to be 24.522 m^3, while 24.466 m^3 of the sediment transport was accumulated in a storm event from June to October 2009. Thereby, 0.056 m^3 of the accumulated sediment transport in the dry season was determined.

In conclusion, 99.77% of the accumulated sediment transport occurs in the wet season, so it could be said that sediment transport significantly occurs in a storm event.

4.4 Evaluation

Sediment transport rate (m^3/d)--depending on the water discharge--and the cadmium concentration in stream sediment (mg/kg) are the main factors of the cadmium transport rate in the sediment (g/d) as displayed in Eq. (3.66). Table 4-9 shows the maximum values of the sediment transport rate and cadmium transport rate at each station.

Table 4-9 Maximum values of the sediment transport rate and cadmium transport in stream sediment at each station in the study area

Station	Date	Sediment transport (m^3/d)	Cadmium contamination (mg/kg)	Cadmium transport rate (g/d)
1	16/08/09	0.815	33.93	53.18
2	16/08/09	0.572	13.34	14.66
3	16/08/09	6.661	6.07	77.66
4	16/08/09	35.903	28.79	1,987
5	16/08/09	0.007	LD	LD
6	16/08/09	2.894	15.05	83.71
7	15/08/09	5.491	1.12	11.82
8	15/08/09	2.749	1.45	7.645
9	15/08/09	1.188	1.35	3.080
10	17/08/09	0.450	LD	LD

* Assumption: density of wet sediment = 1922 kg/m^3

33.93 mg of cadmium per kg of stream sediment was found at station 1, the outlet of the Mae Tao subcatchment, while the 2009 annual amount of accumulated sediment transport at the downstream was equal to 47.131×10^3 kg (see Figure 4-31). The later value was computed with the following: 24.522 m^3 of accumulated sediment transport and a density of wet sediment assumed to be 1922 kg/m^3. Thus, the annual cadmium transport amount from the Mae Tao subcatchment could be estimated at 1.599 kg for the year 2009.

CHAPTER V

CONCLUSION AND RECOMMENDATIONS

5.1 Conclusion

Field observations in the wet season of 2009 produced the flow measurement results in accordance with the area-velocity method. The water discharge along Mae Tao Creek varied from 0.65 to 2.43 m^3/s. Moreover, water in the creek was slightly alkali (pH = 8.16 to 8.46), therefore cadmium was mostly in the insoluble form and could not be widespread in the body of water. In addition, the hydrological data, which were provided by government departments, and water flow characteristics from field observations were applied together as the inputs of MIKE SHE coupled with MIKE 11 for determining the time series-hydrodynamic results, namely water depth and water discharge for the year 2009. The results show that water depth and water discharge in the wet season were much greater than they were in the dry season.

The stream sediment in Mae Tao Creek classified by the grain size distribution method following the USCS was primarily sand; hence, the non-cohesive sediment transport module in MIKE 11 was applied to acquire the sediment transport results. The simulated results also illustrated the difference between the wet and dry seasons were similar to that of the hydrodynamic results. The accumulated sediment transport at the downstream area in year 2009 was equal to 24.522 m^3, whereas 24.466 m^3 (99.77%) of the sediment was distributed out from the subcatchment in the wet season. As a result, only 0.056 m^3 (0.23%) of accumulated sediment transport was moved from the area in the dry season.

There are two main hydrological components that mainly affect the hydrodynamic results namely the overland flow to the river and groundwater drainage to the river. The uncertainty analysis showed that the overland flow to the river process played a significant role in the stream sediment transport in the area since the groundwater drainage to the river compartment was insensitive to the parameters. Moreover, the unknown impervious layer level might have affected the results.

The Mae Tao subcatchment is a highly contaminated with cadmium area, which was evident by the measured cadmium concentrations in the sediment along the creek. At some upstream stations, the concentrations were detected at around 1.305 mg/kg, representing the notable amount of background cadmium. Concurrently, much higher cadmium levels in stream sediment were discovered in the vicinity of the zinc mines. Thus, the two mines can be identified as the main sources of cadmium contamination in the area. In particular, 33.93 mg of cadmium per kg of stream sediment was detected downstream of the subcatchment (station 1), which was characterized as the most significant station that was responsible for cadmium spreading out from the area.

The spread of cadmium contamination due to stream sediment transport in the Mae Tao subcatchment mainly occurred during storm events. In 2009, approximately 1.599 kg of cadmium was distributed out from Mae Tao subcatchment; this value was calculated using the annual accumulated sediment transport value of 24.522 m^3 and the cadmium per kg of stream sediment value of 33.93 mg. This circumstance may intensively aggravate cadmium contamination problems in the area as well as conterminous areas.

5.2 Recommendations

The cadmium concentration at each position along Mae Tao Creek could help the screening locations of the contaminated area. Thus, there should be some suggestions for the locals to solve the cadmium contamination problems. For example, eatable plants, especially rice, should be prohibited from being cultivated in any area with a high potential of cadmium contamination, i.e., one located downstream from a zinc deposit. Constructing a weir would also be a great choice for slowing the movement of sediment. A suggested location for a weir is around station 4 so that the sediment can be blocked after moving out from the zinc deposit. The sediment might be excavated for sediment treatment. Finally, project evaluations should be conducted after running applicable projects for monitoring the cadmium concentration.

Since MIKE SHE is the integrated hydrological model extensively covering all hydrological processes, much data and details of the study area are required. However, in this study there was uncertainty in the results due to insufficient information on the system. Therefore, large amount of input data should be provided to get more reliable simulated results. As well as, the sediment transport modules and equations applied in the model should be scrutinized in more detail.

Even though the cadmium concentration in stream sediment was higher than the concentration in suspended sediment, the cadmium contaminated suspended sediment could still pose health risks. Thus, suspended sediment should be studied in the future.

REFERENCES

Ali, M., Ali, R., Hodgson, G., Juul, M., and Nikraz, H. 2008. MIKE SHE Integrated Hydrological Modelling (One Water – One Resource – One Model) [slide]. Clayton South, Victoria, Australia: CSIRO Land and Water.

American Society for Testing and Materials (ASTM) International. 2009. ASTM C136 - 06 Standard Test Method for Sieve Analysis of Fine and Coarse Aggregates [Online]. Available from: http://www.astm.org/Standards/C136.htm [2009, August 1]

American Society for Testing and Materials (ASTM) International. 2009. ASTM D422 - 63(2007) Standard Test Method for Particle-Size Analysis of Soils [Online]. Available from: http://www.astm.org/Standards/D422.htm [2009, August 1]

American Society for Testing and Materials (ASTM) International. 2009. ASTM D2487 - 10 Standard Practice for Classification of Soils for Engineering Purposes (Unified Soil Classification System) [Online]. Available from: http://www.astm.org/Standards/D2487.htm [2009, August 1]

Anan Paengnoy. 2004. Aid ‘depends on central govt action’ [Online]. Available from: http://library.pcd.go.th/Multimedia/News/2547/7/26/4.pdf [2009, July 2] (in Thai)

Anan Paengnoy. 2004. Mae Sot's deadly harvest [Online]. Available from: http://library.pcd.go.th/Multimedia/News/2547/7/26/4.pdf [2009, July 2] (in Thai)

Anderson, M. P., and Woessner, W. W. 1992. Applied Groundwater Modeling: Simulation of Flow and Advective Transport. San Diego: Academic Press.

Bear, J. 1972. Dynamics of Fluids in Porous Media. New York: Dover Publications.

Brassington, R. 1988. Field Hydrogeology. Milton Keynes: Open University Press.

Cunderlik, J. 2003. Hydrologic Model Selection for the CFCAS Project: Assessment of Water Resource Risk and Vulnerability to Changing Climatic Condition. [Online]. Available from: http://www.eng.uwo.ca/research/iclr/fids/publications/cfcas-climate/reports/Report%20I.pdf [2009, July 1]

DHI Water • Environment • Health. 2009. MIKE 11 Reference Manual. Hørsholm, Denmark: DHI.

DHI Water • Environment • Health, 2009. MIKE 11 Short Introduction Tutorial version 2009. Hørsholm, Denmark: DHI.

DHI Water • Environment • Health, 2009. MIKE 11 User Guide. Hørsholm, Denmark: DHI.

DHI Water • Environment • Health, 2009. MIKE SHE – Basic Exercises. Hørsholm, Denmark: DHI.

DHI Water • Environment • Health, 2009. MIKE SHE User Manual – Volume 1: User Guide. Hørsholm, Denmark: DHI.

DHI Water • Environment • Health, 2009. MIKE SHE User Manual – Volume 2: Reference Guide. Hørsholm, Denmark: DHI.

Friberg, L., Piscator, M., Nordberg, G. F., Kjellstrom, T. 1976. Cadmium in the Environment. 2nd edition. Cleveland, Ohio: CRC Press.

Fulkerson, W., and Goeller, H.E. 1973. Cadmium: the Dissipated Element. Oak Ridge, Tennessee: Oak Ridge National Laboratory.

Haas, E. M., 2003. Staying Healthy with Nutrition: The Complete Guide to Diet and Nutritional Medicine: Berkeley, California: Celestial Arts.

International Cadmium Association, 2009. Cadmium [Online]. Available from: http://www.cadmium.org [2009, April 1]

Johnson, A. I., 1967. Specific yield - compilation of specific yields for various materials. U.S. Geological Survey Water Supply Paper 1662-D: 74.

Liu, W., Yang, Y. S., Zhou, Q., Xie, L., Li, P., and Sun, T., 2007. Impact assessment of cadmium contamination on rice (*Oryza sativa* L.) seedlings at molecular and population levels using multiple biomarkers. Chemophere 67 (2007): 1155-1163.

Ministry of Environmental and Forest (India), Central Pollution Control Board. 2007. Cadmium Levels In Environment [Online]. Available from: http://www.cpcb.nic.in/oldwebsite/News%20Letters/Latest/cadmium/ch8-CADMIUM.htm [2009, April 1]

Ministry of Industry, Department of Primary Industries and Mines. 2006. Study of the causes of cadmium contamination in soil in Mae Sot district, Tak province. Bangkok. (in Thai)

Ministry of Natural Resources and Environment, Department of Water Resources. XXX. Study of cadmium contamination in Mae Tao subcatchment, Mae Sot district, Tak province [Online]. Available from: http://www.waterlab-dwr.com/wizContent.asp?wizConID=100&txtmMenu_ID=7 [2009, 1 April]

Ministry of Science and Technology, Pollution Control Department. 1998. Cadmium. 2nd edition. Bangkok: Integrated Promotion Technology (in Thai)

Ministry of Science and Technology, Pollution Control Department. 2009. Thai Environment Regulations [Online]. Available from: http://www.pcd.go.th/info_serv/en_regulation.html [2009, May 5]

Parada Maneewong. 2005. Cadmium distribution in stream sediment and suspended solids along Huai Mae Tao and Huai Mae Ku, Mae Sot district, Tak province. Master’s Thesis, Environmental Management Graduate School Chulalongkorn University.

Piotrowski, J. K. and Coleman, D. O. 1980. Environmental hazards of heavy metals: Summary evaluation of lead, cadmium and mercury. London: Monitoring and Assessment Research Centre (MARC).

Piyarat Kaowichakorn. 2006. GIS Application For Mineral Resource And Envionmental Management: Case Study On Zinc Deposit, Mae Sot district, Tak province. Master’s Thesis, Environmental Management Graduate School Chulalongkorn University.

Refsgaard, A. and Kjelds, J. 2001. MIKE SHE groundwater model selected as best management tool in US [Online]. Available from: http://www.dhigroup.com/News/NewsArchive/2001/MIKESHEGroundwaterModelSelectedAsBestManagementToolInUS.aspx [2009, March 22]

Reuters. Thailand backs away from rice cartel plan. The International Herald Tribune (7 May 2008)

Scheffer, B. and Blankenburg, J. 1993. The determination of the bulk density of peat soils. Agricultural and Biological Research 46: 46–53.

Schnoor, J. L. 1996. Environmental Modeling: fate and transport of pollutants in water, air, and soil. New York: John Wiley & Sons, Inc.

Simmons, R. W., Noble, A. D., Pongsakul, P., Sukreeyapongse, O., and Chinabut, N. 2009. Cadmium-hazard mapping using a general linear regression model (Irr-Cad) for rapid risk assessment. Environmental Geochemistry and Health. 31: 71-79.

The Nations. 2004. Tak villagers to be tested for Cadmium [Online]. Available from: http://library.pcd.go.th/Multimedia/News/2548/6/27/9.pdf [2009, July 2] (in Thai)

United States Environmental Protection Agency. 2009. Method 3051A Microwave Assisted Acid Digestion of Sediments, Sludge, Soils, and Oils [Online]. Available from: http://www.quimlab.com.br/PDF-LA/Digest%E3o%20de%20amostras%20por%20microondas.pdf [2009, October 10]

United States Public Health Service, Agency for Toxic Substances and Disease Registry. 1993. Cadmium [Online]. Available from: http://www.eco-usa.net/toxics/cadmium.shtml [2009, February 3]

United States Public Health Service, Agency for Toxic Substances and Disease Registry. 2008. Toxicological Profile For Cadmium [Online]. Available from: http://www.atsdr.cdc.gov/toxprofiles/tp5.html [2009, February 3]

Vinit Chovichien. 2004. Soil Mechanics. 7th edition. Bangkok: Vinit Chovichien. (in Thai)

Yan, J. and Zhang, J. 1999. Evaluation of the MIKE SHE Modeling System. Agricultural non-point source water quality models 2004: 83-91.

Yunus, R., 2005. Fate and Transport of Contaminants: Lecture 4 [slide]. Malaysia: Universiti Putra Malaysia: Department of Chemical and Environmental Engineering.

Zarcinas, B. A., Pichit Pongsakul, McLaughlin, M. J., and Cozens, G. 2003. Heavy metals in soils and crops in South East Asia. 2. Thailand. Environmental Geochemistry and Health 26: 359-371.

APPENDICES

APPENDIX A

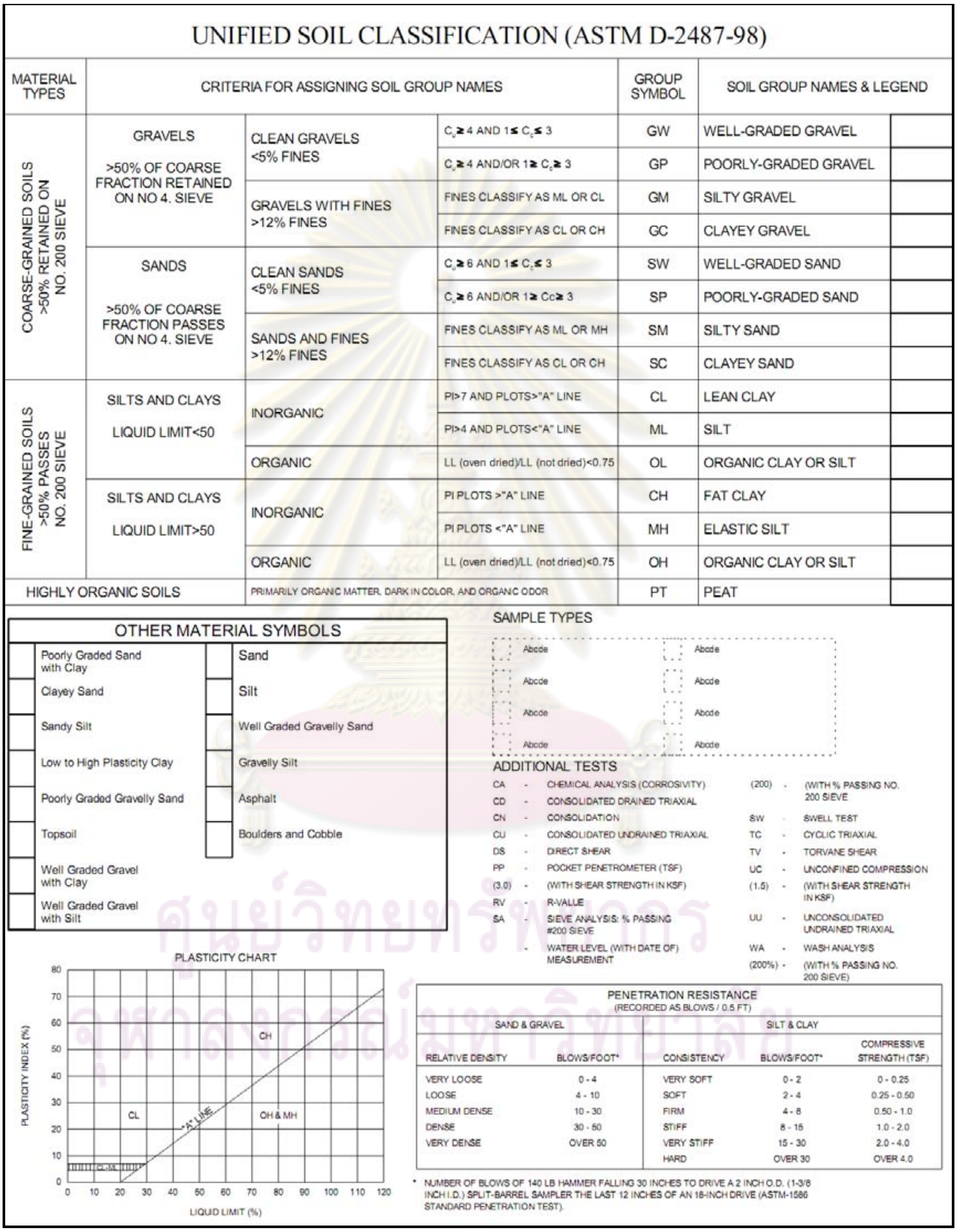

UNIFIED SOIL CLASSIFICATION (ASTM D-2487-98)

MATERIAL TYPES	CRITERIA FOR ASSIGNING SOIL GROUP NAMES			GROUP SYMBOL	SOIL GROUP NAMES & LEGEND	
COARSE-GRAINED SOILS >50% RETAINED ON NO. 200 SIEVE	GRAVELS >50% OF COARSE FRACTION RETAINED ON NO 4. SIEVE	CLEAN GRAVELS <5% FINES	$C_u \geq 4$ AND $1 \leq C_c \leq 3$	GW	WELL-GRADED GRAVEL	
			$C_u \geq 4$ AND/OR $1 \geq C_c \geq 3$	GP	POORLY-GRADED GRAVEL	
		GRAVELS WITH FINES >12% FINES	FINES CLASSIFY AS ML OR CL	GM	SILTY GRAVEL	
			FINES CLASSIFY AS CL OR CH	GC	CLAYEY GRAVEL	
	SANDS >50% OF COARSE FRACTION PASSES ON NO 4. SIEVE	CLEAN SANDS <5% FINES	$C_u \geq 6$ AND $1 \leq C_c \leq 3$	SW	WELL-GRADED SAND	
			$C_u \geq 6$ AND/OR $1 \geq Cc \geq 3$	SP	POORLY-GRADED SAND	
		SANDS AND FINES >12% FINES	FINES CLASSIFY AS ML OR MH	SM	SILTY SAND	
			FINES CLASSIFY AS CL OR CH	SC	CLAYEY SAND	
FINE-GRAINED SOILS >50% PASSES NO. 200 SIEVE	SILTS AND CLAYS LIQUID LIMIT<50	INORGANIC	PI>7 AND PLOTS>"A" LINE	CL	LEAN CLAY	
			PI>4 AND PLOTS<"A" LINE	ML	SILT	
		ORGANIC	LL (oven dried)/LL (not dried)<0.75	OL	ORGANIC CLAY OR SILT	
	SILTS AND CLAYS LIQUID LIMIT>50	INORGANIC	PI PLOTS >"A" LINE	CH	FAT CLAY	
			PI PLOTS <"A" LINE	MH	ELASTIC SILT	
		ORGANIC	LL (oven dried)/LL (not dried)<0.75	OH	ORGANIC CLAY OR SILT	
HIGHLY ORGANIC SOILS		PRIMARILY ORGANIC MATTER, DARK IN COLOR, AND ORGANIC ODOR		PT	PEAT	

OTHER MATERIAL SYMBOLS

	Poorly Graded Sand with Clay		Sand
	Clayey Sand		Silt
	Sandy Silt		Well Graded Gravelly Sand
	Low to High Plasticity Clay		Gravelly Silt
	Poorly Graded Gravelly Sand		Asphalt
	Topsoil		Boulders and Cobble
	Well Graded Gravel with Clay		
	Well Graded Gravel with Silt		

SAMPLE TYPES

Abcde	Abcde
Abcde	Abcde
Abcde	Abcde
Abcde	Abcde

ADDITIONAL TESTS

CA	-	CHEMICAL ANALYSIS (CORROSIVITY)	(200)	-	(WITH % PASSING NO. 200 SIEVE
CD	-	CONSOLIDATED DRAINED TRIAXIAL			
CN	-	CONSOLIDATION	SW	-	SWELL TEST
CU	-	CONSOLIDATED UNDRAINED TRIAXIAL	TC	-	CYCLIC TRIAXIAL
DS	-	DIRECT SHEAR	TV	-	TORVANE SHEAR
PP	-	POCKET PENETROMETER (TSF)	UC	-	UNCONFINED COMPRESSION
(3.0)	-	(WITH SHEAR STRENGTH IN KSF)	(1.5)	-	(WITH SHEAR STRENGTH IN KSF)
RV	-	R-VALUE			
SA	-	SIEVE ANALYSIS: % PASSING #200 SIEVE	UU	-	UNCONSOLIDATED UNDRAINED TRIAXIAL
	-	WATER LEVEL (WITH DATE OF) MEASUREMENT	WA	-	WASH ANALYSIS
			(200%)	-	(WITH % PASSING NO. 200 SIEVE)

PENETRATION RESISTANCE
(RECORDED AS BLOWS / 0.5 FT)

SAND & GRAVEL		SILT & CLAY		
RELATIVE DENSITY	BLOWS/FOOT*	CONSISTENCY	BLOWS/FOOT*	COMPRESSIVE STRENGTH (TSF)
VERY LOOSE	0 - 4	VERY SOFT	0 - 2	0 - 0.25
LOOSE	4 - 10	SOFT	2 - 4	0.25 - 0.50
MEDIUM DENSE	10 - 30	FIRM	4 - 8	0.50 - 1.0
DENSE	30 - 50	STIFF	8 - 15	1.0 - 2.0
VERY DENSE	OVER 50	VERY STIFF	15 - 30	2.0 - 4.0
		HARD	OVER 30	OVER 4.0

* NUMBER OF BLOWS OF 140 LB HAMMER FALLING 30 INCHES TO DRIVE A 2 INCH O.D. (1-3/8 INCH I.D.) SPLIT-BARREL SAMPLER THE LAST 12 INCHES OF AN 18-INCH DRIVE (ASTM-1586 STANDARD PENETRATION TEST).

Figure A-1 Unified Soil Classification Sheet

APPENDIX B

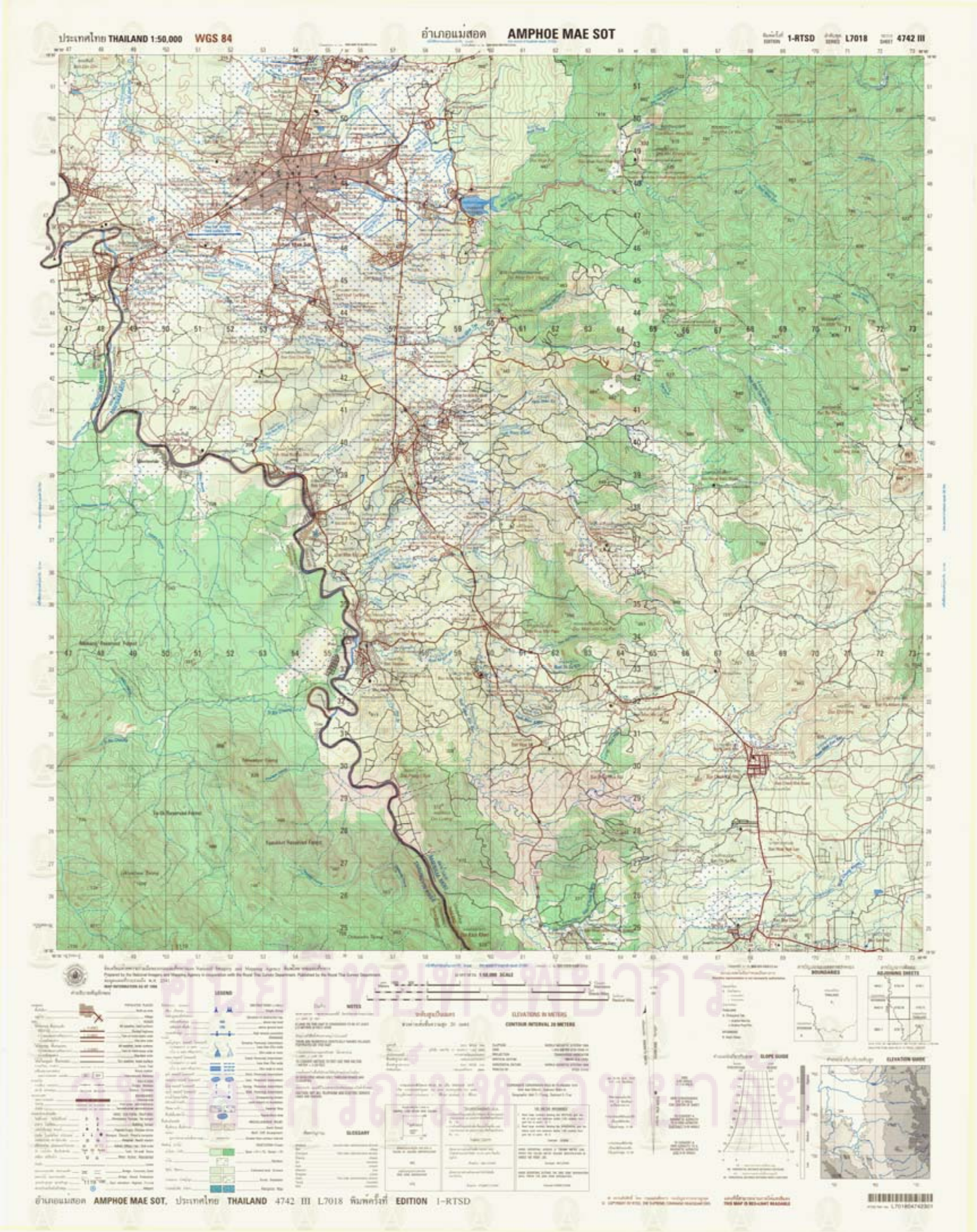

Figure B-1 **The topographic map 1:50,000 scale, sheet 4742III, series L7018, edition 1-RTSD**

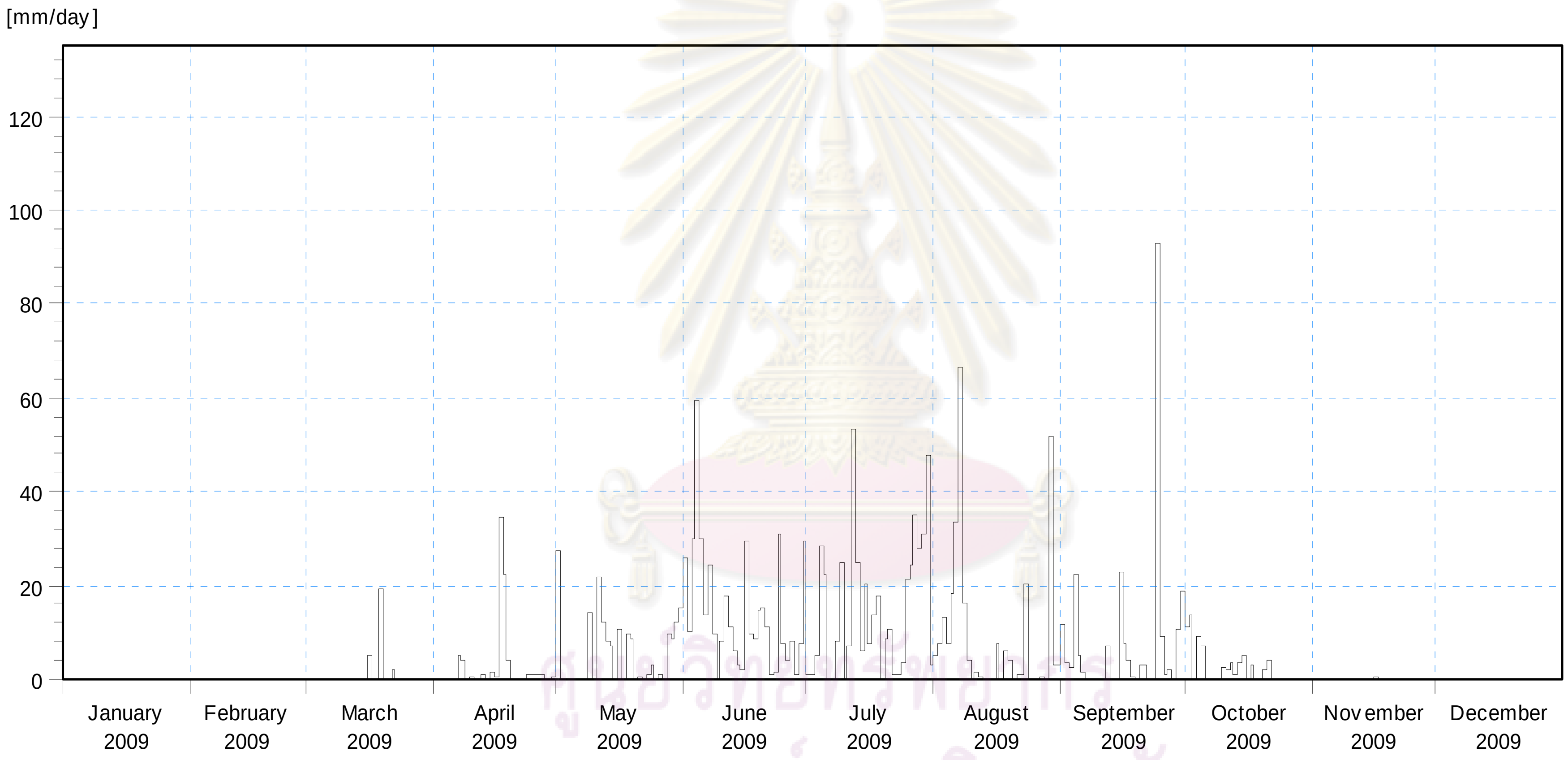

Figure B-2 Rainfall rate in year 2009 (unit: mm/day) (TMD)

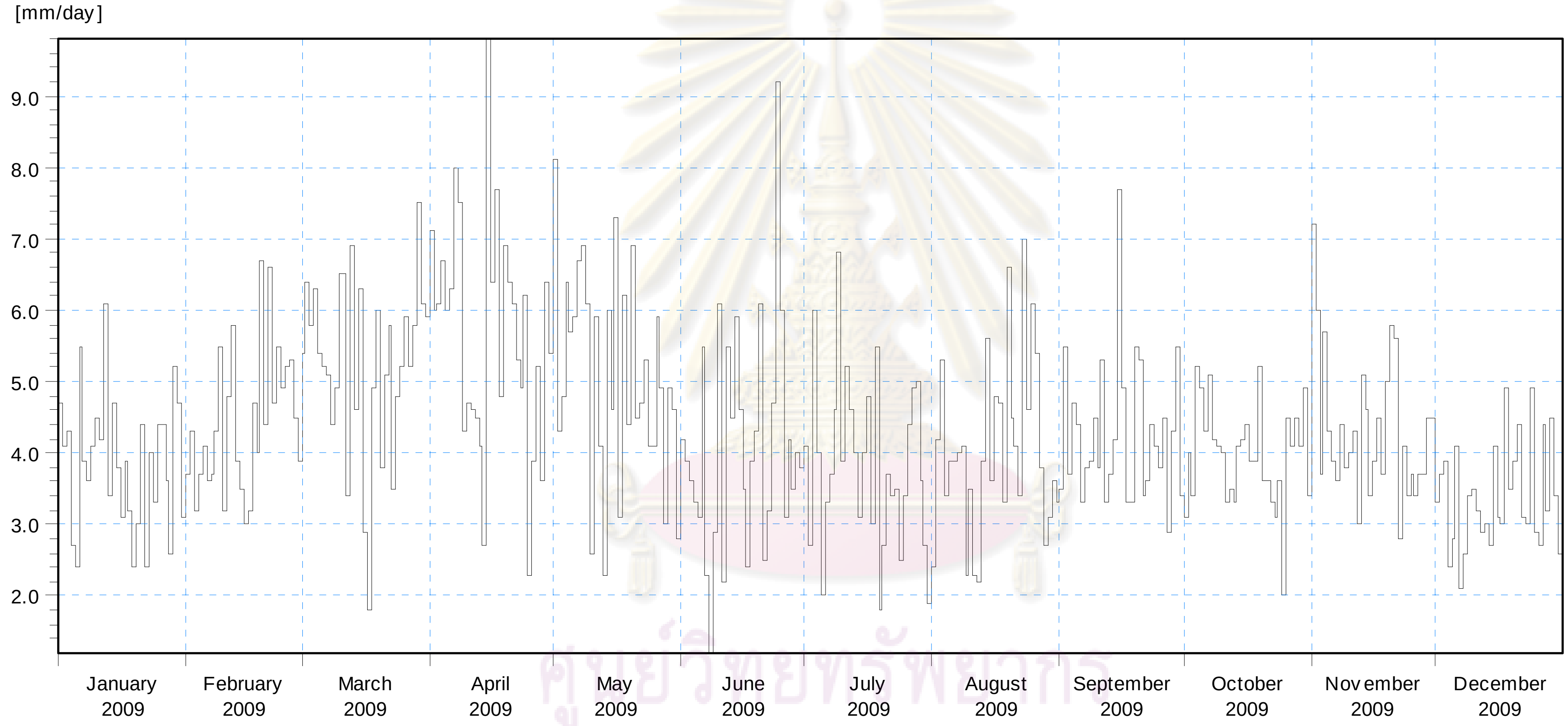

Figure B-3 Evaporation rate in year 2009 (unit: mm/day) (TMD)

Table B-1 Daily rainfall rate data in year 2009 (unit: mm/d) (TMD)

Date	**Jan**	**Feb**	**Mar**	**Apr**	**May**	**Jun**	**Jul**	**Aug**	**Sep**	**Oct**	**Nov**	**Dec**
1	0	0	0	0	0.3	15.3	29.3	2.9	3	18.9	0	0
2	0	0	0	0	27.2	26.1	1	4.9	11.9	11.1	0	0
3	0	0	0	0	0	10.3	1.1	7.6	3.5	13.9	0	0
4	0	0	0	0	0	29.9	4.9	13.1	2.6	0.1	0	0
5	0	0	0	0	0	59.6	28.5	7.4	22.1	9	0	0
6	0	0	0	0	0	29.8	22.3	18.1	5.2	7.3	0	0
7	0	0	0	0	0	13.8	0	33.4	1.6	0	0	0
8	0	0	0	5.1	0	24.6	0	66.7	0	0	0	0
9	0	0	0	4.3	0	9.5	7.9	16.1	0	0	0	0
10	0	0	0	0.2	14	0	24.7	4	0	0	0	0
11	0	0	0	0.5	0.2	8	0.1	0	0	2.5	0	0
12	0	0	0	0	21.9	18	7.2	1.3	0	1.9	0	0
13	0	0	0	0	12.4	11	53.3	0.4	6.9	3.6	0	0
14	0	0	0	1.2	7.9	6.1	24.8	0	0.2	1.2	0	0
15	0	0	0	0.2	7	2.8	5.9	0	0	3.6	0	0

Date	Jan	Feb	Mar	Apr	May	Jun	Jul	Aug	Sep	Oct	Nov	Dec
16	0	0	0	1.3	0.1	1.9	20.5	0	23.1	5	0	0
17	0	0	5	0.3	10.9	29.5	7.7	7.6	7.8	0	0.3	0
18	0	0	0.1	34.7	0	9.6	13.6	0	3.9	2.8	0	0
19	0	0	0	22.3	9.9	8.6	17.6	6.1	0.4	0	0	0
20	0	0	19.5	4.2	8.4	14.8	0.2	4.1	0	0	0	0
21	0	0	0	0	0	15.3	8.5	0.2	3	1.9	0	0
22	0	0	0	0	0.5	11.3	10.8	0.9	3	4.2	0	0
23	0	0	2.2	0	0	1.2	1.1	1	0	0	0	0
24	0	0	0	0	0.9	1.4	0.8	20.4	0	0	0	0
25	0	0	0	1.2	3.1	30.8	3.5	0.1	92.7	0	0	0
26	0	0	0	0.9	0	7.8	21.1	0	9.3	0	0	0
27	0	0	0	0.8	1	4.3	24.2	0	1.1	0	0	0
28	0	0	0	0.8	0	8.3	34.9	0.5	1.8	0	0	0
29	0	-	0	0	9.4	1.2	28.1	0.2	0	0	0	0
30	0	-	0	0	8.5	7.5	31.2	52	10.8	0	0	0
31	0	-	0	-	12	-	47.7	3.1	-	0	-	0

Table B-2 Daily evaporation rate data in year 2009 (unit: mm/d) (TMD)

Date	Jan	Feb	Mar	Apr	May	Jun	Jul	Aug	Sep	Oct	Nov	Dec
1	4.2	3.1	3.9	5.9	5.4	2.8	3.8	1.9	3.3	3.4	3.4	4.5
2	4.7	3.7	5.4	7.1	8.1	4.2	4.1	2.4	3.5	3.1	7.2	3.3
3	4.1	4.3	6.4	6.0	4.3	N/A	2.7	4.2	5.5	4.0	6.0	3.7
4	4.3	3.2	5.8	6.1	4.8	3.6	6.0	5.3	3.7	3.4	3.7	3.9
5	2.7	3.7	6.3	6.7	6.4	N/A	N/A	3.4	4.7	5.2	5.7	2.4
6	2.4	4.1	5.4	6.0	5.7	3.1	2.0	3.9	4.4	4.9	4.3	2.8
7	5.5	3.6	5.2	6.3	5.9	5.5	3.3	N/A	3.3	4.3	3.9	4.1
8	3.9	3.7	5.1	8.0	6.7	2.3	3.7	N/A	3.8	5.1	3.6	2.1
9	3.6	4.3	4.4	7.5	6.9	1.2	4.6	4.1	3.9	4.2	4.4	2.6
10	4.1	5.5	4.9	4.3	6.1	2.9	6.8	2.3	4.5	4.1	3.8	3.4
11	4.5	3.2	6.5	4.7	2.6	6.1	3.9	3.5	3.8	4.0	4.0	3.5
12	4.2	4.8	6.5	4.6	5.9	2.2	5.2	2.3	5.3	3.3	4.3	3.2
13	6.1	5.8	3.4	4.5	N/A	5.5	N/A	2.2	3.3	3.5	3.0	2.9
14	3.4	3.9	6.9	4.1	2.3	4.5	4.0	3.9	3.7	3.3	5.1	3.0
15	4.7	3.5	4.6	2.7	6.0	5.9	3.1	5.6	4.2	4.1	4.6	2.7

Date	Jan	Feb	Mar	Apr	May	Jun	Jul	Aug	Sep	Oct	Nov	Dec
16	3.8	3.0	6.3	9.8	4.6	4.6	4.0	3.6	7.7	4.2	3.4	4.1
17	3.1	3.2	2.9	6.4	7.3	N/A	4.8	4.8	4.9	4.4	3.9	3.1
18	3.9	4.7	1.8	7.7	3.1	2.4	3.0	4.7	3.3	3.9	4.5	3.0
19	3.2	4.0	4.9	4.8	6.2	3.9	5.5	3.3	3.3	3.9	3.7	4.9
20	2.4	6.7	6.0	6.9	4.4	4.3	1.8	6.6	5.5	5.2	5.0	3.5
21	3.0	4.4	3.8	6.4	6.9	6.1	2.7	4.5	5.3	3.6	5.8	3.9
22	4.4	6.6	5.1	6.1	4.5	2.5	3.7	4.1	3.4	3.6	5.6	4.4
23	2.4	4.7	5.8	5.3	4.7	3.2	3.4	3.4	3.6	3.3	2.8	3.1
24	4.0	5.5	3.5	4.9	5.3	4.7	3.5	7.0	4.4	3.1	4.1	3.0
25	3.3	4.9	4.8	6.2	4.1	9.2	2.5	4.6	N/A	3.6	3.4	4.9
26	4.4	5.2	5.2	2.3	4.1	6.0	N/A	6.1	3.8	2.0	3.7	2.9
27	4.4	5.3	5.9	3.9	5.9	3.1	4.4	5.4	4.5	4.5	3.4	2.7
28	3.6	4.5	5.2	5.2	4.9	4.2	4.9	3.8	2.9	4.1	3.7	4.4
29	2.6	-	5.8	3.6	3.0	3.5	5.0	2.7	4.3	4.5	3.7	3.2
30	5.2	-	7.5	6.4	4.9	4.0	3.6	N/A	5.5	4.1	4.5	4.5
31	4.7	-	6.1	-	4.6	-	-	3.6	-	4.9	-	3.4

APPENDIX C

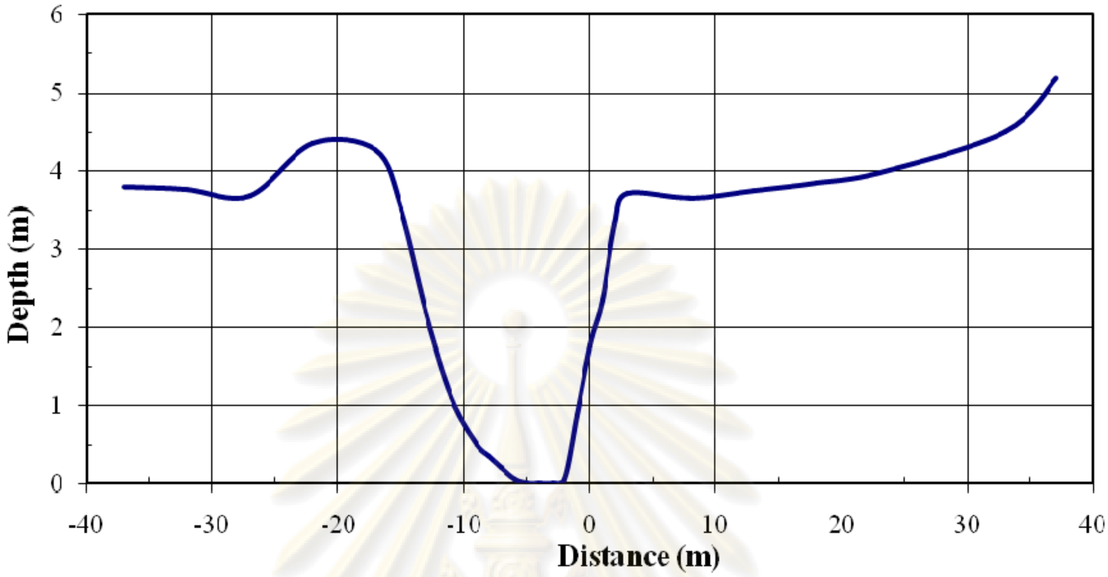

Figure C-1   Cross-section profile of Station 1 (N = 1843017, E = 457998)

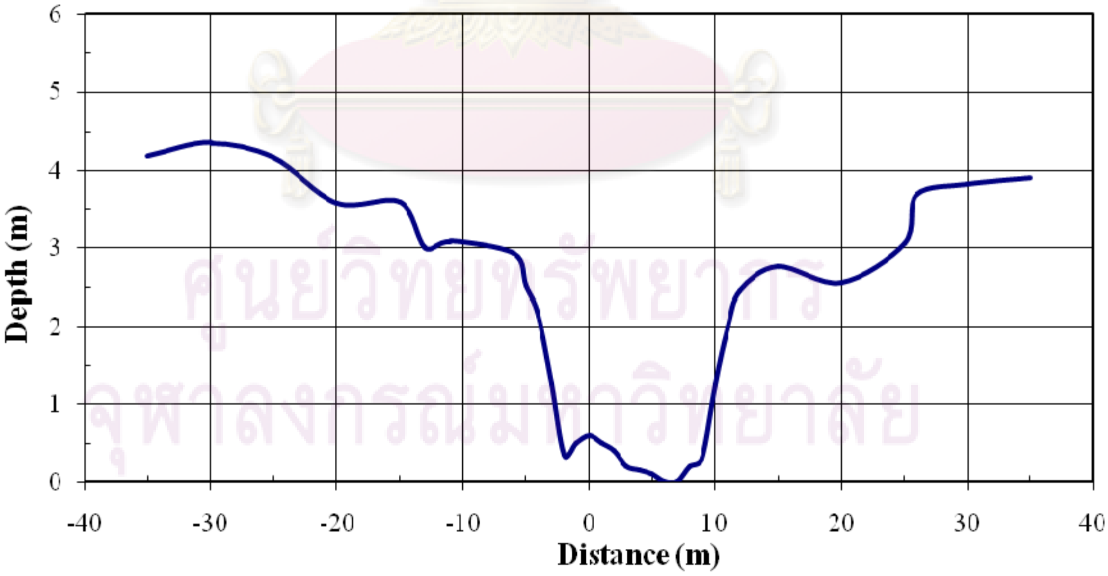

Figure C-2   Cross-section profile of Station 2 (N = 1843330, E = 459400)

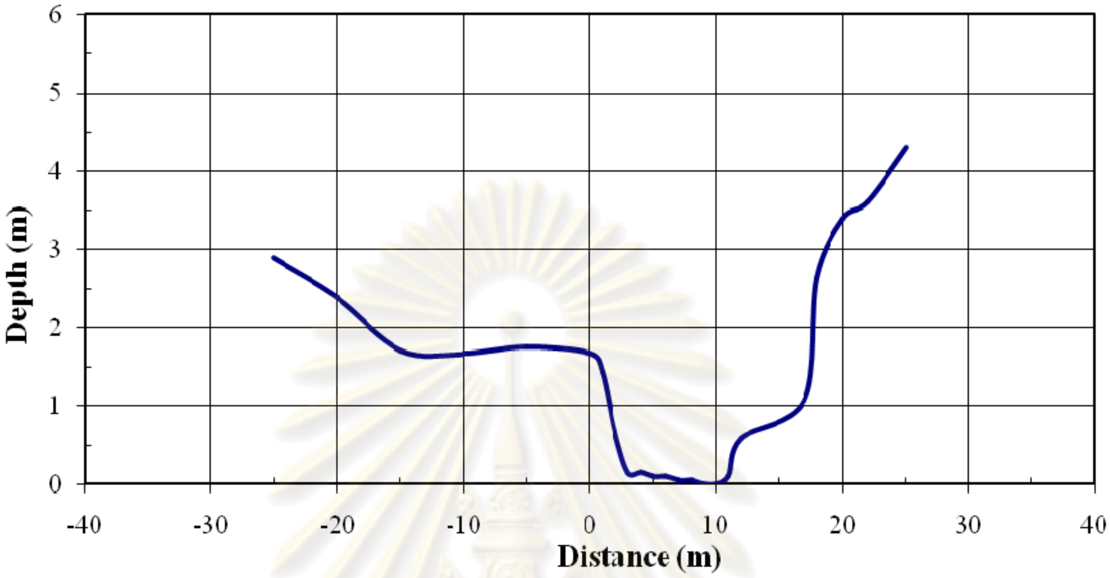

Figure C-3 Cross-section profile of Station 3 (N = 1843034, E = 461274)

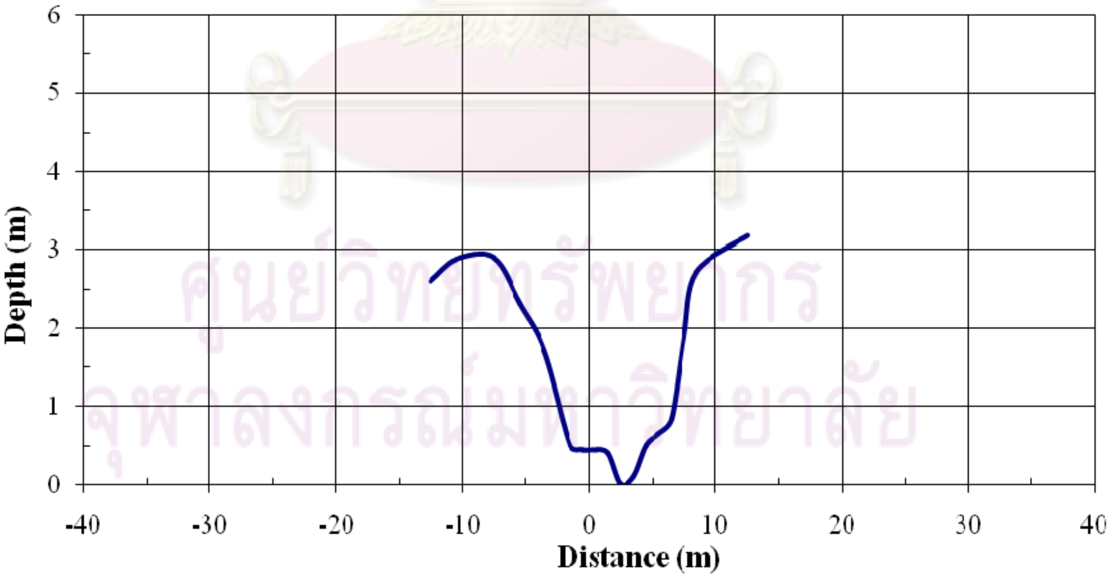

Figure C-4 Cross-section profile of Station 4 (N = 1843110, E = 461376)

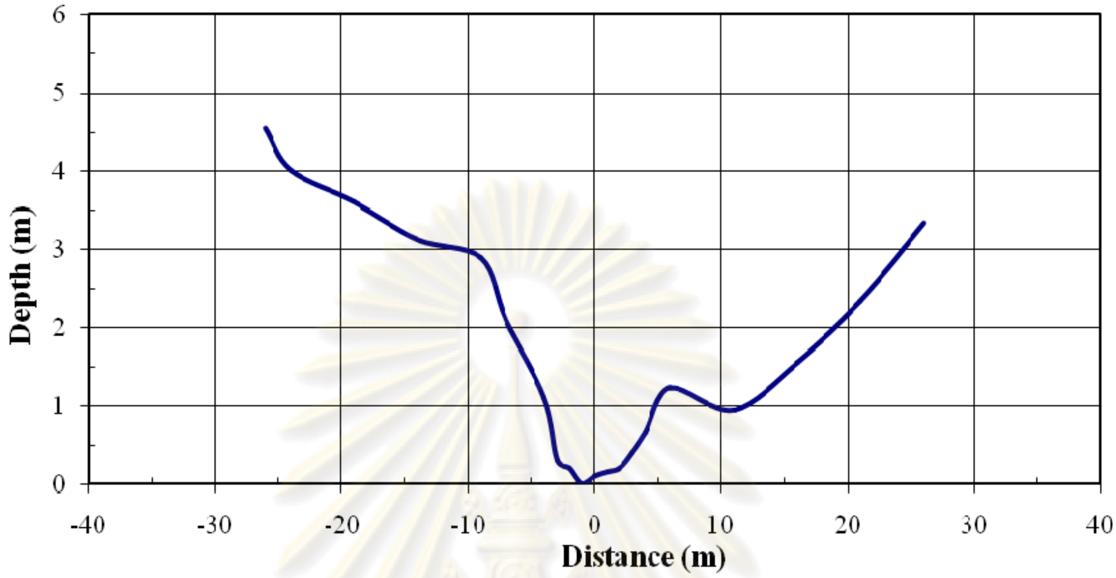

Figure C-5 Cross-section profile of Station 5 (N = 1843286, E = 461438)

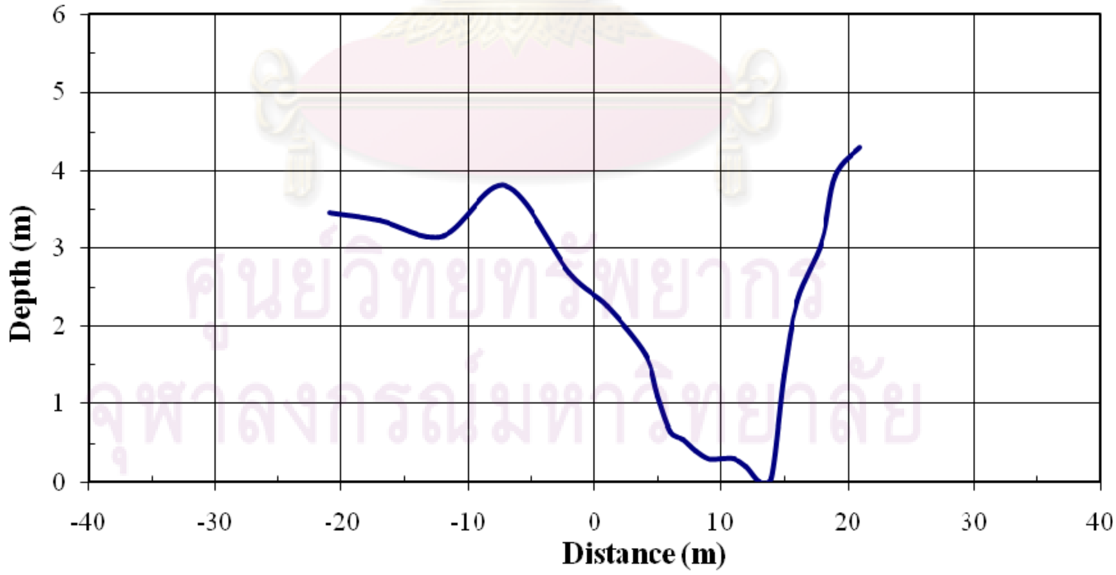

Figure C-6 Cross-section profile of Station 6 (N = 1842870, E = 462046)

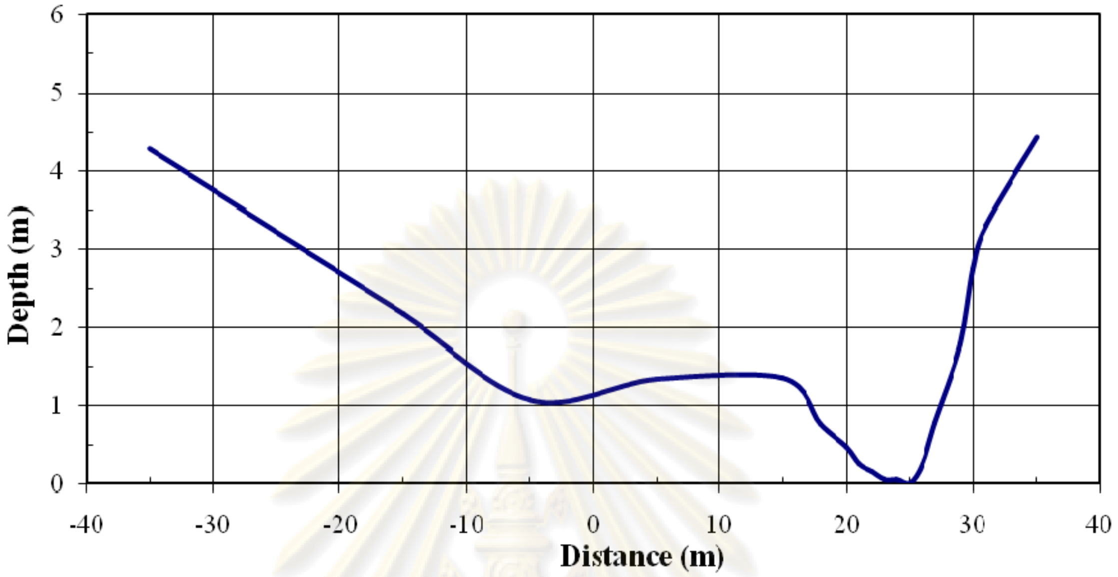

Figure C-7 Cross-section profile of Station 7 (N = 1842718, E = 465638)

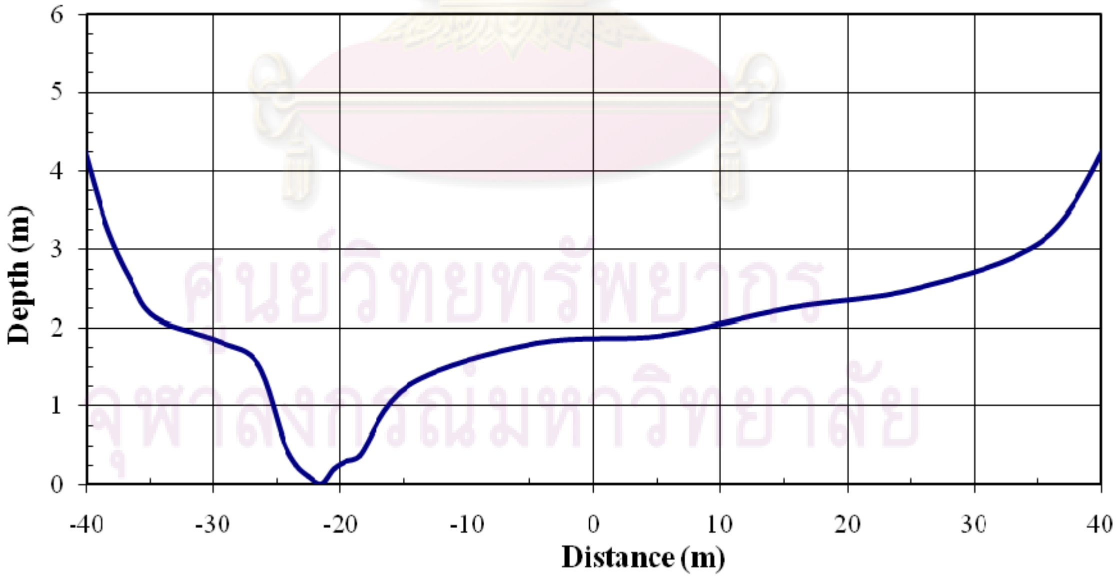

Figure C-8 Cross-section profile of Station 8 (N = 1842750, E = 466937)

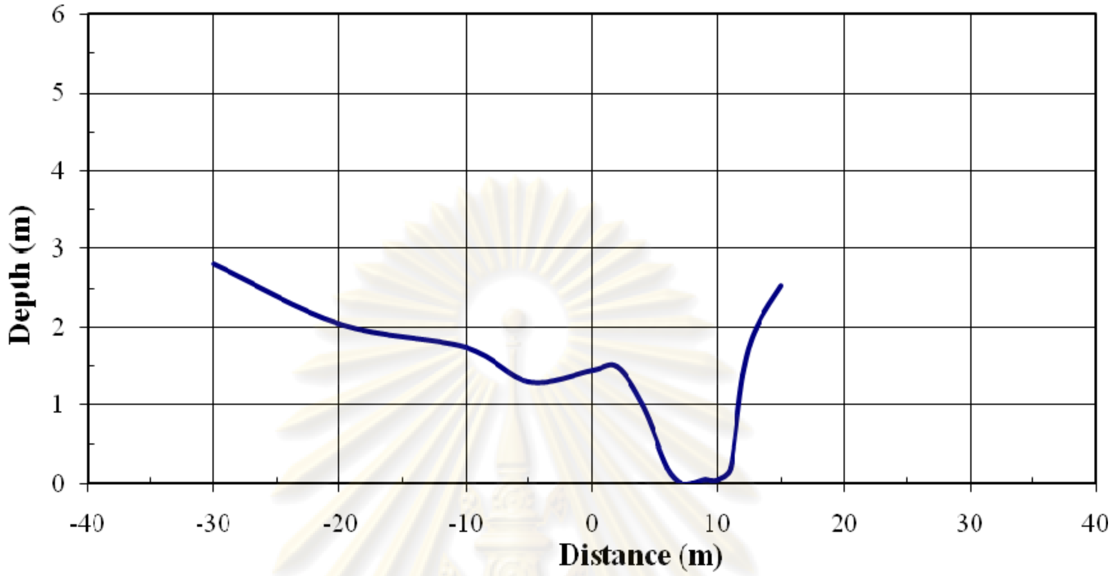

Figure C-9 Cross-section profile of Station 9 (N = 1842559, E = 467228)

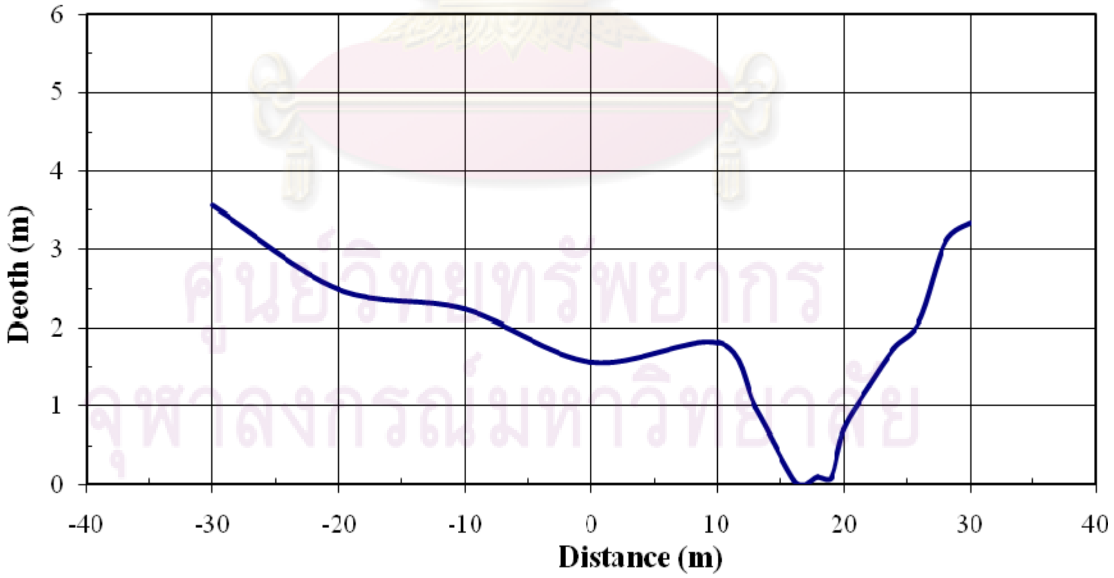

Figure C-10 Cross-section profile of Station 10 (N = 1842736, E = 467088)

BIOGRAPHY

Miss Pimprapa Karoonmakphol was born on August 7, 1986 in Bangkok. She graduated with a bachelor’s degree in Environmental Engineering from Chulalongkorn University in the year 2007. After that, she pursued a master’s degree though the International Postgraduate Programs in Environmental and Hazardous Waste Management of the National Center of Excellence in Environmental and Hazardous Waste Management at Chulalongkorn University from May 2008 to May 2010.